

Copyright
by
Chang Hyuk Kim
2014

**The Dissertation Committee for Chang Hyuk Kim Certifies that this is the approved
version of the following dissertation:**

**Performance of Concrete Panels Strengthened using Carbon Fiber
Reinforced Polymers (CFRP)**

Committee:

James O. Jirsa, Supervisor

Wassim M. Ghannoum, Co-Supervisor

Oguzhan Bayrak

Jinying Zhu

Harovel G. Wheat

**Performance of Concrete Panels Strengthened using Carbon Fiber
Reinforced Polymers (CFRP)**

by

Chang Hyuk Kim, B.S.E.; M.E.

Dissertation

Presented to the Faculty of the Graduate School of
The University of Texas at Austin
in Partial Fulfillment
of the Requirements
for the Degree of

Doctor of Philosophy

**The University of Texas at Austin
December, 2014**

Dedication

To my parents

Acknowledgements

This research was able to be conducted only with help from many individuals. First of all, my most sincere thanks go to my supervisor Dr. James O. Jirsa, for his perceptive criticism and kind encouragement. His comprehensive knowledge enabled this research to reach valuable conclusions. I also would like to thank Dr. Wassim Ghannoum, my co-supervisor, for his thoughtful guidance for my research and technical study. Their advice and comments were indispensable for my dissertation work. Furthermore, I would like to thank the committee members, Dr. Oguzhan Bayrak, Dr. Jinying Zhu, and Dr. Harovel G. Wheat for their help with my dissertation.

I would like to extend thanks to the members of my research group: Jose Garcia, Wei Sun, William Shekarchi, Nawaf Alotaibi, and Helen Wang. I could only carry out my experiments with their help. The technical support provided by the Ferguson Structural Engineering Laboratory staffs is greatly acknowledged. I would like to give thanks to Andrew Valentine, Blake Stasney, Dennis Phillip, Eric Schell, Mike Wason, and David Braley. Also, I would like to thank the administrative staff, Barbara Howard, Anise Langley, and Michelle Damvar. In addition, I would like to give thanks to my FSEL friends – Guillermo Huaco, Jinwoo Lee, Sungyeob Shin, Kiyeon Kwon, Yungon Kim, Jongkwon Choi, and Jinhan Kwon. I truly appreciate their friendship, assistance and advice.

Funding from the Texas Department of Transportation and generous donation of sufficient CFRP materials from Scott Arnold of Fyfe Co. LLC are greatly acknowledged. Their help made this research possible.

Finally I would like to sincere and the deepest thank my parents Namhae Kim and Junghee Lee. I could accomplish all my work and study with their endless and immensurable love and support. Sincere thanks go to my lovely family.

Performance of Concrete Panels Strengthened using Carbon Fiber Reinforced Polymers (CFRP)

Chang Hyuk Kim, Ph.D.

The University of Texas at Austin, 2014

Supervisor: James O. Jirsa

Co-Supervisor: Wassim M. Ghannoum

Many bridges are handling heavier loads than those expected at design, making it increasingly necessary to strengthen existing members or conduct repairs on damaged structural members. Carbon Fiber Reinforced Polymer (CFRP) materials have been broadly used to repair and strengthen reinforced concrete structures. Using CFRP materials as the strengthening material is an excellent solution because of their mechanical properties. CFRP has properties of high strength, corrosion resistance, and light weight.

CFRP materials are being widely used for shear and flexural strengthening. Most studies have focused on uni-directional layout of CFRP strips in high shear regions of beams. Recent shear tests on full-scale I-girders have shown that the use of bi-directional CFRP layouts with CFRP anchors led to much higher shear strength increases than when

using uni-directional layouts. The objective of the study is to determine the mechanism that governs shear strengthening of bridge girders using bi-directional CFRP and, in doing so, demonstrate the feasibility of using bi-directional CFRP for shear strengthening of large bridge I- and U-beams.

Small-scale panel tests have been conducted to investigate parameters that influence the shear strength provided by bi-directional CFRP layouts. Panels were tested under compressive forces to simulate the compression struts that develop in the webs of I-beams. The applied loads generated bottle-shaped compressive struts. CFRP anchors were used to prevent early failure due to CFRP strip delamination from the panel surface. The panels, while not fully reproducing the boundary condition of girder webs, were tested ahead of full-scale girders to investigate a wide range of parameters in a cost-effective manner. The variables considered include the amount of CFRP and steel reinforcement, the inclination of CFRP fibers, and the layout and spacing of CFRP strips. The panel tests provide qualitative comparisons between the influence of the various parameters. The relative strength contributions of CFRP strips, steel stirrups, and concrete were evaluated.

Table of Contents

LIST OF TABLES	XII
LIST OF FIGURES	XIII
CHAPTER 1 INTRODUCTION.....	1
1.1 Overview.....	1
1.2 CFRP anchors for strengthening with CFRP sheets	1
1.3 Objectives and Scope.....	2
CHAPTER 2 BACKGROUND	3
2.1 Carbon Fiber Reinforced Polymers (CFRP).....	3
2.2 Shear Strengthening CFRP system	5
2.2.1 Wrapping schemes	5
2.2.2 Failure mode of CFRP reinforcement.....	6
2.2.3 Shear strengthening using CFRP materials.....	6
2.2.4 Bi-directional CFRP for shear strengthening of I-girder	7
2.3 CFRP Anchor.....	10
2.3.1 Development of CFRP anchors	10
2.3.2 CFRP anchor detail.....	12
2.4 Panel Tests	14
2.4.1 Specimen details	14
2.4.2 Observations	15

CHAPTER 3 EXPERIMENTAL STUDY 16

3.1 Test Specimens 16

 3.1.1 General16

 3.1.2 Design Considerations18

3.2 Test Setup and Instruments 28

 3.2.1 Universal Testing Machine (UTM)28

 3.2.2 UT vision system30

 3.2.3 Strain gage34

3.3 Material Properties..... 35

 3.3.1 Concrete35

 3.3.2 CFRP.....38

 3.3.3 Steel.....39

CHAPTER 4 ANALYSIS OF THE TEST RESULTS..... 41

4.1 Overview of the Test Results 41

4.2 Control Panel Results..... 44

 4.2.1 Comparison between the two 5 ksi control specimens (with and without steel).....44

 4.2.2 Control panel cracking and failure mode.....47

4.3 Behavior of typical panel test 52

4.4 Effect of CFRP strip inclination 54

 4.4.1 Panels reinforced with uni-directional CFRP strips.....54

 4.4.2 Panels reinforced with bi-directional CFRP strips.....64

4.5 Effect of CFRP layout..... 75

 4.5.1 Panels reinforced with CFRP strips without steel reinforcement75

 4.5.2 Panels reinforced with CFRP strips and bars.....84

4.6 Effect of amount of CFRP, steel reinforcement, and intermediate anchor 93

 4.6.1 Amount of CFRP material93

4.6.2	Intermediate CFRP anchors	95
4.6.3	Amount of steel reinforcement	99
4.7	Load contribution of CFRP strips and steel reinforcement	104
4.8	Effect of concrete strength	107
4.9	Trends observed in panels and I-beams	108
CHAPTER 5 SUMMARY AND CONCLUSIONS		109
5.1	Summary	109
5.2	Conclusions	110
5.3	Future work	112
APPENDIX A		113
APPENDIX B		118
APPENDIX C		121
APPENDIX D		131
REFERENCES		136
VITA		138

LIST OF TABLES

Table 2.1 Typical tensile properties of fibers used in FRP systems (ACI 440.2R).....	4
Table 2.2 Tensile properties of FRP laminates with 40 to 60% fiber volume.....	4
Table 3.1 Test specimen variables	17
Table 3.2 Stiffness comparison.....	24
Table 3.3 Camera properties.....	32
Table 3.4 Cylinder test results	37
Table 3.5 Material properties of Tyfo [®] SCH 11-UP composite	38
Table 4.1 Test result summary.....	43
Table 4.2 Comparisons of load contributions of steel and CFRP to panel strength at 0.004 strain	105
Table 4.3 Load increase in bi-directional CFRP strengthened panels	108

LIST OF FIGURES

Figure 2.1 Material properties of steel and CFRP laminate.....	5
Figure 2.2 Typical wrapping schemes for shear strengthening (ACI 440.2R).....	6
Figure 2.3 CFRP shear strengthening configurations.....	7
Figure 2.4 I-girders reinforced with various CFRP layouts (Kim et al, 2012).....	8
Figure 2.5 LVDTs configuration for shear strain calculation (Kim, 2011).....	8
Figure 2.6 Load-strain response of test results.....	9
Figure 2.7 Panel test concept.....	10
Figure 2.8 Use of anchors for flexural strengthening (Kim et al. 2006).....	11
Figure 2.9 CFRP anchor detail.....	12
Figure 2.10 Isometric view of U-wrap with CFRP anchorage system (Kim, 2011).....	13
Figure 2.11 Bottle-shaped strut and associated strut-and-tie model (Brown, 2005).....	14
Figure 3.1 Notation for the panels.....	18
Figure 3.2 Loading region of panels with CFRP confinement.....	19
Figure 3.3 Panels with steel plates.....	19
Figure 3.4 Diagonal cracks of I-beam (Picture from Kim 2011).....	20
Figure 3.5 Various CFRP strip inclinations for the uni-directional CFRP layout.....	21
Figure 3.6 CFRP reinforced panels.....	22
Figure 3.7 Variation of CFRP amount.....	23
Figure 3.8 Variation of #3 stirrup.....	25
Figure 3.9 Different number of CFRP anchors.....	26
Figure 3.10 CFRP layouts for the high strength (11.5 ksi) concrete.....	27
Figure 3.11 600 kips Universal Testing Machine (UTM).....	28
Figure 3.12 Testing frame.....	29
Figure 3.13 UT Vision system (UTVS).....	31
Figure 3.14 Strain comparison plot for specimen U5-0-2-5.....	33
Figure 3.15 Locations of targets used to estimate the average horizontal strain over panel height.....	34
Figure 3.16 Steel strain gage.....	35

Figure 3.17 Locations of the strain gages	35
Figure 3.18 Concrete compressive strength from cylinder tests (5,000 psi)	36
Figure 3.19 Concrete compressive strength from cylinder tests (11,000 psi)	36
Figure 3.20 Small beam test for the CFRP material properties	39
Figure 3.21 Stress-strain responses for calculation of CFRP material properties	39
Figure 3.22 #3 bar tension test.....	40
Figure 3.23 Stress-strain response of #3 bars	40
Figure 4.1 C0-0-0-5 (without bars).....	44
Figure 4.2 C0-0-2-5 (with bars).....	44
Figure 4.3 Load comparison between control specimens.....	45
Figure 4.4 Horizontal strain contours for C0-0-0-5	46
Figure 4.5 Horizontal strain contours for C0-0-2-5	47
Figure 4.6 C0-0-0-5 panel in the universal testing machine, UTM.....	48
Figure 4.7 Failure mode of specimen C0-0-0-5.....	48
Figure 4.8 C0-0-0-11 Panel in the test frame.....	49
Figure 4.9 Failure mode of specimen C0-0-0-11	49
Figure 4.10 Control panel, C0-0-2-5.....	50
Figure 4.11 Failure mode of specimen C0-0-2-5.....	51
Figure 4.12 Horizontal strain contours for typical panel (B5-45-2-5).....	53
Figure 4.13 Load-strain responses for uni-directional CFRP strip layouts	55
Figure 4.14 Horizontal strain contours for panels reinforced with uni-directional CFRP strips.....	56
Figure 4.15 Failure modes of panels reinforced with various CFRP inclinations	58
Figure 4.16 Load comparison of the specimens reinforced with uni-directional CFRP layouts, no reinforcement	59
Figure 4.17 Load-strain responses for uni-directional CFRP strip layouts with reinforcement.....	60
Figure 4.18 Horizontal strain contours for panels reinforced with uni-directional CFRP strips and reinforcement	61
Figure 4.19 Failure modes of panels reinforced with various CFRP inclinations and steel reinforcement	62

Figure 4.20 Load comparison of the uni-directional CFRP layout, panels with reinforcement.....	63
Figure 4.21 Load-strain responses for bi-directional CFRP strip layouts, $f_c'=5$ ksi	64
Figure 4.22 Horizontal strain contours for panels reinforced with bi-directional CFRP strips	66
Figure 4.23 Load comparison of the bi-directional CFRP layout specimens ($f_c'=5$ ksi)	67
Figure 4.24 Failure mode of panels reinforced with different inclinations of bi-directional CFRP layouts ($f_c'=11$ ksi).....	69
Figure 4.25 Load comparison of the bi-directional CFRP layout specimens ($f_c'=11$ ksi)	70
Figure 4.26 Load-Strain responses for bi-directional CFRP strips layouts with reinforcement.....	71
Figure 4.27 Horizontal strain contours for panels reinforced with bi-directional CFRP strips and reinforcement	73
Figure 4.28 Load comparison of bi-directional CFRP layouts, panels with reinforcement.....	74
Figure 4.29 Failure modes of bi- vs. uni-directional CFRP layouts at 0 and 90 degrees ..	76
Figure 4.30 Load comparison of 0 and 90 degrees CFRP layout, no reinforcement.....	77
Figure 4.31 Failure modes of bi- vs. uni-directional CFRP layouts at 45 degrees	79
Figure 4.32 Load comparison of 45 degrees CFRP layout, no reinforcement	80
Figure 4.33 Failure modes of bi- vs.uni-directional CFRP layouts at 30 and 60 degrees.....	82
Figure 4.34 Load comparison of 30 and 60 degrees CFRP layout, no reinforcement.....	83
Figure 4.35 Failure modes of bi- vs. uni-directional CFRP layouts at 45 degrees	85
Figure 4.36 Load-strain responses of bi- and uni-directional CFRP layouts at 45 degrees from horizontal.....	86
Figure 4.37 Horizontal strain contours for panels reinforced with a 45 degrees CFRP layouts	87
Figure 4.38 Load comparison for panels with a 45 degrees CFRP strip layouts, with reinforcement.....	88

Figure 4.39 Failure modes of bi- vs. uni-directional CFRP layouts at 30 and 60 degrees.....	89
Figure 4.40 Load-strain responses of bi-and uni-directional CFRP layouts at 30 and 60 degrees from horizontal.....	90
Figure 4.41 Horizontal strain contours for panels reinforced with 30 and 60 degrees CFRP strip layouts.....	91
Figure 4.42 Load comparison of 30 and 60 degrees CFRP layout.....	92
Figure 4.43 Load-Strain responses of strip vs. fully reinforced panel.....	93
Figure 4.44 Failure modes of strip vs. fully reinforced panel, no reinforcement	94
Figure 4.45 Effect of the CFRP amount	95
Figure 4.46 Load-strain responses of panels with intermediate CFRP anchors	96
Figure 4.47 Horizontal strain contours for panels with intermediate CFRP anchors	97
Figure 4.48 Effect of intermediate CFRP anchors.....	98
Figure 4.49 Failure modes of panels reinforced with different amounts of reinforcement.....	99
Figure 4.50 Load-strain responses of panels reinforced with different steel ratios	100
Figure 4.51 Horizontal strain contours for panels reinforced with various steel ratios...	102
Figure 4.52 Effect of steel reinforcement ratio.....	103
Figure 4.53 Load-strain responses of panels reinforced with various reinforcements ...	104
Figure 4.54 Horizontal strain contours for panels reinforced with different materials ...	106
Figure 4.55 Load contribution of CFRP strip to panel strength	107
Figure A.1 Strain gage installation	114
Figure A.2 Surface preparation for CFRP installation.....	115
Figure A.3 CFRP application.....	117
Figure B.1 Layout of steel reinforcement	118
Figure B.2 CFRP anchor detail (Kim, 2011)	119
Figure C.1 C0-0-0-5.....	121
Figure C.2 B36-0-0-5-0an.....	122
Figure C.3 B36-0-0-5-4an.....	122
Figure C.4 B36-0-0-5-6an.....	123
Figure C.5 U5-0-0-5.....	123

Figure C.6 U5-30-0-5.....	124
Figure C.7 U5-45-0-5.....	124
Figure C.8 U5-60-0-5.....	125
Figure C.9 B5-0-0-5.....	125
Figure C.10 B5-45-0-5.....	126
Figure C.11 B5-60-0-5.....	126
Figure C.12 C0-0-2-5.....	127
Figure C.13 U5-0-1-5.....	127
Figure C.14 U5-0-2-5.....	128
Figure C.15 U5-30-2-5.....	128
Figure C.16 U5-45-2-5.....	129
Figure C.17 U5-60-2-5.....	129
Figure C.18 B5-45-2-5.....	130
Figure C.19 B5-60-2-5.....	130
Figure D.1 Locations of the strain measurement.....	131
Figure D.2 C0-0-2-5.....	132
Figure D.3 U5-0-1-5.....	132
Figure D.4 U5-0-2-5.....	133
Figure D.5 U5-30-2-5.....	133
Figure D.6 U5-45-2-5.....	134
Figure D.7 U5-60-2-5.....	134
Figure D.8 B5-45-2-5.....	135
Figure D.9 B5-60-2-5.....	135

CHAPTER 1 INTRODUCTION

1.1 OVERVIEW

As traffic loads rise and bridge infrastructure ages, it is becoming increasingly necessary to repair or strengthen existing bridge members. Externally applied Carbon Fiber Reinforced Polymer (CFRP) materials have been broadly used to repair and strengthen reinforced concrete structures. Strengthening concrete members using CFRP is a cost-effective and rapid retrofit technique, which can be implemented while members are in service. Moreover, CFRP materials offer additional benefits over traditional materials because of their high strength-to-weight ratio, corrosion resistance, and limited architectural impact.

1.2 CFRP ANCHORS FOR STRENGTHENING WITH CFRP SHEETS

In most CFRP strengthening applications, interface bond capacity between the concrete surface and the CFRP is important to realize the role of CFRP reinforcement. Full capacity of the strengthening material cannot be utilized when debonding failure occurs. Therefore, a conservative approach to avoid premature debonding failure has to be taken into account.

The use of CFRP anchors provides a means of precluding debonding failure. The CFRP strengthening materials can reach their ultimate capacity through the use of CFRP anchors. Therefore, CFRP anchors were implemented for the CFRP strip reinforcement in this study.

1.3 OBJECTIVES AND SCOPE

Many experimental studies have been conducted to evaluate CFRP shear strengthening effects on shear regions of beams and girders. However, the strengthening of bi-directional CFRP layouts led to increases in shear strength compared with that of the uni-directional CFRP layouts. Therefore, the objective of this study was to demonstrate the feasibility of using bi-directional CFRP for shear strengthening. More specifically, the effects of bi-directional CFRP layouts on the strength of bottle-shaped struts were investigated. Panel tests were conducted considering a number of variables. The parameters affecting CFRP strengthening applications were identified in this study.

Chapter 2 contains background information for this experimental study regarding CFRP strengthening systems as well as CFRP anchor details. Test specimen and design considerations are introduced in Chapter 3. The first series of the panels was reinforced with uni-directional CFRP strips and the second series was reinforced with bi-directional CFRP strips. Subsequently, the test setup and instrumentation are presented in Chapter 3. In Chapter 4, test results are evaluated in terms of the load capacities and deformations of the panels. Chapter 5 contains a summary of the experimental study and conclusions.

CHAPTER 2 BACKGROUND

CFRP laminates are commonly used in flexural strengthening despite high material cost. Most of the studies using CFRP materials focused on the behavior of flexural structural members. However, strengthening of shear regions with CFRP anchors has not been studied as extensively.

Early debonding failure of CFRP strips from the concrete surface leads to ineffective use of the CFRP material. To maximize the development of CFRP material capacity, delamination failure has to be prevented during the life time of the reinforced members. Several anchorage systems have been studied to prevent CFRP strip delamination failure.

2.1 CARBON FIBER REINFORCED POLYMERS (CFRP)

Fiber reinforced polymers are composite materials that consist of fibers in a polymer matrix. There are three commonly used fibers: glass, carbon, and aramid. Table 2.1 shows typical tensile properties of fibers used in FRP materials. Generally FRP fibers are used with epoxy resin. Tensile properties for CFRP, GFRP, and AFRP laminates are shown in Table 2.2. These mechanical properties are measured in the fiber orientation.

CFRP is most commonly used for structural members. For reinforced concrete structures, steel embedded in the concrete matrix is used because of its higher elastic modulus and lower cost compared with the CFRP materials. However, the lightweight of CFRP and the possibility of rapid application make CFRP material attractive for retrofit of structures.

Table 2.1 Typical tensile properties of fibers used in FRP systems (ACI 440.2R)

Fiber	Elastic modulus (ksi)	Ultimate strength (ksi)	Rupture strain (%)
Carbon (High-strength)	32,000 to 34,000	550 to 700	1.4
Glass (E-glass)	10,000 to 10,500	270 to 390	4.5
Aramid (High-performance)	16,000 to 18,000	500 to 600	1.6

Table 2.2 Tensile properties of FRP laminates with 40 to 60% fiber volume

Fiber	Young's modulus (ksi)	Ultimate strength (ksi)	Rupture strain (%)
Carbon (High-strength)	15,000 to 21,000	150 to 350	1.0 to 1.5
Glass (E-glass)	3,000 to 6,000	75 to 200	1.5 to 3.0
Aramid (High-performance)	7,000 to 10,000	100 to 250	2.0 to 3.0

Figure 2.1 shows specified material properties for grade 60 steel and the CFRP laminates used in this study. As can be seen in this plot, the CFRP laminate has no yield point or ductile behavior characterizes steel behavior after reaching yield stress. The modulus of elasticity of CFRP is about 15,000 ksi, which is roughly half that of Grade 60 steel. Ultimate stress of the CFRP laminate, however, is approximately 150 ksi. CFRP material is brittle and ruptures 1 %. The material comparisons in Figure 2.1 indicate that large strains need to develop in structural members to utilize CFRP material capacity effectively. Large deformations and wide crack openings could therefore occur when the full capacity of CFRP is mobilized, but the deformations have to remain in an acceptable range for serviceability considerations.

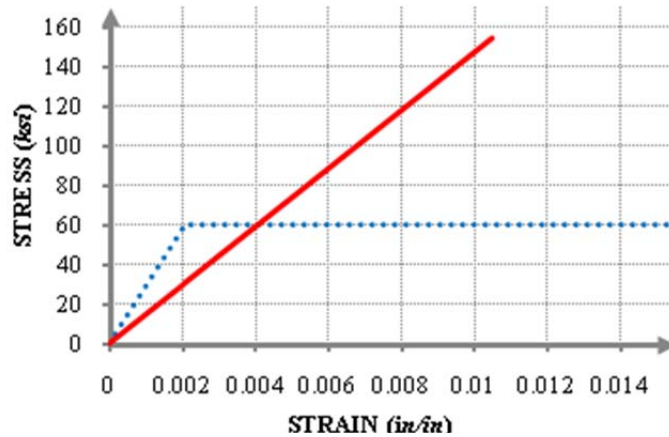


Figure 2.1 Material properties of steel and CFRP laminate

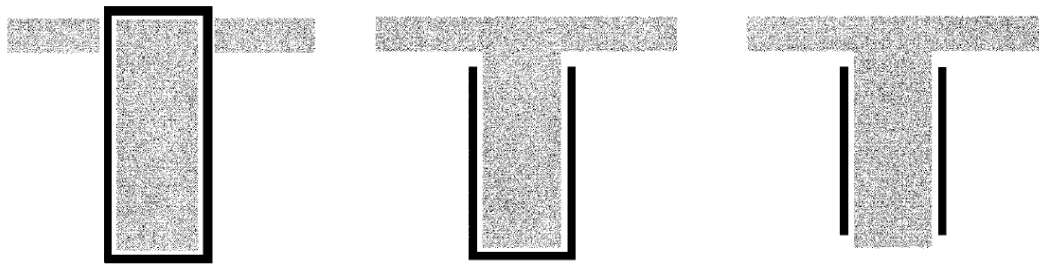
2.2 SHEAR STRENGTHENING CFRP SYSTEM

2.2.1 Wrapping schemes

FRP systems can be used to increase shear strength of existing concrete beams and columns (Malvar 1995, Chajes 1995, Norris 1997, Kachlakev and McCurry 2000). Three different wrapping schemes are commonly used in shear strengthening. Typical schemes are shown in Figure 2.2.

Completely wrapping the FRP (Figure 2.2(a)) around the section on all four sides is the most efficient wrapping scheme and is most commonly used in column applications where access to all four sides of the column is usually available. In beam applications where an integral slab makes it impractical to completely wrap the member, the shear strength can be improved by wrapping the FRP system around three sides of the member (Figure 2.2(b)), or bonding to two opposite sides of the member (Figure 2.2(c)).

Although all three techniques have been shown to improve the shear strength of a member, completely wrapping the section is the most efficient, followed by the three-sided U-wrap. Bonding to two sides of a beam is the least efficient scheme.



(a) *Completely wrapped* (b) *3-sided “U-wrap”* (c) *2 sides*

Figure 2.2 Typical wrapping schemes for shear strengthening (ACI 440.2R)

2.2.2 Failure mode of CFRP reinforcement

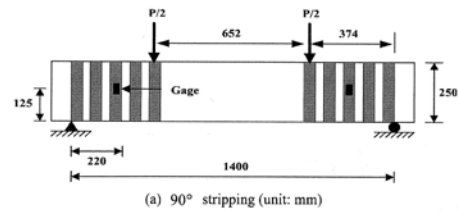
Concrete crushing, rupture of the CFRP strips, and delamination failure between the CFRP strips and the concrete surface are typical failure modes of CFRP strengthened systems. The most favorable failure mode is CFRP rupture since the full capacity of the CFRP material will be utilized. Concrete crushing failure has to be prevented because the CFRP materials are ineffective once crushing occurs. Delamination failure of the CFRP is triggered by concrete cracking or bond failure between the concrete surface and CFRP material. Delamination can spread rapidly and lead to failure of the strengthening system.

2.2.3 Shear strengthening using CFRP materials

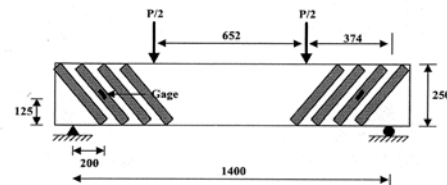
Figure 2.3 shows different FRP strengthening configurations for shear tested by Monti and Liotta (2005) and by Sim et al. (2005). Most of the failure modes were brittle with the CFRP strip debonding from the concrete surface prior to reaching the fracture strain of the CFRP strips. Because of the CFRP debonding failure, the strengthened specimens were not able to reach expected shear capacities.

STRENGTHENING APPLICATION	STRENGTHENING TYPE	FIBRES ANGLE	NAME	STRENGTHENING CONFIGURATION	EXP. SHEAR STRENGTH TH (kN)
	NONE	-	REF		95.0
SIDE BONDING	STRIPS width 150 mm spacing 300 mm	90°	SS90*		100.0
		45°	SS45		101.0
		60°, 45°, 30°	SSVA		105.0
	SHEETS	90°	SF90		112.5
U-JACKETING	STRIPS width 150 mm spacing 300 mm	90°	US90*		95.0
		60°	US60		111.0
		60°, 45°, 30°	USVA		120.0
		60°, 45°, 30°	USVA+		135.0
		45°	US45+		126.0
		90°	US90(2)*		90.0
	SHEETS	90°	UF90		125.0
	STRIPS width 50mm spacing 100 mm		US45++		133.5
			UF45++A		158.5
	SHEETS		UF45++B		167.0
			UF45++C		172.0
		US45++F		182.85	
STRIPS width 150 mm spacing 225 mm		US45++E		150.15	
		US45+ D		163.45	
WRAPPING	STRIPS width 50mm spacing 100 mm		WS45++		114.5

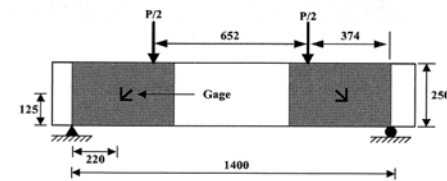
* In these tests, the shear cracks did not fully activate the FRP strips, which then did not contribute to the shear strength.



(a) 90° stripping (unit: mm)



(b) 45° stripping (unit: mm)



(c) II, U wrapping (unit: mm)

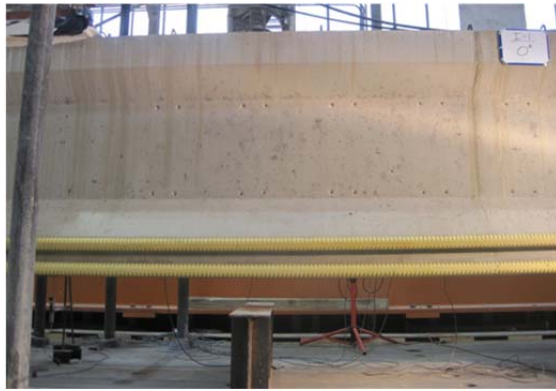
(a) Monti and Liotta (2005)

(b) Sim et al. (2005)

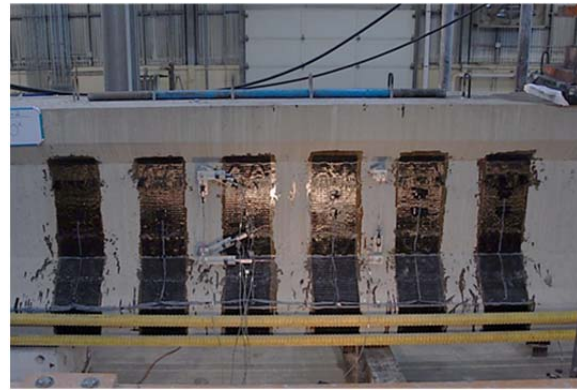
Figure 2.3 CFRP shear strengthening configurations

2.2.4 Bi-directional CFRP for shear strengthening of I-girder

Four 54 inch deep I-girders with both uni- and bi-directional CFRP strips were tested at the University of Texas at Austin sponsored by Texas Department of Transportation (Kim et al, 2012). As can be seen in Figure 2.4, the deep I-girders were reinforced with various CFRP strip layouts. Girders were monotonically loaded to failure. Cracking and ultimate loads were recorded. Six LVDTs were used to record shear deformation of the I-beam tests (Figure 2.5). Shear strains could be calculated with triangularly arranged LVDTs.



(a) Control, No CFRP strips



(b) Uni-directional strips



(c) Bi-directional fully wrapped beam



(d) bi-directional strips

Figure 2.4 I-girders reinforced with various CFRP layouts (Kim et al, 2012)

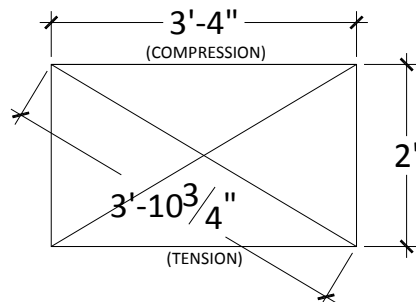


Figure 2.5 LVDTs configuration for shear strain calculation (Kim, 2011)

Figure 2.6 shows load-shear strain responses for the girder tests. The figure shows that having CFRP in both directions increased the ultimate shear strength by 38 % and increased the shear-cracking load. The responses of the bi-directional strip reinforced girder and the bi-directionally reinforced fully wrapped girder were identical, even though the fully wrapped girder had more than twice the CFRP materials as the strip reinforced girder. The results show that the use of a bi-directional CFRP strip layout improves the performance of the member with much less materials than a fully wrapped layout.

Based on the observed behavior of the I-beams, the panel test concept is illustrated in Figure 2.7. Load is applied over a defined area to generate a bottle-shaped compressive strut between loading and reaction points. The panel loaded in this manner is intended to simulate the compression strut in the web regions. However, direct design data cannot be obtained since boundary conditions of the panel test are different compared with full scale specimens.

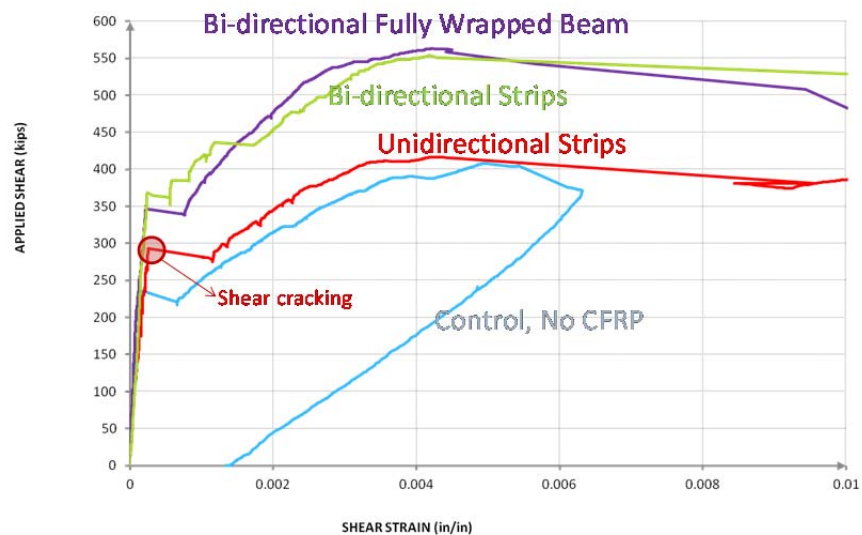


Figure 2.6 Load-strain response of test results

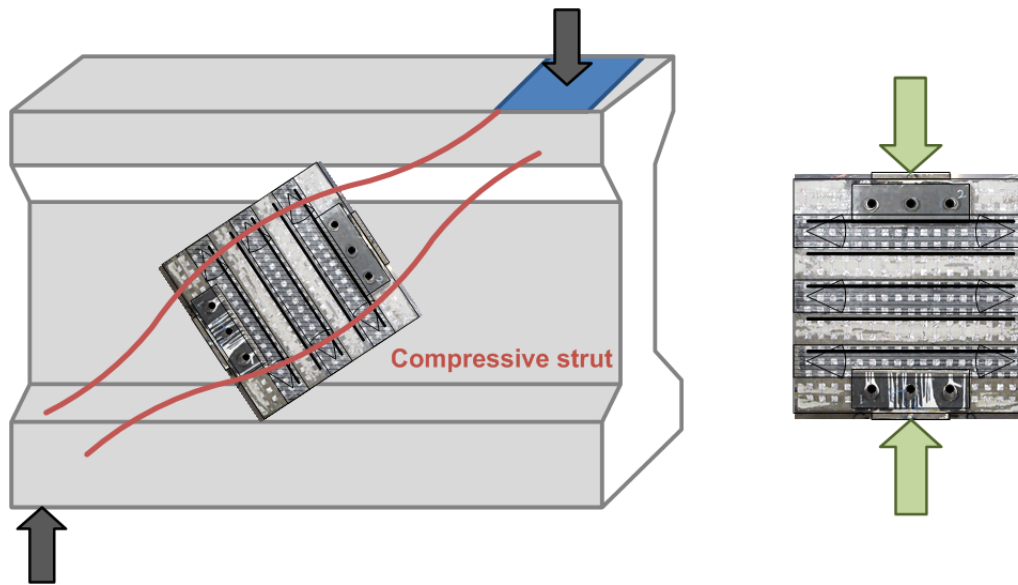


Figure 2.7 Panel test concept

2.3 CFRP ANCHOR

CFRP anchors have a significant effect on the CFRP sheet reinforcing system. To utilize the full capacity of the CFRP material, premature CFRP debonding failure has to be prevented. CFRP anchors can allow CFRP strips to reach full capacity. Many experimental studies have examined the use of CFRP anchors to improve reinforced concrete member strength.

2.3.1 Development of CFRP anchors

CFRP anchors were used to provide continuity of CFRP sheets in a CFRP layout that was intersected by walls (Kobayashi, 2001). Penetration holes were drilled through the wall close to the column surface. The CFRP anchors were made of the same material that strengthened the concrete member. The anchors were inserted into the penetration holes and fanned out over the CFRP sheets. The CFRP anchor can be used for beams

with slabs, or in-filled shear walls in frames. For example, in the test conducted by Kim et al. (2006), CFRP sheets were used to improve the flexural behavior of specimens.

As shown in Figure 2.8, two beams were strengthened with CFRP sheets. In the case of the beam without the CFRP anchors (Figure 2.8(a)), CFRP sheet delamination from the concrete surface was the main failure mode and the CFRP strain at failure was 0.0053. On the other hand, the improvement was apparent and the strains developed in the CFRP sheets nearly doubled when CFRP anchors were used. Figure 2.8(b) shows the specimen with the CFRP anchors. The maximum strain at failure was 0.0097. The CFRP anchors allowed the CFRP sheet to reach fracture and prevented the CFRP strip delamination failure.

Experimental studies by Orton (2007) and Kim (2008) indicated that the CFRP anchors had to be inserted at least 2 inches into the core of the concrete specimen to prevent concrete cover separation. The tests showed that a total cross-section area of the CFRP anchor should be two times greater than that of the CFRP sheet to develop rupture of the sheet.



(a) Beam without CFRP anchors



(b) Beam with CFRP anchors

Figure 2.8 Use of anchors for flexural strengthening (Kim et al. 2006)

In addition, surface preparation was unimportant when the CFRP sheets were well anchored. Quality control of the materials was indispensable for successful CFRP anchor installation.

2.3.2 CFRP anchor detail

A CFRP anchor consists of two parts. One is a roll of CFRP material that is inserted into the concrete hole and the other is a 6 inch long CFRP fan that is placed over the CFRP sheet. In this experimental study, the CFRP anchor details were based on the recommendations of Kobayashi (2001). Figure 2.9 shows the fan of the CFRP anchor detail for the installation. As can be seen in the figure, a 6 inch long CFRP anchor fan was splayed out over the CFRP sheet with 60 degree fan angle. The inserted CFRP anchor portion was 4 in. long. The area of anchor hole was 40 % larger than the anchor area (Kim, 2008). In order to facilitate installation, a large enough anchor hole should be used so that the anchor can be inserted easily. On the other hand, too large an anchor hole could lead to pull out failure of the CFRP anchor and other quality control problems. To reduce stress concentration of the CFRP anchor, ACI 440.2R recommends a radius of 0.5 inch of hole chamfer.

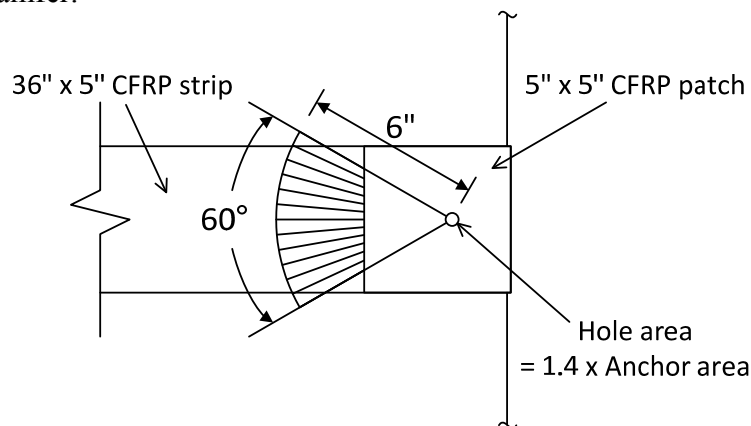


Figure 2.9 CFRP anchor detail

Figure 2.10 illustrates the CFRP anchor installation used by Kim (2011) on the panel specimen. To distribute stresses from the CFRP strip to the anchor, two 5 inch square CFRP patches were applied on the strip. CFRP anchor failure before the CFRP strip rupture could be prevented by the installation of the patches (Kobayashi, 2001). The first patch was applied on the CFRP strip with fibers perpendicular to the main CFRP strip fibers. After the CFRP anchor installation, the second patch was installed covering a portion of the anchor fan and with fibers oriented parallel to those of the CFRP strip.

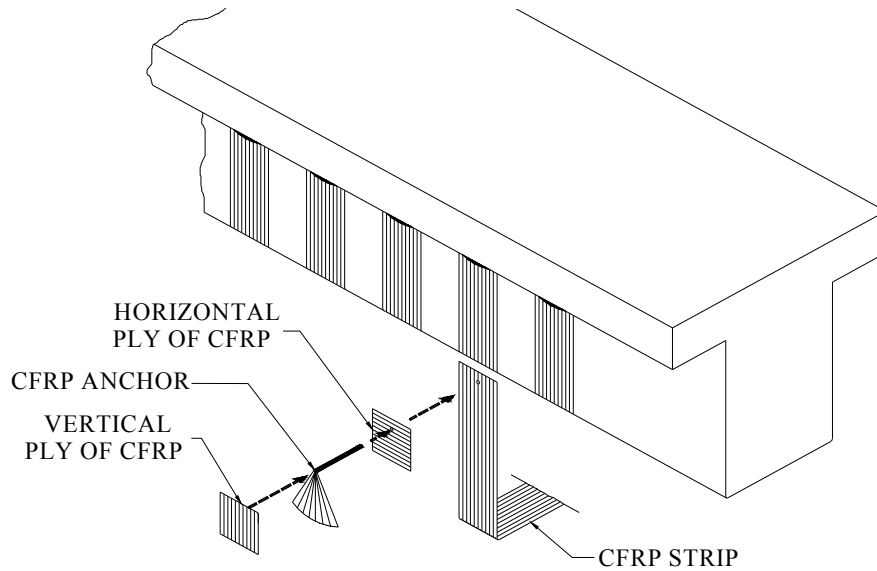


Figure 2.10 Isometric view of U-wrap with CFRP anchorage system (Kim, 2011)

2.4 PANEL TESTS

2.4.1 Specimen details

Small-scale panel tests were successfully conducted at the Ferguson Structural Engineering Laboratory to investigate the effects of bi-directional steel reinforcements of bottle-shaped strut. Based on these tests, panels seemed to be an ideal way to assess the behavior of bi-directional CFRP strengthening of compression struts.

In order to examine the behavior of bottle-shaped struts, 26 concrete panels as shown in Figure 2.11 were tested to failure (Brown, 2005). The typical specimen size was 36 x 36x 6 in. and 12 x 6 x 2 in. steel bearing plates were installed. The amount of steel reinforcement was calculated based on the variables. Five basic reinforcement layouts were considered for the experimental study.

- Unreinforced: To evaluate the contribution of the concrete alone, four plain concrete panels were tested.

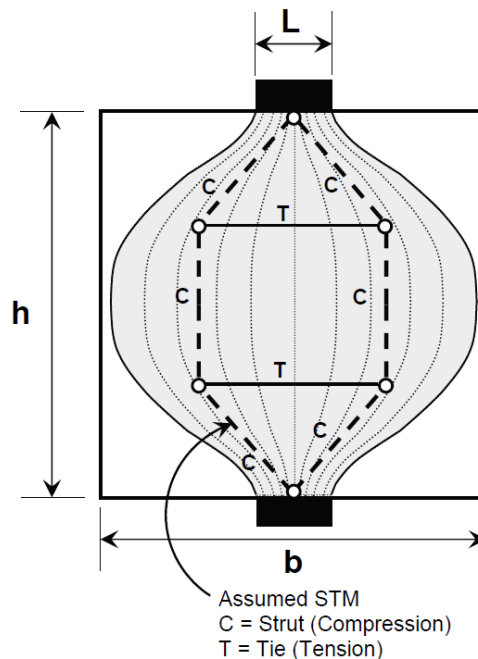


Figure 2.11 Bottle-shaped strut and associated strut-and-tie model (Brown, 2005)

- Orthogonal mats: The second series of the panels were reinforced with two different orthogonal mats of steel. The reinforcements consisted of # 2 and # 3 deformed bars. In addition, the effect of the bar mat angle was investigated using rotated orientation.
- Uni-directional mats: Next series of panels were reinforced with uni-directional bars. The reinforcement was either uniformly distributed or concentrated at locations of maximum tensile stress.
- Panel width: To determine effects of the panel width, 36 inch and 60 inch width panels were constructed and tested.
- Panel thickness: Typical panels had 6 inch thickness. In addition, two specimens with 10 inch thickness were considered in this category.

The panel specimens were tested under a monotonically increasing load using a universal testing machine (UTM). A thin layer of hydrostone was applied to provide uniform stress distribution under the bearing plates and a spherical head was placed on the bearing plate to eliminate load eccentricities.

2.4.2 Observations

The failure of the panel tests was caused by concrete crushing of the strut around the node. The panel test results indicated that the load when a splitting crack forms is not affected by the reinforcement in the panel; which is in agreement with general reinforced concrete behavior. Based on the panel specimen test results, deep beam tests were performed to obtain similar data (Brown, 2005). With such data, specimen behavior in more complex members could be compared to the simplified tests.

CHAPTER 3 EXPERIMENTAL STUDY

3.1 TEST SPECIMENS

3.1.1 General

The different types of panels and their design considerations will be described. Then, test setups and instrumentation will be introduced. The last section of this chapter describes the mechanical properties of concrete, CFRP, and steel used.

A total of 27 panels from five different concrete batches were constructed and tested to develop an understanding of the strengthening effectiveness of bi-directional CFRP layouts. All the panels were constructed and tested at the Ferguson Structural Engineering Laboratory at the University of Texas at Austin.

The following key parameters were studied:

- CFRP strip inclination, relative to crack orientation
- Uni- versus bi-directional CFRP layout
- With/without anchors in the CFRP strips
- Amount of steel reinforcement in panel
- Concrete strength of panel

The web thickness of prestressed concrete I-beams typically varies from 6 inches to 8 inches. The main objective of this study was to evaluate the effect of CFRP materials used to strengthen a web subjected to shear. Therefore, a 6 inch panel thickness was considered in this study to minimize the concrete contribution to shear and to magnify the effect of reinforcement-steel stirrups or CFRP strips.

The plain concrete panels had dimensions of $36 \times 36 \times 6$ in. Compressive load was applied on the concrete panel through $12 \times 6 \times 1$ in. steel plates. To provide uniform load distribution between the steel plate and the panel surface, hydrostone was placed at the concrete-steel plate interface.

Table 3.1 Test specimen variables

Concrete strength	Steel Reinforcement	CFRP layout	CFRP strip inclination	Notation
Normal strength	None	Non-reinforced	n/a	C0-0-0-5
		Uni-direction	0°	U5-0-0-5
			30°	U5-30-0-5
			45°	U5-45-0-5
			60°	U5-60-0-5
		Bi-direction	0°, 90°	B5-0-0-5
			45°	B5-45-0-5
			30°, 60°	B5-60-0-5
		Fully wrapped In both directions	0°, 90°	B36-0-0-5-0an
	0°, 90°		B36-0-0-5-4an	
	0°, 90°		B36-0-0-5-6an	
	Rebar mat	Non-reinforced	n/a	C0-0-2-5
		Uni-direction	0°	U5-0-1-5
			0°	U5-0-2-5
			30°	U5-30-2-5
45°			U5-45-2-5	
60°			U5-60-2-5	
Bi-direction		0°, 90°	B5-0-2-5	
		45°	B5-45-2-5	
		30°, 60°	B5-60-2-5	
High strength	None	Non-reinforced	n/a	C0-0-0-11
		Bi-direction	0°, 90°	B5-0-0-11
			45°	B5-45-0-11
			30°, 60°	B5-60-0-11

3.1.2 Design Considerations

Nomenclature for the specimens is shown in Figure 3.1. Terms in the nomenclature are separated by dashes. The first term represents the layout of the CFRP strips and the number indicates CFRP strip width. The second term represents the angle of CFRP strips measured from a horizontal axis. The third term is for the amount of steel reinforcement, with 0 indicating plain concrete panels. A reinforcing bar mat consisted of 5-#3 rebars in the horizontal direction. The last term is the nominal concrete strength. The first series of specimens consisted of 4 panels from the same concrete batch. At the outset of the experimental program, 2 layers of 18 inch by 18 inch CFRP patches were applied on the loading and bearing areas in an orthogonal direction as can be seen in Figure 3.2(a) to prevent local concrete failure at the loading and reaction areas. However, as shown in Figure 3.2(b), it was found that the CFRP patches could not confine the concrete sufficiently to prevent local crushing before the capacity of the panel was reached. Therefore, two pairs of 18 by 6 by 1 in. steel plates shown in Figure 3.3 were

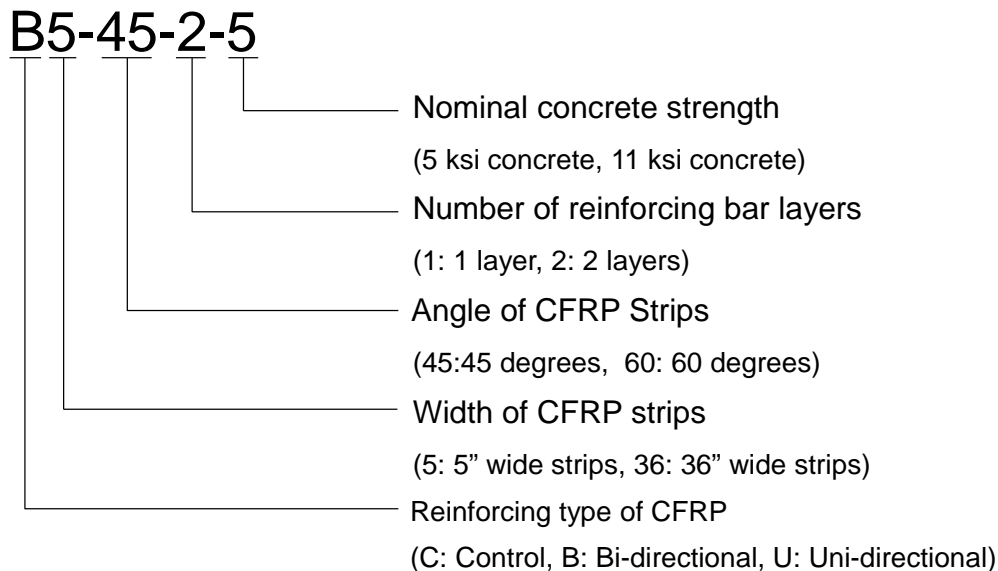
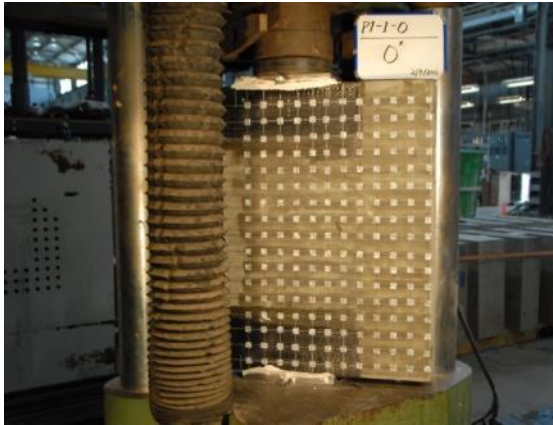


Figure 3.1 Notation for the panels



(a) Panel with CFRP



(b) Funnel-shaped concrete crushing

Figure 3.2 Loading region of panels with CFRP confinement

installed at the top and bottom of the panels to provide confinement of the concrete in the critical loading regions. Bolts through the panels were torqued to improve confinement of the loading region. Hydrostone was applied between the concrete and the steel plates to provide uniform confinement when the bolts were tightened.



(a) Steel plates



(b) Steel plates on the panel

Figure 3.3 Panels with steel plates

3.1.2.1 Uni-directional CFRP strip inclination

Diagonal cracks in the shear span of a reinforced concrete beam can be seen in Figure 3.4. As seen here, the diagonal cracks form at various angles. Various orientations of the diagonal cracks can be simulated by the varying CFRP strip inclinations.

Uni-directional CFRP strip inclinations of 0, 30, 45, and 60 degrees from the horizontal as shown in Figure 3.5 were installed. Subsequently, the same inclinations were applied to a bi-directional CFRP layout (Figure 3.6).



(a) Unreinforced I-beam

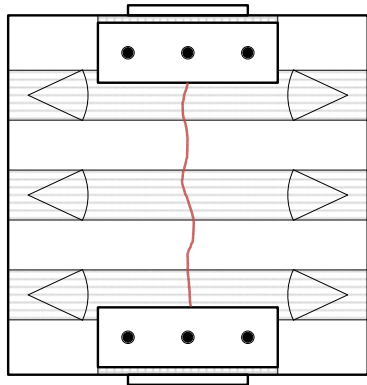


(b) Example of uni-directional CFRP layout

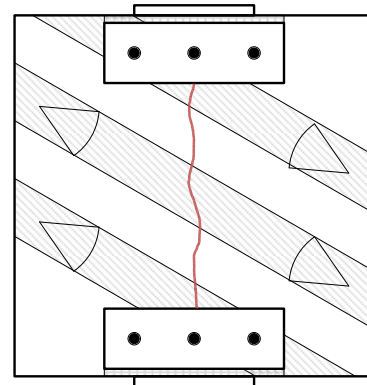


(c) Example of bi-directional CFRP layout

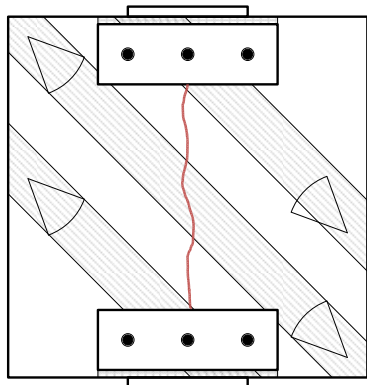
Figure 3.4 Diagonal cracks of I-beam (Picture from Kim 2011)



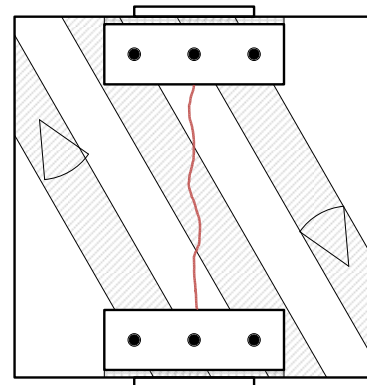
(a) CFRP strips at 0° degrees
U5-0-0-5



(b) CFRP strips at 30° degrees
U5-30-0-5



(c) CFRP strips at 45° degrees
U5-45-0-5



(d) CFRP strips at 60° degrees
U5-60-0-5

Figure 3.5 Various CFRP strip inclinations for the uni-directional CFRP layout

3.1.2.2 Bi-directional CFRP strip inclination

Three bi-directional CFRP strip layouts are shown in Figure 3.6. All the inclinations are based on the horizontal line. The seven test specimens permit evaluation of uni- versus bi-directional layouts, as well as the influence of the inclination of the CFRP strips relative to the critical crack. A CFRP strip width of 5 in. was used for all the specimens and the spacing of the strips was 10 inches, center to center. CFRP anchors were installed on each strip to prevent CFRP failure when strip delamination occurred.

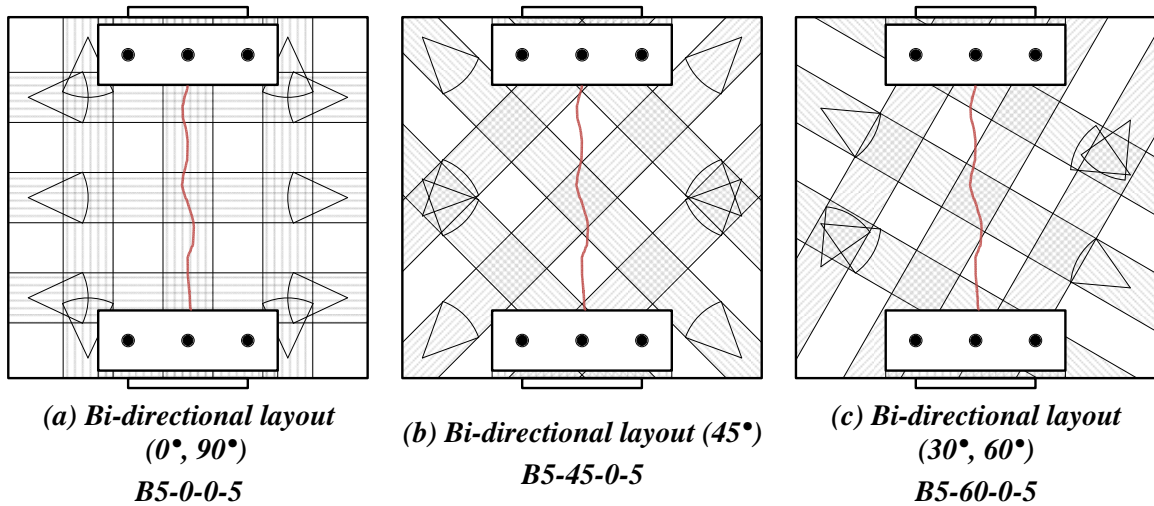


Figure 3.6 CFRP reinforced panels

3.1.2.3 Amount of CFRP

The shear capacity of the I-girder that was reinforced with a fully wrapped CFRP layout was similar to that of the bi-directional CFRP strip layout (Figure 2.4). As can be seen in Figure 3.7, three panels were designed to simulate these layouts. CFRP strips with a 0.02 in. thickness, a 5 in. width, and a 5 in. clear space between were used for all the panels. One panel was reinforced with uni-directional CFRP strips (Figure 3.7(a)). The second panel had a bi-directional layout as shown in Figure 3.7(b). The third panel had full CFRP sheets applied in both directions. First, a 36 in. \times 36 in. vertical sheet was applied front and back of the panel. Then a horizontal CFRP strip that was 36 inches wide and 90 inches long was installed over the vertical strips. The horizontal strip overlapped 6 inches on one edge of the panel. By using a continuous strip in the horizontal direction, CFRP delamination was not expected to load to failure.

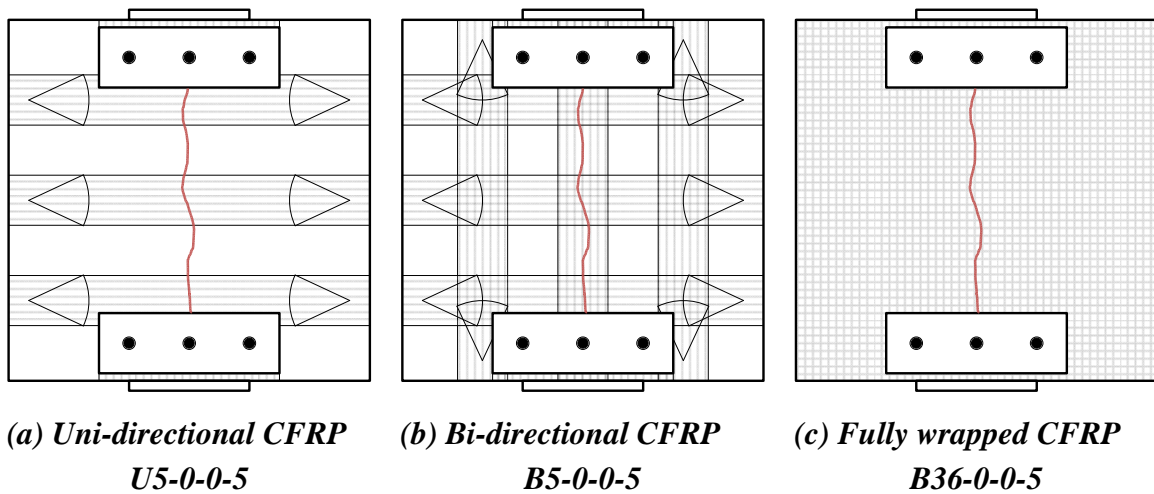


Figure 3.7 Variation of CFRP amount

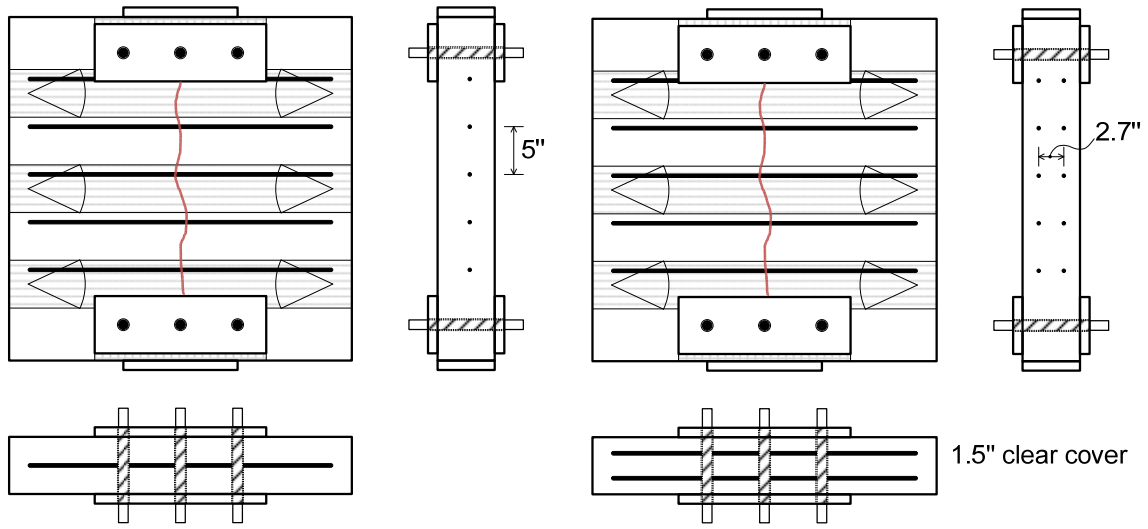
3.1.2.4 Amount of steel reinforcement

Another variable was the amount of steel reinforcement crossing the critical crack. To evaluate the effect of steel reinforcement, two panels were constructed with bars in the horizontal direction as shown in Figure 3.8. The CFRP strips were installed in a horizontal direction as in Figure 3.7(a). Figure 3.8(a) shows 1 layer of bars and Figure 3.8(b) shows 2 layers of bars. Spacing of the bars was 5 inches. The panel reinforced with a uni-directional CFRP strip layout (Figure 3.7(a)) in horizontal direction is the control test (no bars) for these specimens.

Table 3.2 shows calculated stiffness of the reinforcing materials. The stiffness was calculated using EA/L , and the effective length of material (L) was assumed to be identical. The stiffness of the horizontal reinforcement of U5-0-2-5 is 4 times that of the uni-directional CFRP strip without bar layers.

Table 3.2 Stiffness comparison

	CFRP strip (Figure 3.7(a))	Steel reinforcement (with Uni-directional CFRP)	
		1 layer (Figure 3.8(a))	2 layers (Figure 3.8(b))
Elastic Modulus (ksi)	15,600	33,300	33,300
Total Area (in ²)	0.6	0.55	1.1
Stiffness	9,400	18,300	36,600



(a) 1 layer stirrup, U5-0-1-5

(b) 2 layers stirrup, U5-0-2-5

Figure 3.8 Variation of #3 stirrup

3.1.2.5 CFRP anchors

As can be seen in Figure 3.9, CFRP anchors were added to evaluate the effect of distance between anchors. Anchor details are described in Appendix B. Bi-directional CFRP sheet layouts were the same as in Figure 3.7(c). The horizontal CFRP strips were overlapped side of the specimen to provide a continuous wrap. The intermediate anchors reduce the distance over which debonding can occur and should improve the stiffness of the CFRP sheets. The behavior with intermediate anchors will be compared with the behavior of a fully-wrapped panel (B36-0-0-5, Figure 3.7(c)).

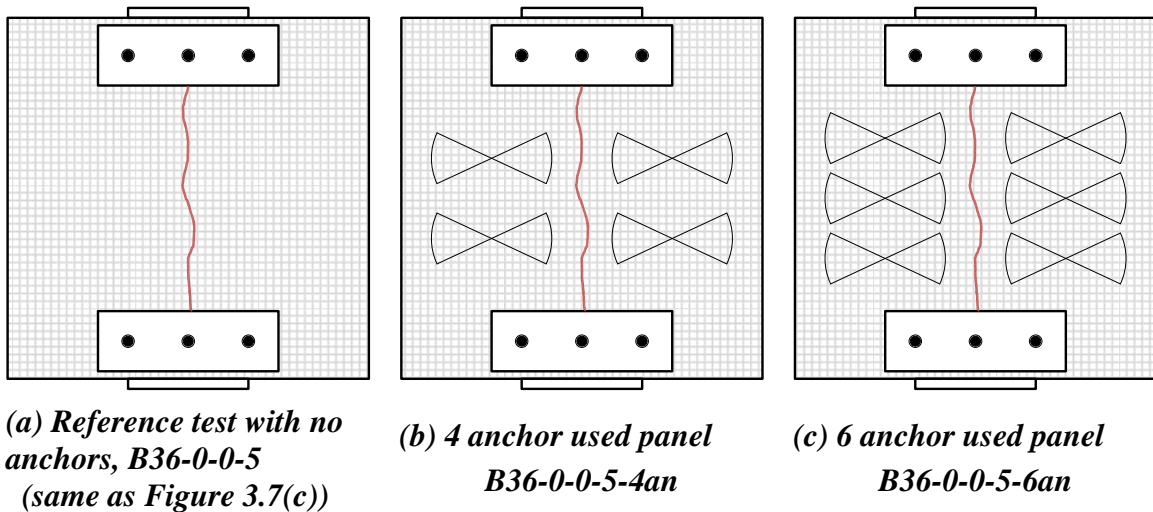


Figure 3.9 Different number of CFRP anchors

3.1.2.6 Concrete strength

The purpose of this test series was to study the effect of CFRP strengthening on panels with high strength concrete. Four out of twenty seven panels were constructed with 11.5 ksi strength concrete. Figure 3.10 shows CFRP layouts for the high strength concrete panels. The bi-directionally reinforced panel behavior will be compared with C0-0-0-11, and with the same CFRP layout, and 5 ksi concrete strength.

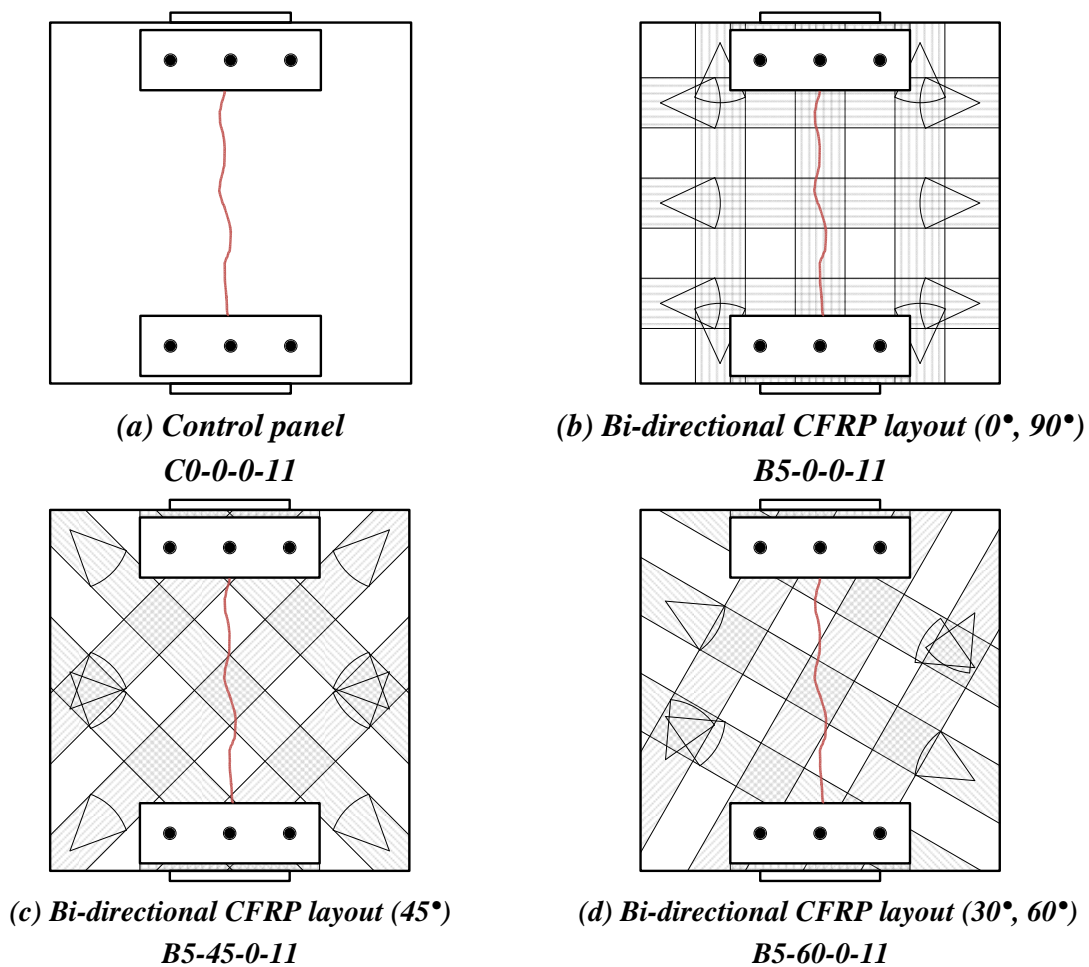


Figure 3.10 CFRP layouts for the high strength (11.5 ksi) concrete

3.2 TEST SETUP AND INSTRUMENTS

3.2.1 Universal Testing Machine (UTM)

Load was applied to the 3 ft. by 3 ft. panels using a universal testing machine (UTM) or a ram. A steel bearing plate (12 by 6 by 1 in.) was placed on the panel. For uniform load distribution between the steel plate and the panel surface, hydrostone was placed at the concrete-steel plate interface. In addition to the bearing plates, a spherical head was placed between the steel plate and loading head to assure concentric loading of the panel.

Eight panels were tested in a 600 kips capacity UTM shown in Figure 3.11. The highest maximum load applied on the panels was about 570 kips which was close to the UTM capacity. The entire panel surface cannot be seen with this test set up because of narrow opening of the UTM. These drawbacks led to the use of another test apparatus.



Figure 3.11 600 kips Universal Testing Machine (UTM)

Figure 3.12(a), this test frame was used for the remainder of the panels. In the test frame, a 400 ton (882 kips) capacity hydraulic cylinder (Figure 3.12(b)) was placed as shown in Figure 3.12(a). A 1000 kips load cell (Figure 3.12(d)) was placed between a spherical head (Figure 3.12(c)) and the hydraulic cylinder.



(a) Test frame



(b) Hydraulic cylinder



(c) Spherical head



(d) 1,000 kips load cell

Figure 3.12 Testing frame

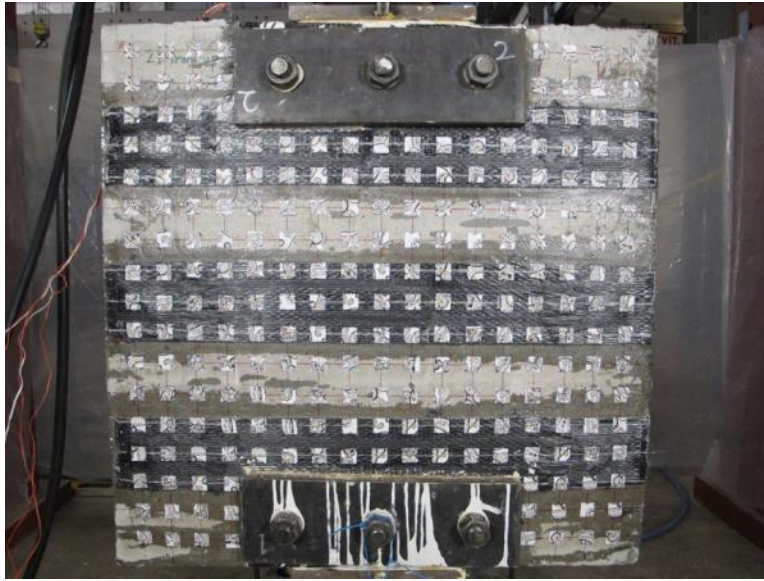
3.2.2 UT vision system

3.2.2.1 Overview of system

In order to determine the characteristics of the load transfer mechanism from CFRP strips to CFRP anchors, strains need to be measured along the strip between anchors. While strain gages affixed on the surface of CFRP can produce reliable strain measurements, they are impractical to use for obtaining a complete surface-strain profile due to cost and installation time considerations. Recently, Digital Image Correlation (DIC) systems were introduced in structural engineering to measure surface deformations (Choi, Cheung, Kim, & Ahn, 2011; Helfrick, Niezrecki, Avitabile, & Schmidt, 2011; Jurjo, Magluta, Roitman, & Gonçalves, 2010; Lee & Shinozuka, 2006; Olaszek, 1999; Stephen, Brownjohn, & Taylor, 1993; Wahbeh, Caffrey, & Masri, 2006).

In some cases, speckled paint patterns are used to a specimen surface for the DIC system to track movements. In others, targets that offer high contrast patterns are affixed on the surface of specimens. Digital cameras are used to capture successive images during testing, from which movement of targets are extracted.

The UT Vision System (UTVS), a high-resolution DIC system developed at the Ferguson Structural Engineering Laboratory, was used in this study to record the movements of targets affixed on the surface of panels as shown in Figure 3.13(a). The DIC system allows tracking of the movements of as many targets as can be fit on a specimen. The system can therefore monitor the progression of the complete surface-strain profile of a specimen throughout a test.



(a) Paper targets on the specimen surface



(b) Camera used by the UTVS



(c) UTVS computer

Figure 3.13 UT Vision system (UTVS)

The UTVS was developed to allow surface-strain measurement of full-scale structural systems and members. The system is able to resolve surface strains on the order of 10^{-4} over a field of view of 8 ft and a gage length of 2.5 in. (63 mm). Similar strain resolutions were achieved in this study but for a much smaller gage length of approximately 2 in.

3.2.2.2 *UTVS Hardware and software*

The UTVS hardware consists of a high-resolution camera (Proscilica GE4900, Figure 3.13(b)) connected to a computer. The main properties of the camera are shown in Table 3.3. In the case of the panel tests, only one camera was used since only in-plane deformations were expected. The computer triggers frame-grabbing and records coordinates of the targets (Figure 3.13(c)). Once the camera is connected to the computer and ready to grab an image, the computer software issues a command to capture the subsequent images simultaneously. The network router can be connected to a Data Acquisition system (DAQ) such that frame numbers can be sent to the DAQ. This feature allows the UTVS data to be synchronized with DAQ data in post-processing. LabVIEW (National Instruments) software is used to grab and synchronize frame numbers and pictures. Matlab (Mathworks) is used to calibrate and process the target data.

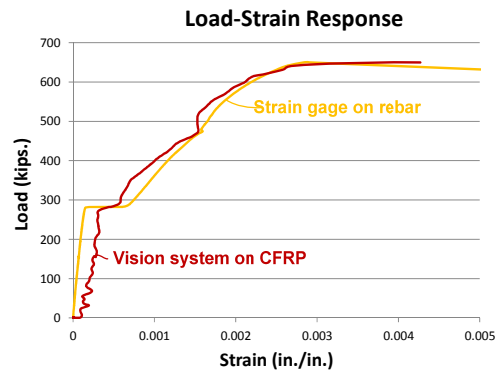
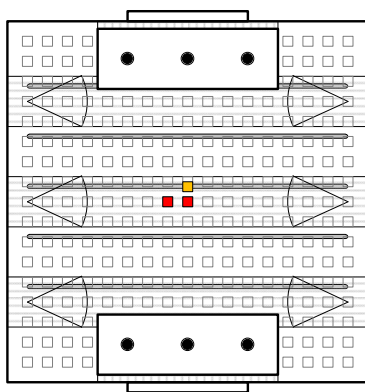
Table 3.3 Camera properties

Sensor Size, H x V (mm)	36.1 x 24.0
Pixels (H x V)	4872 x 3248
Maximum Frame Rate (fps)	3
Pixel Size, H x V (μm)	7.4 x 7.4
Image Type	Grayscale, 8 bit, raw format

Figure 3.14 shows a comparison of strains determined using the vision system and steel strain gage readings. The load strain plots of other specimens are shown in Appendix D. As can be seen in Figure 3.14(a), there are two locations represented by red and yellow colors. The red squares indicate the location of the two surface targets used to obtain the surface strain using the vision system. Selected targets were close to the location of the strain gage on the bar (yellow square). A vertical crack formed adjacent to steel gage and between the surface targets used in the comparison.

Despite the difference in the curves before cracking load, the overall load-strain responses were nearly identical for both measuring systems during the test. The results showed the surface strains acquired using the vision system were comparable to the steel strain gage readings. Thus, surface strain measurements at cracks provided a reasonable estimate of internal steel strains.

Figure 3.15 shows 11 layers of targets used to obtain average horizontal strains over the clear height of panels. In Chapter 4, applied load values and average horizontal strains are used to examine the specimen behavior.



(a) Location of strain measurement (b) Load-Strain response

Figure 3.14 Strain comparison plot for specimen U5-0-2-5

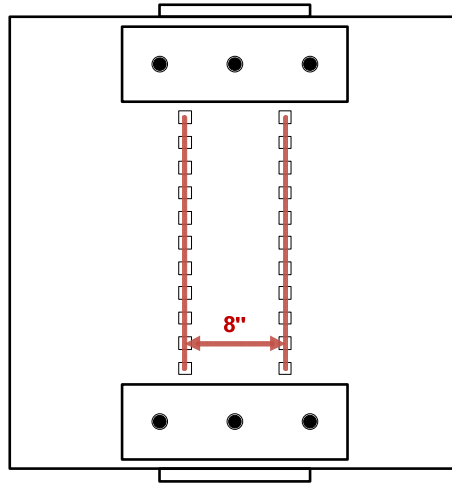


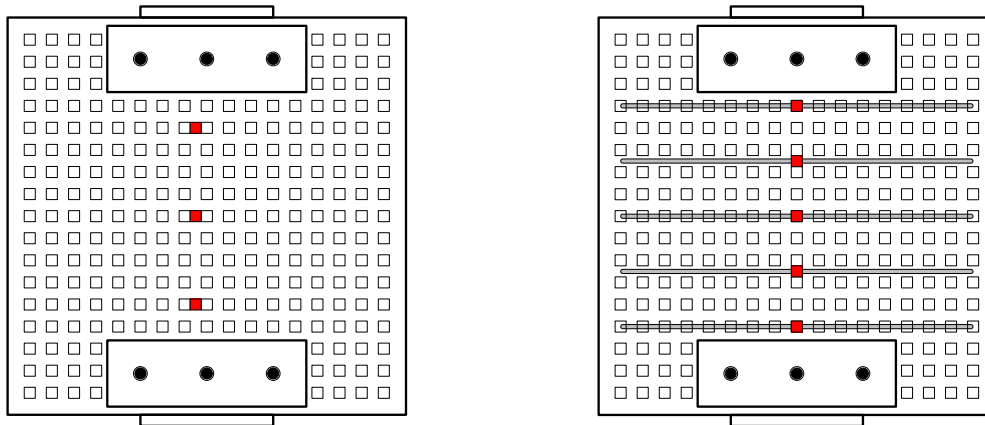
Figure 3.15 Locations of targets used to estimate the average horizontal strain over panel height

3.2.3 Strain gage

In the first several panel tests, strain gages were attached on the concrete surfaces and the CFRP strips to compare the strain readings between the strain gage and vision system. Figure 3.17(a) shows the location of the concrete strain gages (red squares) on a control panel surface. All the strain gages were on the concrete surfaces. Gage locations for panels with steel bars are shown in Figure 3.17(b). A strain gage used on the bars is shown in Figure 3.16. This strain gage is for general purpose use and has 3% maximum elongation capacity.



Figure 3.16 Steel strain gage



(a) plain concrete panel

(b) steel reinforced panel

Figure 3.17 Locations of the strain gages

3.3 MATERIAL PROPERTIES

3.3.1 Concrete

Two different concrete compressive strengths (5 and 11 ksi) were designed to evaluate the effect of the concrete strength on the CFRP behavior. Concrete cylinders (4 × 8 in.) were cast from all concrete batches. The cylinders were tested in accordance with

ASTM C39 “Standard Test Method for Compressive Strength of Cylindrical Concrete Specimens”.

Average concrete compressive strength versus age can be seen in Figure 3.18 and Figure 3.19. The average 28 day compressive strengths were 5,370 psi and 11,450 psi. Table 3.4 shows the cylinder test results.

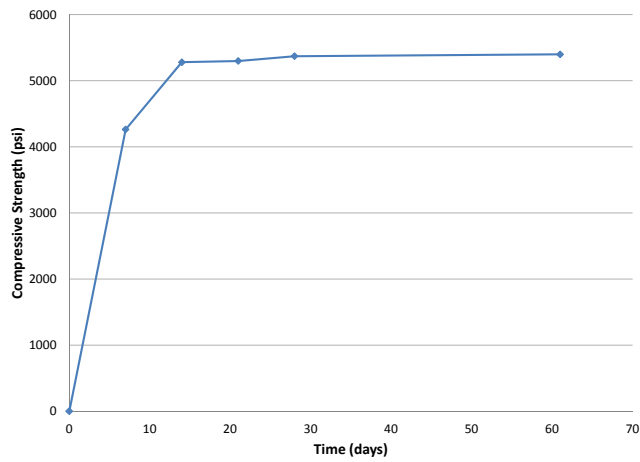


Figure 3.18 Concrete compressive strength from cylinder tests (5,000 psi)

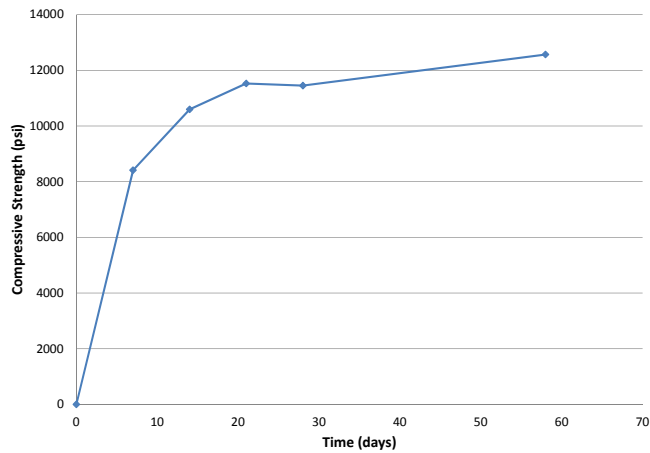


Figure 3.19 Concrete compressive strength from cylinder tests (11,000 psi)

Table 3.4 Cylinder test results

Cylinder Test	Average concrete strength (psi)	
	5,000 psi	11,000 psi
7 day	4,260	8,410
14 day	5,280	10,600
21 day	5,300	11,530
28 day	5,370	11,450
Test day	5,400	12,570

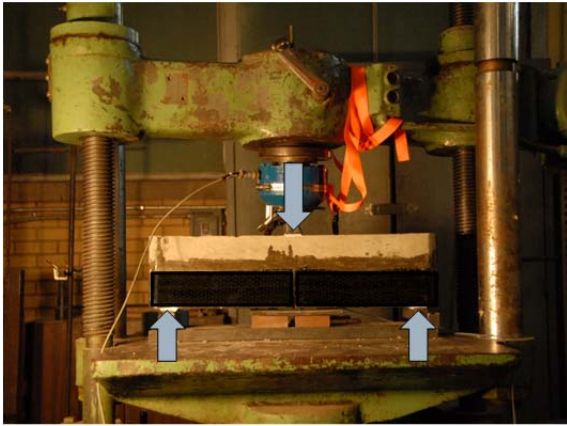
3.3.2 CFRP

Tyfo[®] SCH 11-UP CFRP material was used in the study. Material properties of Tyfo[®] SCH 11-UP composite from FYFE Co. LLC can be seen in Table 3.5. Tyfo[®] S Epoxy was used as the adhesive. The properties of the CFRP were determined using ASTM D-3039.

Small beams tested at the beginning of this research project were used to develop stress-strain response of the CFRP laminate. Figure 3.20(a) shows the test setup for the small beams. The dimensions of the small beam were 6 inches by 6 inches by 24 inches and a CFRP strip was installed at the bottom of the specimen. Strain gages were installed at the center of the CFRP strip to measure CFRP strip strain. Specimens that failed by CFRP rupture were chosen for the CFRP material calculation. Stress-strain response was calculated using applied load on the beam and strain recording from the gages. Figure 3.21(a) shows overall stress-strain responses of the CFRP strips. Elastic modulus of the CFRP strips was calculated using the responses after cracking to eliminate the concrete contribution to the capacity before cracking (Figure 3.21(b)).

Table 3.5 Material properties of Tyfo[®] SCH 11-UP composite

Property	Manufacturer's provided typical test values	Test Result of small beams
Typical Dry Fiber		
Tensile Strength	550,000 psi	
Tensile Modulus	33.4 x 10 ⁶ psi	
Ultimate Elongation	1.7 %	
Composite Gross Laminate		
Tensile Strength	143,000 psi	150,000 psi
Tensile Modulus	15.3 x 10 ⁶ psi	15.6 x 10 ⁶ psi
Ultimate Elongation	0.93 %	0.96 %

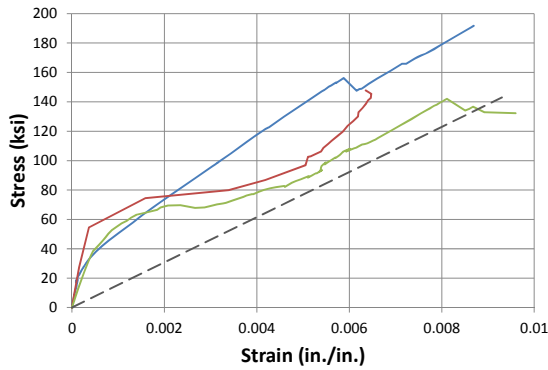


(a) Test setup

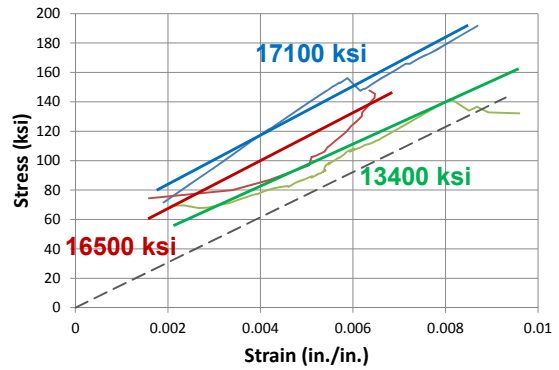


(b) CFRP strip rupture

Figure 3.20 Small beam test for the CFRP material properties



(a) Overall test results



(b) Test results after concrete cracking

Figure 3.21 Stress-strain responses for calculation of CFRP material properties

3.3.3 Steel

Tension tests were conducted to determine the properties of the steel rebars. ASTM A615 Grade 60 No. 3 bars were used for the panels. The test setup for the bars

can be seen in Figure 3.22(a). Figure 3.22(b) shows a strain gage that was installed on the bar. Stress-strain response for the bar tests is shown in Figure 3.23. A 0.2 % offset method was used for this material test since the stress-strain curves did not exhibit a distinct yield plateau. From the tests, the average yield stress of the bars was 80 ksi.



(a) Test setup



(b) Strain gage on the bar

Figure 3.22 #3 bar tension test

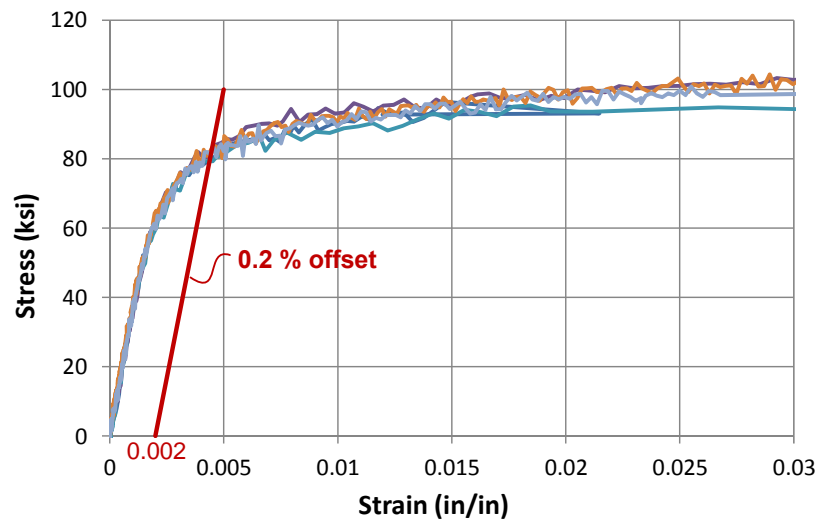


Figure 3.23 Stress-strain response of #3 bars

CHAPTER 4 ANALYSIS OF THE TEST RESULTS

4.1 OVERVIEW OF THE TEST RESULTS

A total of 27 panels were tested. Table 4.1 shows a summary of test results of all the panels. Cracking and maximum loads, as well as the percentage increase in the maximum load relative to the maximum load of the comparable control panel are shown in the table.

A typical specimen failure was triggered by crushing of the compressive strut between the loading and reaction bearing plates, which led to large horizontal deformations and vertical cracking along panel centerline. As mentioned in the section 3.1.2, the bearing regions of the first few specimens (indicated with a * in Table 4.1) were only reinforced with CFRP patches and experienced funnel-shaped concrete crushing at those regions. Subsequent panels were reinforced with two pairs of steel plates to prevent local concrete crushing.

Test results are evaluated in terms of the load capacity and the deformation of the panels in the horizontal direction (splitting strains). Average horizontal strains determined from the vision system as described in Section 3.2.2 were selected as a primary criterion for examining the panel behavior. In cases of premature failure, such as when CFRP anchors failed or in cases where failure occurred near the loading plates due to poor confinement, initial stiffness and cracking loads could only be used to assess specimen behavior. In the first few tests, strain gages were applied on the concrete surface of test specimens to validate the strain measurements obtained from the vision system. In subsequent tests, only the vision system was used to measure surface strains. In this Chapter, panel tests are categorized in six different groups to evaluate the effects

of CFRP strengthening with respect to: 1), 2) inclination of CFRP from principle crack in uni- and bi-directional CFRP layouts, 3) effect of CFRP layout, 4) effect of amount of reinforcing materials, 5) load contribution of CFRP strips and steel reinforcement, 6) effect of concrete strength.

Table 4.1 Test result summary

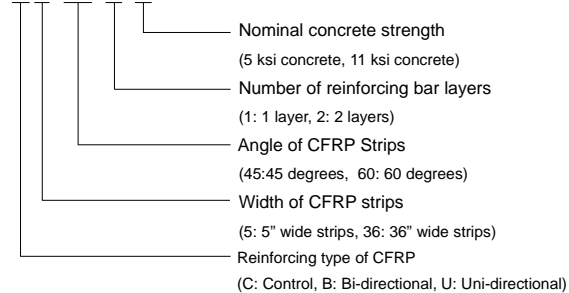
Specimen	Cracking load (kips)	Maximum load (kips)	Increment from control specimen	
			kips	%
C0-0-0-4*	226	363	0	0
B24-0-0-4-I*	236	413	50	14
B24-0-0-4-II*	224	365	2	0
B36-0-0-4*	161	404	41	11
C0-0-0-5	220	364	0	0
U5-0-0-5	201	486	122	34
U5-30-0-5	198	472	108	30
U5-45-0-5	202	448	84	23
U5-60-0-5	204	474	110	30
B5-0-0-5	232	475	111	31
B5-45-0-5**	210	431	67	18
B5-60-0-5**	227	462	98	27
B36-0-0-5-0an	289	540	176	48
B36-0-0-5-4an	290	572	208	57
B36-0-0-5-6an	284	563	199	55
C0-0-2-5	269	590	0	0
U5-0-1-5	274	635	45	8
U5-0-2-5	275	650	60	10
U5-30-2-5	265	588	-2	0
U5-45-2-5	292	626	36	6
U5-60-2-5	263	566	-24	-4
B5-45-2-5	309	656	66	11
B5-60-2-5	310	629	39	7
C0-0-0-11	298	617	0	0
B5-0-0-11*	328	595	-22	-4
B5-45-0-11	381	749	132	21
B5-60-0-11	405	733	116	19

Bold: Control panel

*: Unconfined bearing area (No steel plates)

** : Anchor failure

B5-45-2-5



4.2 CONTROL PANEL RESULTS

4.2.1 Comparison between the two 5 ksi control specimens (with and without steel)

The load versus average horizontal strain responses for C0-0-0-5 (without steel reinforcement) and C0-0-2-5 (with two layers of steel reinforcement) are shown in Figure 4.1 and Figure 4.2, respectively. As can be seen in these plots, the panel behavior before the cracking was almost identical. However, in the case of C0-0-0-5, a large strain increase was observed after cracking and the strain reading was 0.0075 when the peak load was reached. Higher stiffness can be observed in C0-0-2-5 right after cracking due to the steel reinforcement. The peak load of C0-0-2-5 was about 590 kips at an average horizontal strain was 0.0034. Four load levels (1~4 in the plots) were chosen for the strain contour: 1-before the cracking, 2-after the cracking, 3-increased load after the cracking, 4-before the peak load was reached.

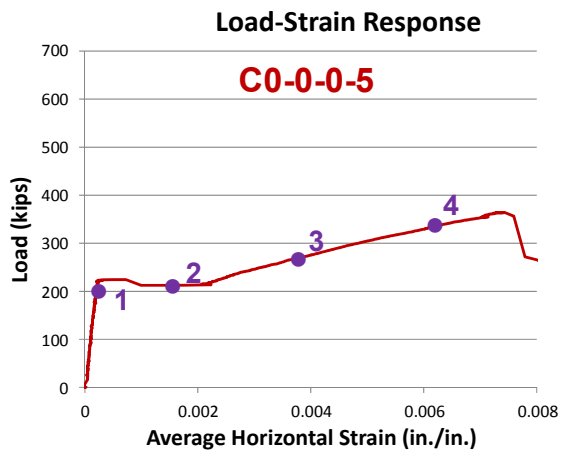


Figure 4.1 C0-0-0-5 (without bars)

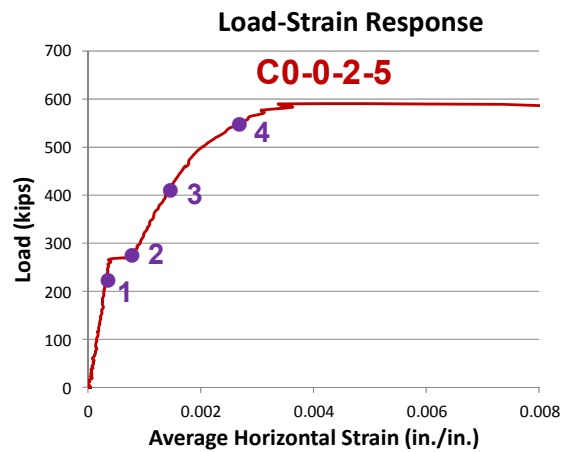


Figure 4.2 C0-0-2-5 (with bars)

Figure 4.4 and Figure 4.5 show the strain contours at four different load levels for C0-0-0-5 and C0-0-2-5, respectively. Strain scales can be seen to the right of the contours and the values vary from 0 to 0.006. The orientation of the strain contour is in the horizontal direction. Notable change of strain cannot be seen before the cracking in both control panels. In Figure 4.4, the vertical crack formed in C0-0-0-5 when a load of 212 kips was reached. Subsequent strain increments were localized in this initial crack location. A narrow band of high strains indicates a crack that opened wider as the test progressed. A wider strain distribution and lower strain readings were exhibited in C0-0-2-5 at all load levels (Figure 4.5). Steel reinforcement controlled the crack width in C0-0-2-5

In Figure 4.3, the loads on the control panels are compared. The cracking and the maximum loads with reinforcement were increased by 22 % (49 kips) and 62 % (226 kips) compared to that of the plain concrete specimen (C0-0-0-5).

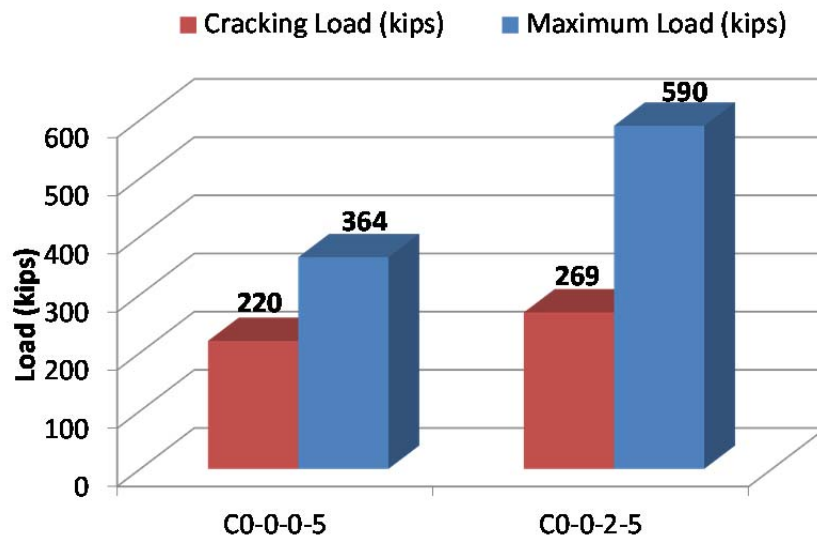
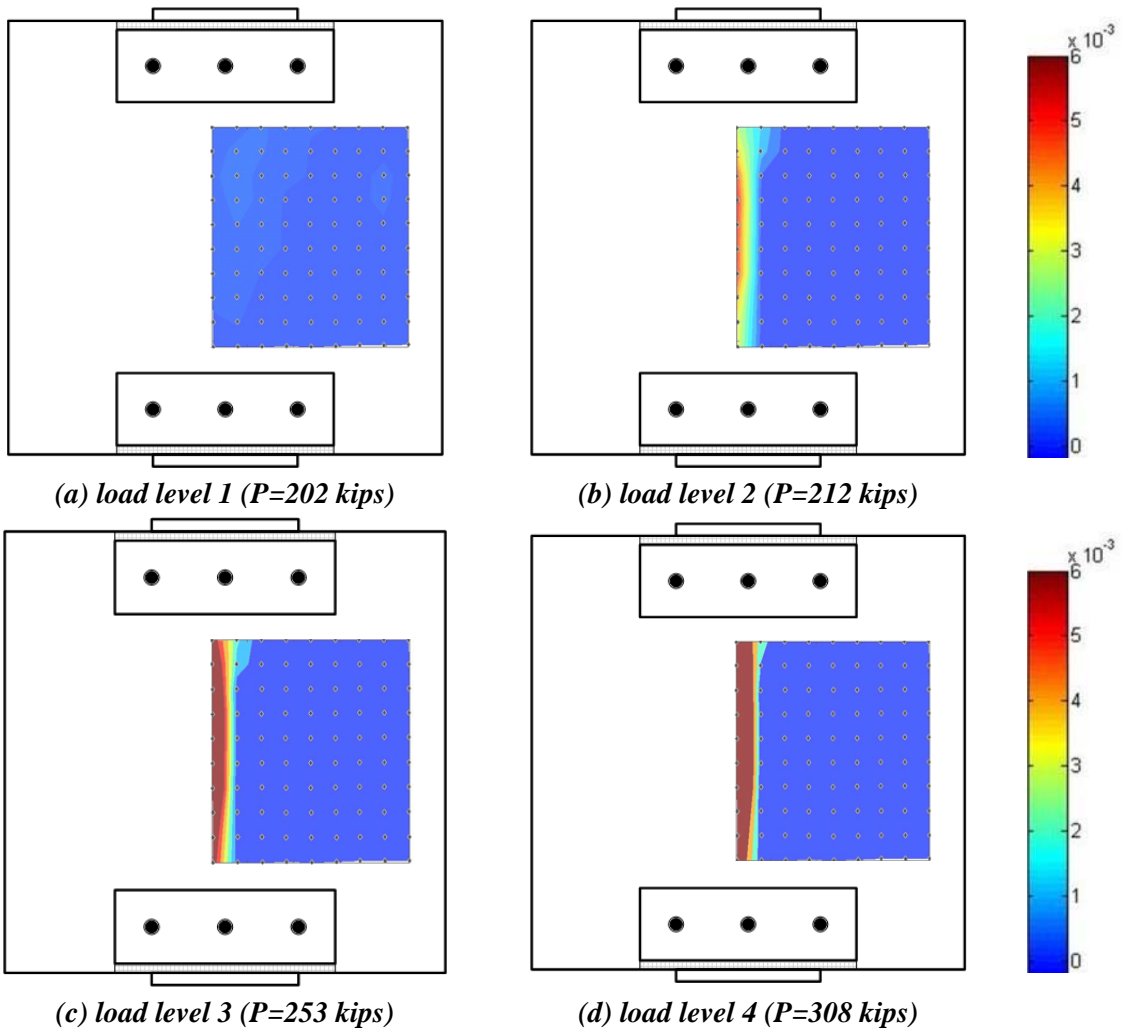


Figure 4.3 Load comparison between control specimens



Note: Only a portion of the surface was monitored because of sight limitations for UTVS in UTM

Figure 4.4 Horizontal strain contours for C0-0-0-5

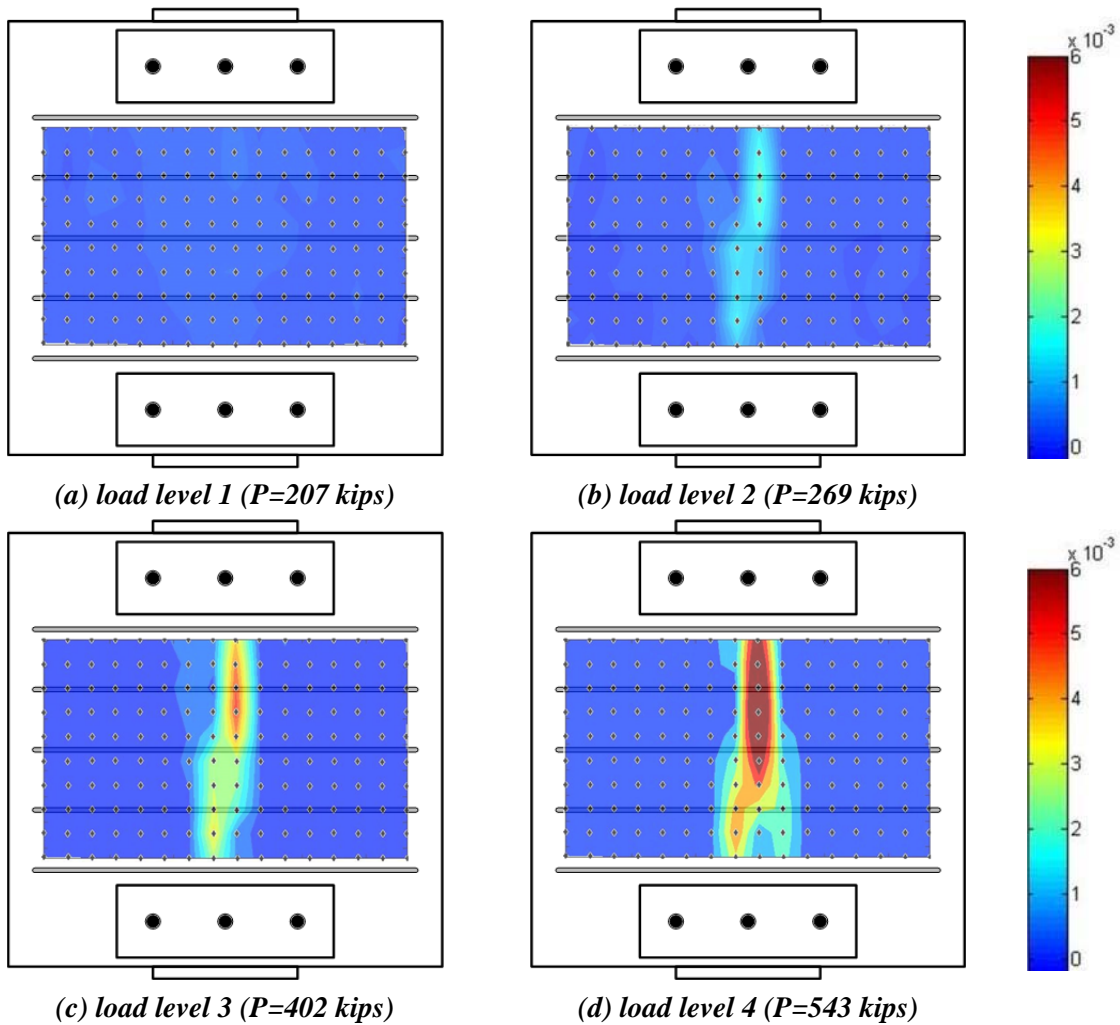


Figure 4.5 Horizontal strain contours for C0-0-2-5

4.2.2 Control panel cracking and failure mode

4.2.2.1 Control test for panels without steel reinforcement (5 ksi concrete)

Figure 4.6 shows the control panel in the test setup (no CFRP strips) and the steel plates installed to prevent localized concrete crushing. Figure 4.7 shows main vertical cracks on the panel surface after the test. The cracking load was about 220 kips and the maximum load was 364 kips. One wide crack was observed after cracking and the panel

separated into three parts after the maximum load was reached. A funnel-shaped concrete, wedge formed at the top bearing plate end can be seen in this specimen after the steel plates were removed.



Figure 4.6 C0-0-0-5 panel in the universal testing machine, UTM



Figure 4.7 Failure mode of specimen C0-0-0-5

4.2.2.2 Control test for panels without steel reinforcement (11 ksi concrete)

Figure 4.8 shows the control specimen for the concrete panels with 11 ksi concrete. The cracking load was about 300 kips, and no notable cracks could be seen until just before the maximum load of 617 kips was reached. The first vertical crack occurred at the center of the panel. As can be seen in Figure 4.9, a number of vertical cracks formed at the maximum load and the failure mode was brittle.



Figure 4.8 C0-0-0-11 Panel in the test frame



Figure 4.9 Failure mode of specimen C0-0-0-11

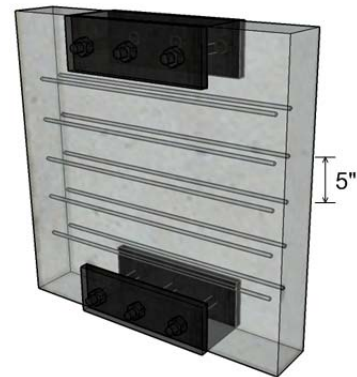
4.2.2.3 Control test for panels with steel reinforcement (5 ksi)

Figure 4.10(a) shows the control panel in the test frame. No CFRP strips were applied on this specimen. Figure 4.10(b) illustrates two layers of 5-#3 bars spaced at 5 in. vertically and 2.5 in. between the layers (from center to center).

Failure of the control specimen is shown in Figure 4.11(a) and (b). As shown in these figures, large concrete spalling of the cover over the bars can be seen on the front and back sides of the panel. The cracking load was about 270 kips and the maximum load was 590 kips.



(a) C0-0-2-5 specimen in the test setup



(b) 3D view of C0-0-2-5

Figure 4.10 Control panel, C0-0-2-5



(a) Concrete crushing of front side

(b) Concrete crushing of back side

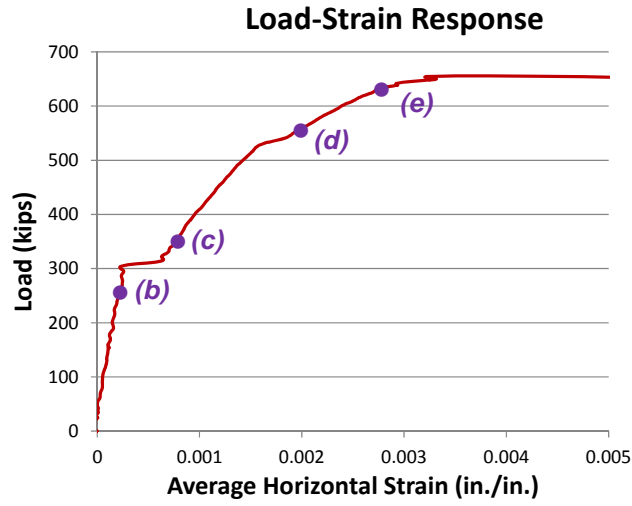
Figure 4.11 Failure mode of specimen C0-0-2-5

4.3 BEHAVIOR OF TYPICAL PANEL TEST

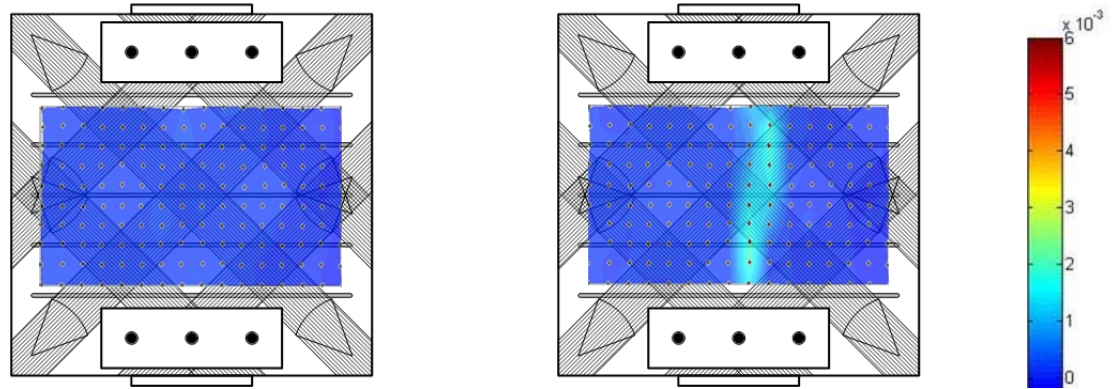
Figure 4.12 represents typical behavior of a panel that was reinforced with two layers of bars and strengthened with a 5 in wide bi-directional CFRP layout with 45 degree angle. The panel failed by concrete crushing between the CFRP strips. All of the strain plots represent average horizontal strains (Figure 4.12)

Figure 4.12(b) shows the strain contour before cracking (250 kips). Average horizontal strain was 0.0002 at this load level. In Figure 4.12(c), tension zone can be clearly seen after the cracking load. The tensile strain outlines the formation of a compressive strut. Strains were higher at the unreinforced concrete surface between CFRP strips (Figure 4.12(d)) and development of well-defined compressive strut is evident in the figure. The strain contour in Figure 4.12(e) was taken before the maximum applied load on the panel. At that load level, the average horizontal strain measured across a gage length of 8" over the height of the panel was 0.003 and localized large strains occurred at concrete-CFRP interface areas.

CFRP strengthened panels had similar strain distributions and progressions during tests. However, the locations of the widest cracks varied according to CFRP strip layout.

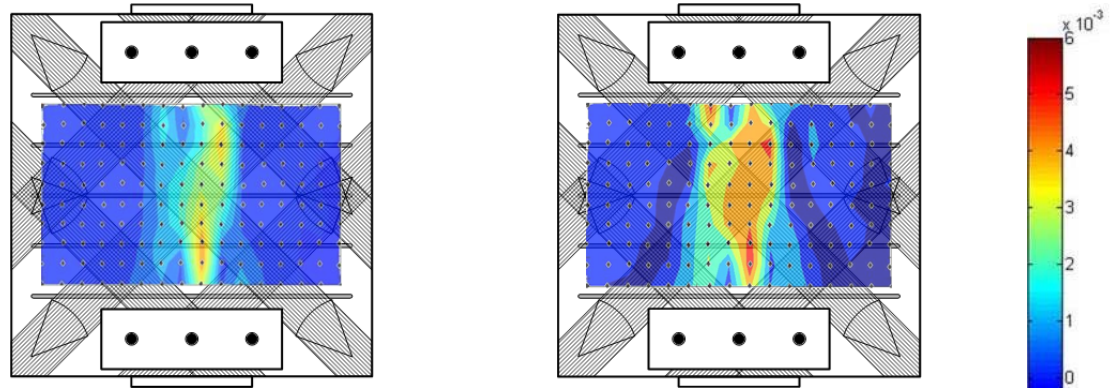


(a) Load-average horizontal strain response of B5-45-2-5



(b) Before cracking ($P=250$ kips)

(c) After cracking ($P=350$ kips)



(d) Between cracking and maximum loads
($P=550$ kips)

(e) Before the maximum load ($P=640$ kips)

Figure 4.12 Horizontal strain contours for typical panel (B5-45-2-5)

4.4 EFFECT OF CFRP STRIP INCLINATION

To evaluate the effects of the CFRP strip inclinations, two series of panels were considered: uni-directional CFRP layouts and bi-directional CFRP layouts.

4.4.1 Panels reinforced with uni-directional CFRP strips

4.4.1.1 Panels without steel reinforcement

The applied load on the panels is plotted against the average strain in the horizontal direction for the uni-directionally reinforced panels in Figure 4.13. The maximum recorded loads of all panels in this series were reached at an average horizontal strain of about 0.006. As can be seen in Figure 4.13, the initial stiffnesses of all the panels up to cracking and the cracking loads (200~220 kips) were almost identical. This observation indicates that, up to the cracking load, the CFRP strips and their inclination did not affect panel behavior significantly. After cracking of uni-directionally reinforced panels, stiffness varied in accordance with the inclination of CFRP strips. CFRP strips with low inclination angles with respect to horizontal exhibited slightly higher post-cracking peak loads and stiffnesses.

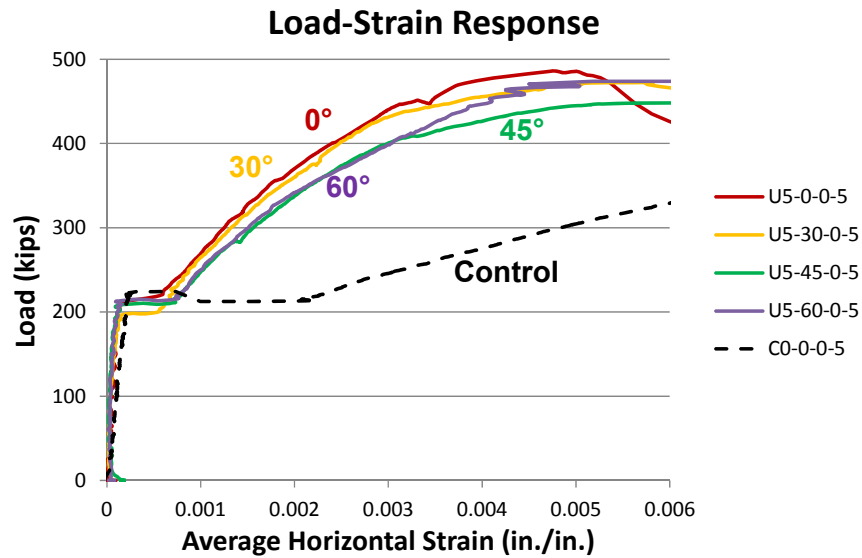
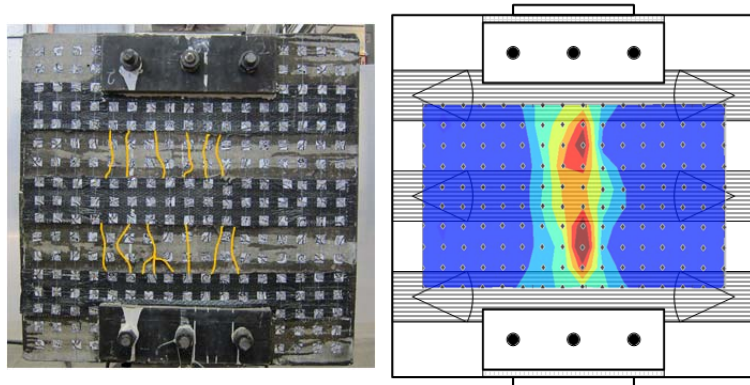


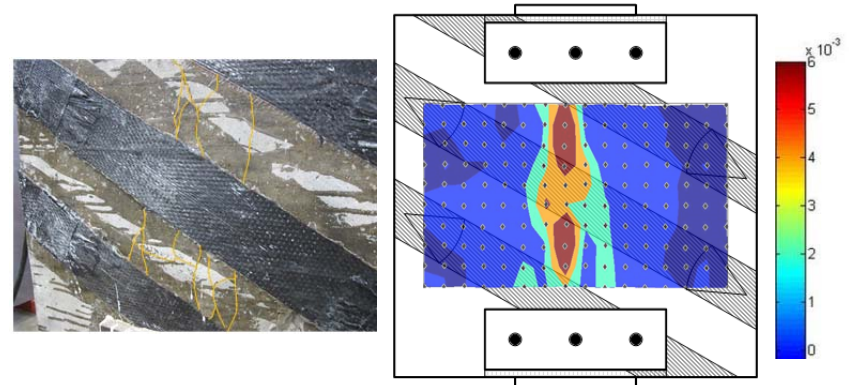
Figure 4.13 Load-strain responses for uni-directional CFRP strip layouts

Figure 4.14 shows horizontal strain contours for the panels reinforced with uni-directional CFRP strips. The strain scale is shown on the right side of each subplot in Figure 4.14. The scale varies from 0 to 0.006.

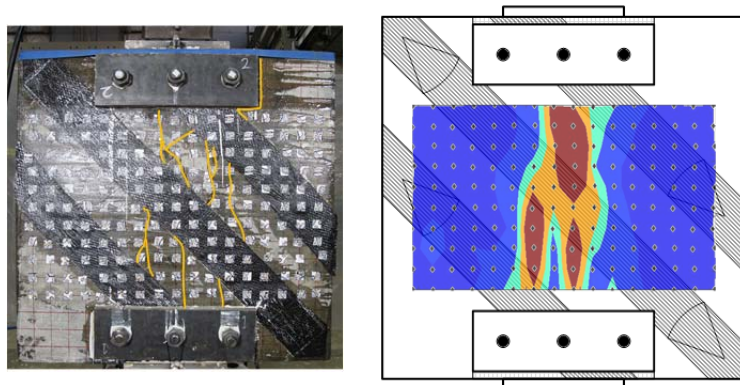
All the strain contours in Figure 4.14 were taken at the load of 447 kips that was the maximum load of specimen U5-45-0-5. As can be seen in these strain contours, large strains occurred at the locations of the unreinforced concrete surfaces (away from the CFRP). Red and dark red areas in the contour plots represent the regions of largest horizontal strains. These areas indicate concrete crushing between CFRP strips, which was corroborated visually as can be seen in Figure 4.15. Figure 4.14 indicates that CFRP strips crossing the principal cracks closer to perpendicular controlled strains more effectively, which resulted in smaller crack widths.



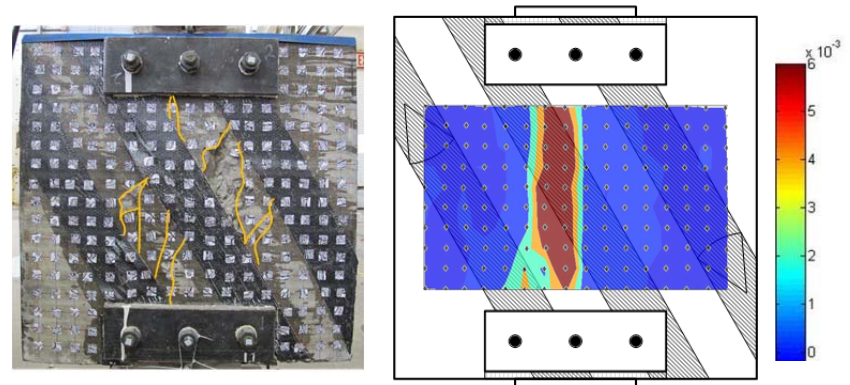
(a) U5-0-0-5 ($P=447$ kips)



(b) U5-30-0-5 ($P=447$ kips)



(c) U5-45-0-5 ($P=447$ kips)



(d) U5-60-0-5 ($P=447$ kips)

Figure 4.14 Horizontal strain contours for panels reinforced with uni-directional CFRP strips

The behavior of the U5-0-0-5 and the U5-30-0-5 specimens was nearly identical as indicated by the load-strain response (Figure 4.13) and the strain contours (Figure 4.14 (a) and (b)). However, the maximum strains in U5-0-0-5 were lower than those in U5-30-0-5. Large horizontal strains developed over the entire depth of the panel in U5-45-0-5 and U5-60-0-5. The difference between the strain contours in U5-0-0-5 and U5-60-0-5 is striking. The CFRP layout parallel to the direction of maximum strain was the most effective in improving panel strength and controlling cracking.

The maximum and cracking loads of the uni-directional CFRP reinforced panels are shown in Figure 4.16. The uni-directional CFRP layout did not significantly change cracking load regardless of the angle of inclination. The panel strength was substantially increased by the uni-directional CFRP layouts. The panel that was reinforced with the horizontal CFRP strips had the highest strength since CFRP fibers crossed the primary cracks in the same direction as the cracks opened, however, the difference in maximum loads was less than 10 %. The maximum loads of the strengthened specimens were 23 to 34 % (84 to 122 kips) greater than the control specimen.



(a) U5-0-0-5



(b) U5-30-0-5



(c) U5-45-0-5



(d) U5-60-0-5

Figure 4.15 Failure modes of panels reinforced with various CFRP inclinations

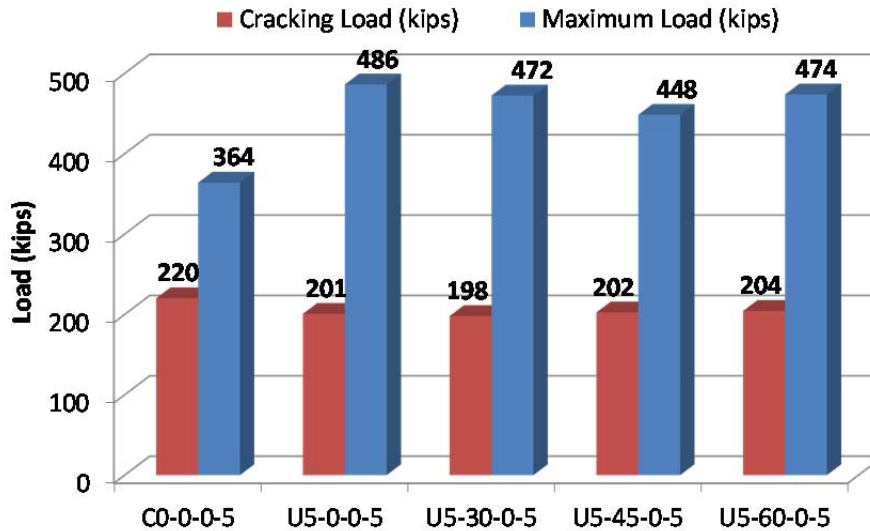


Figure 4.16 Load comparison of the specimens reinforced with uni-directional CFRP layouts, no reinforcement

4.4.1.2 Panels with steel reinforcement

The dashed curve in Figure 4.17 indicates the control panel test result. All panels were reinforced with 2-layers of bars. As can be seen in this figure, the cracking loads of the uni-directional CFRP reinforced panels were similar to each other but post-cracking stiffness was different. The green curve in Figure 4.17 for U5-60-2-5 indicates that the 60 degree uni-directional CFRP strip layout had little influence on behavior because it is nearly identical to C0-0-2-5. The average strains in the strips with lower inclination from horizontal were smaller at all load levels. U5-0-2-5 reached the highest load. In the case of panels with uni-directional CFRP layouts and steel reinforcement increases in maximum loads were much smaller (less than 10 %) than in the panels with no bars.

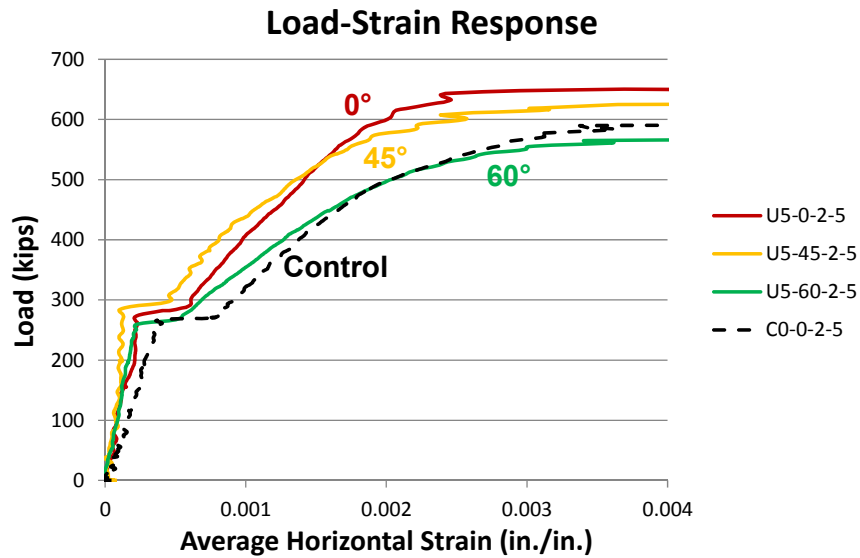
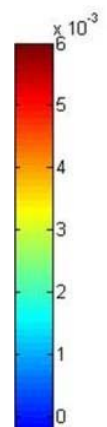
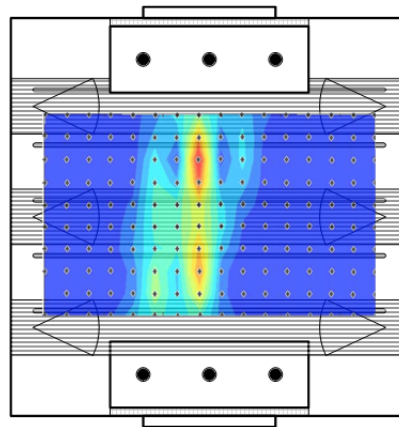
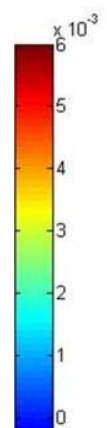
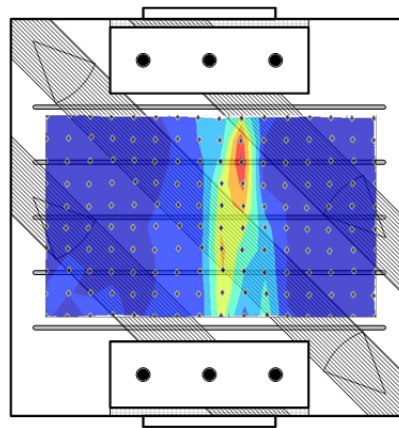


Figure 4.17 Load-strain responses for uni-directional CFRP strip layouts with reinforcement

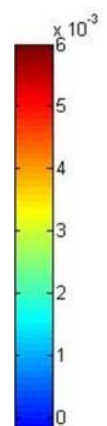
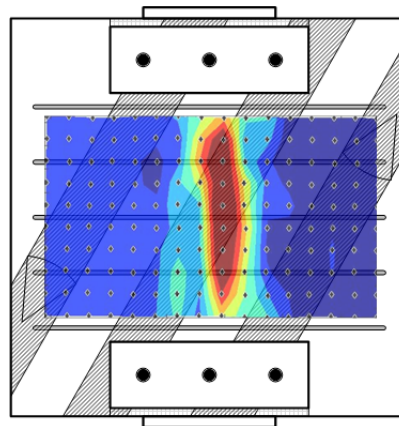
Figure 4.18 shows the strain contours of panel tests in this series. The peak load on U5-60-2-5 was 564 kips and all the strain contours were plotted at this load level. The difference in strain distribution between the U5-0-2-5 and U5-60-2-5 can be observed in Figure 4.18. The panel reinforced with horizontal CFRP strips (Figure 4.18(a)) exhibited lower strains but over a slightly wide area. U5-60-2-5 had large strains over the entire depth of the panel with most strains were higher than 0.006. The 60° inclination of CFRP strips resulted in wider crack opening and a lower maximum load. U5-45-2-5 exhibited strain distributions similar to those of U5-0-2-5. As shown in Figure 4.18(b), a peak strain of 0.005 was observed for the latter specimens in the regions ways from CFRP strips.



(a) U5-0-2-5 ($P=564$ kips)



(b) U5-45-2-5 ($P=564$ kips)



(c) U5-60-2-5 ($P=564$ kips)

Figure 4.18 Horizontal strain contours for panels reinforced with uni-directional CFRP strips and reinforcement

Figure 4.19 shows pictures of specimens highlighting the failure modes of the panels reinforced with uni-directional CFRP strips. U5-0-2-5 and U5-30-2-5 failed due to concrete crushing along the compressive strut, which resulted in CFRP strip rupture.

The cracking and maximum loads of U5-0-2-5 were 275 kips and 650 kips, respectively. The cracking load was increased slightly compared to the control specimen. The maximum load was increased by 10 % (60 kips) when horizontal CFRP strips were added. One vertical crack occurred at the peak load and large deformation after the maximum load led to the CFRP strip rupture. The strip rupture failure on the back side of the panel can be seen in Figure 4.19(a).



(a) U5-0-2-5



(b) U5-30-2-5



(c) U5-45-2-5



(d) U5-60-2-5

Figure 4.19 Failure modes of panels reinforced with various CFRP inclinations and steel reinforcement

U5-30-2-5 failed at a 588 kips. Despite the addition of CFRP strips, the maximum applied load was almost identical to that of the control panel. Figure 4.19(b) shows that a brittle concrete failure occurred between the CFRP strips.

Figure 4.20 shows maximum and cracking loads of the panels reinforced with uni-directional CFRP layouts. Difference between the cracking loads was less than 10 %. However, according to the CFRP strip inclination, the maximum loads varied between the panels. Panel U5-0-2-5 reached the highest load (650 kips) and U5-60-2-5 failed at a load below that of the control panel. The trend of decreasing maximum load with increasing strip inclination was similar to that in the panels without steel reinforcement.

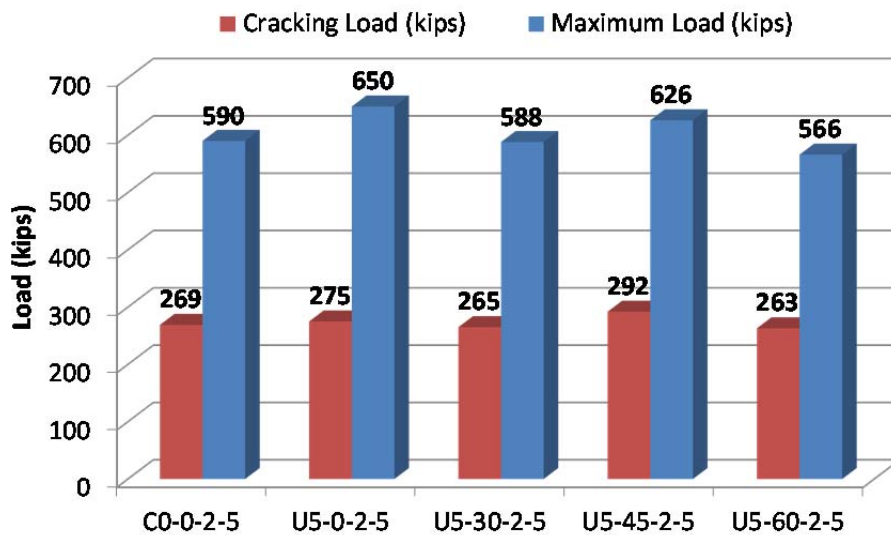


Figure 4.20 Load comparison of the uni-directional CFRP layout, panels with reinforcement

4.4.2 Panels reinforced with bi-directional CFRP strips

4.4.2.1 Panels without steel reinforcement ($f'_c=5$ ksi)

The initial stiffness of all the bi-directional CFRP strip reinforced panels up to cracking (200~220 kips) was almost identical as shown in Figure 4.21. This result indicates that up to the cracking load, the CFRP strips and their inclination did not affect the cracking load. First, it must be noted that B5-45-0-5 and B5-60-0-5 reached peak capacity when the CFRP anchors failed. Therefore, the test data from these two specimens could not be used to evaluate the effect of CFRP inclinations in bi-directional CFRP layout especially at higher load levels. Larger strains were recorded at the same load levels due to the CFRP anchor failure.

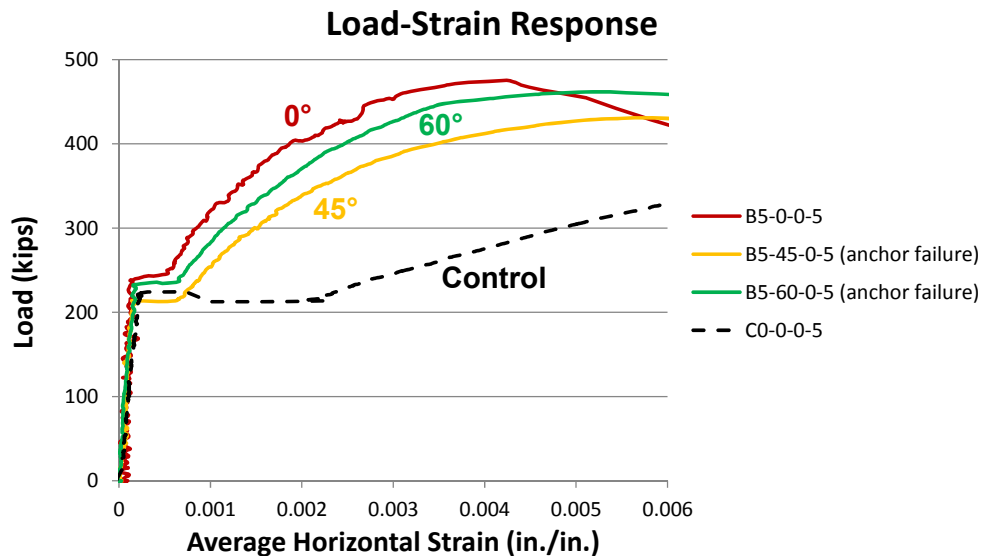
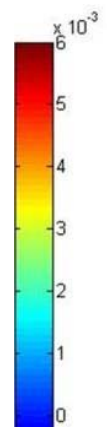
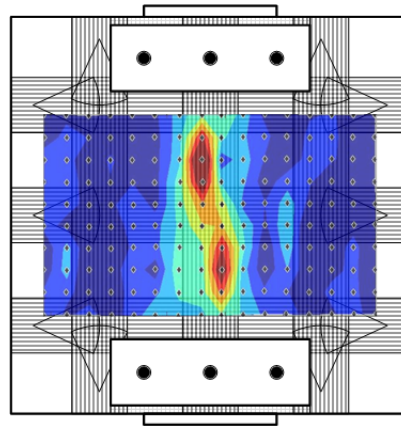


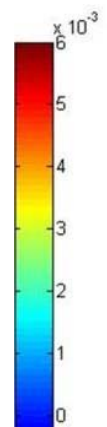
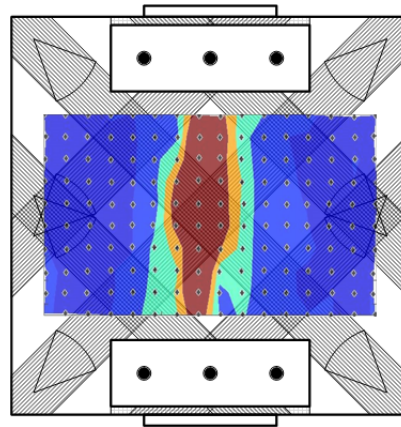
Figure 4.21 Load-strain responses for bi-directional CFRP strip layouts, $f'_c=5$ ksi

Strain contours in Figure 4.22 were plotted at a load of 430 kips that was the maximum load on B5-45-0-5. The strain contour for the entire concrete surface of the B5-60-0-5 could not be obtained due to irregular data from the vision system. A notable feature in the photographs of Figure 4.22 was the inclination of the cracks at failure. The layout of the CFRP strips in Figure 4.22(a) was the only symmetric pattern about the panel center line. The other specimens had an asymmetric pattern due to the CFRP strip layout and the early failure of the CFRP anchors. Unexpected CFRP anchor failures led to the lower maximum loads and early failure of the B5-45-0-5 and the B5-60-0-5 specimens. Due to the CFRP anchor failures, large strains in the horizontal direction could be observed as seen in Figure 4.22(b).

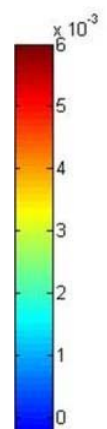
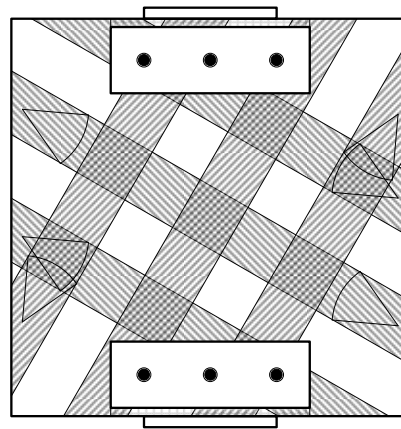
There were relatively small strains in B5-0-0-5 specimen at the load of 430 kips, which was the ultimate load of B5-45-0-5. The contours indicate that the CFRP strip layout was effective in distributing strains across the panel and over the depth of the panel.



(a) B5-0-0-5 ($P=430$ kips)



(b) B5-45-0-5 ($P=430$ kips)



(c) B5-60-0-5

Figure 4.22 Horizontal strain contours for panels reinforced with bi-directional CFRP strips

Figure 4.23 indicates the cracking and peak loads for the bi-directional layouts. The cracking loads were nearly the same for all panels. However, due to anchor failures, the strength of the panels could not be directly compared.

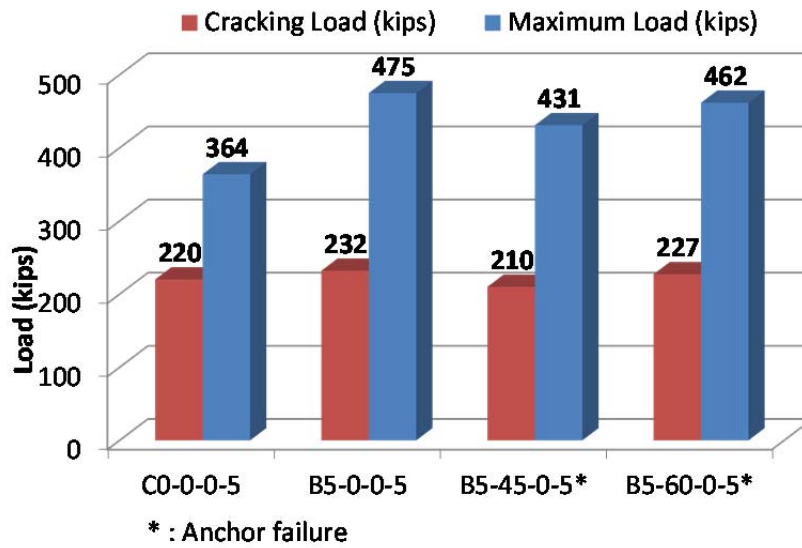


Figure 4.23 Load comparison of the bi-directional CFRP layout specimens ($f'_c=5$ ksi)

4.4.2.2 Panels without steel reinforcement ($f'_c = 11$ ksi)

In Figure 4.24, the main vertical cracks can be seen after the removal of the CFRP strips. As opposed to specimens with 5 ksi concrete, large regions of concrete spalling were not observed in the panels with 11 ksi concrete strength. Most of the cracks formed in the vertical direction between the loading and reaction areas. Rupture of the CFRP strips occurred when the peak load was reached. Figure 4.25 shows the cracking and maximum loads for the panels with high-strength concrete and bi-directional CFRP strip layouts. In the case of B5-0-0-11, the peak load was smaller than that of C0-0-0-11 panel because of poor confinement of the bearing area. In test B5-0-0-11, only two rods were used to pretension the steel plates and a premature bearing failure occurred. Omitting B5-0-0-11, the cracking load with biaxial CFRP strengthening was about 30 % higher than the control specimen and the maximum load was nearly 20 % greater than the control specimen. Strain contours could not be plotted from the vision system because of inexperienced system operation in the beginning of the experiments.



(a) B5-0-0-11



(b) B5-45-0-11



(c) B5-60-0-11

Figure 4.24 Failure mode of panels reinforced with different inclinations of bi-directional CFRP layouts ($f'_c=11$ ksi)

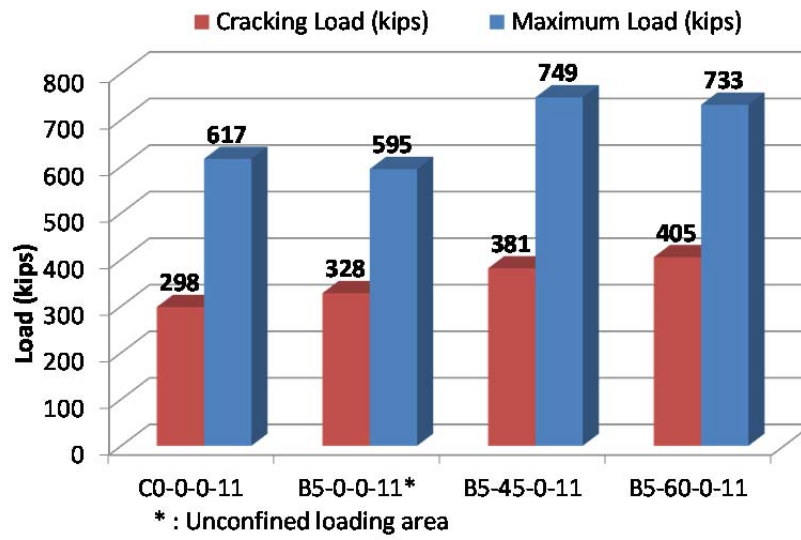


Figure 4.25 Load comparison of the bi-directional CFRP layout specimens ($f'_c=11$ ksi)

4.4.2.3 Panels with steel reinforcement

The dashed curves in Figure 4.26 indicate the response of the control panel reinforced with 2-layers of bars. The effect of the bi-directional CFRP strip inclination layout is shown in Figure 4.26. Test results of U5-0-0-5 and B5-0-0-5 showed ineffective load contribution of vertical CFRP strips (applied load orientation) to the panel strength (Figure 4.30). Therefore, U5-0-2-5 specimen test result was used to represent bi-directional CFRP layout in horizontal and vertical directions.

The cracking loads increased about 30 kips in the case of two inclined bi-directional layouts. The higher cracking loads may be due to the fact that with bi-directional layout. The amount of CFRP material crossing a vertical crack is greater than with horizontal strips. The bi-directional CFRP strip layout resulted in all panels reaching the same capacity regardless of the strip inclination. A relatively small variation in the average horizontal strain at the same loads can be observed with the bi-directional CFRP layouts.

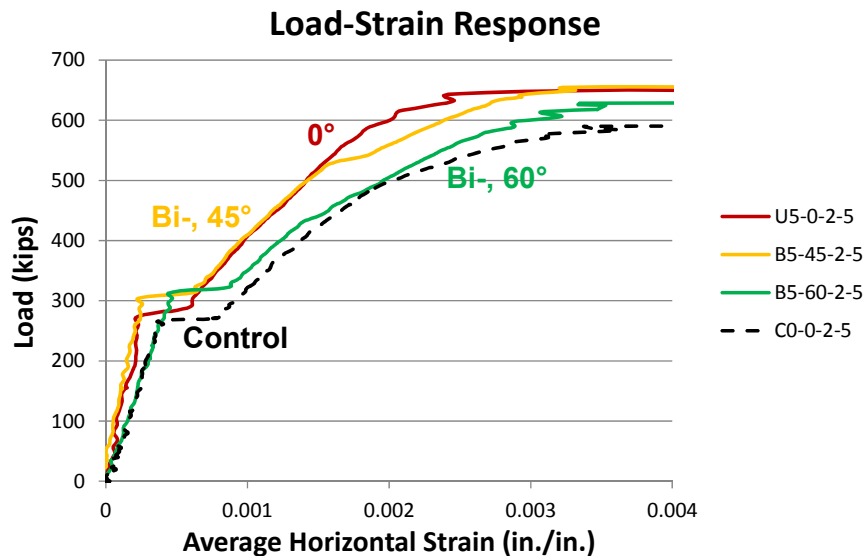
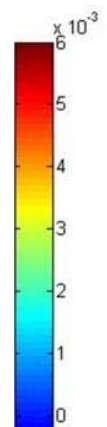
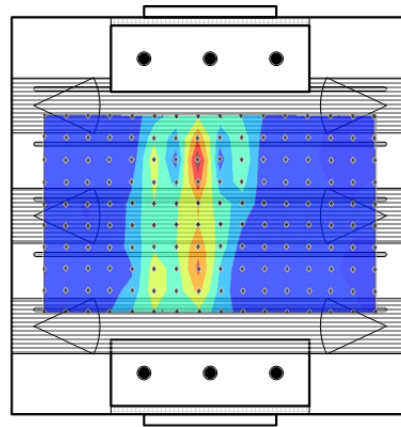


Figure 4.26 Load-Strain responses for bi-directional CFRP strips layouts with reinforcement

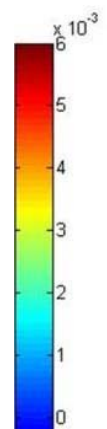
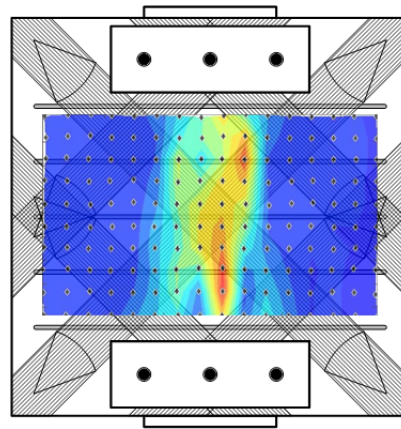
In Figure 4.27, the strain contours of the panels that were reinforced with the bi-directional CFRP layout are shown. Since the effects of the bi-directional CFRP strip layouts without steel reinforcement were influenced by anchor failure, this series of specimens provides important data regarding the effects of bi-directional CFRP layouts.

The lowest ultimate load was 628 kips for B5-60-2-5 specimen. The strain contours were taken at this load for the other specimens to compare the strain distribution at the same load level. There was a wide distribution of strains along the width of panel but the peak strains were moderate (0.004). The maximum tensile strains were observed between the CFRP strips.

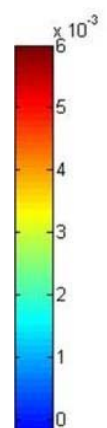
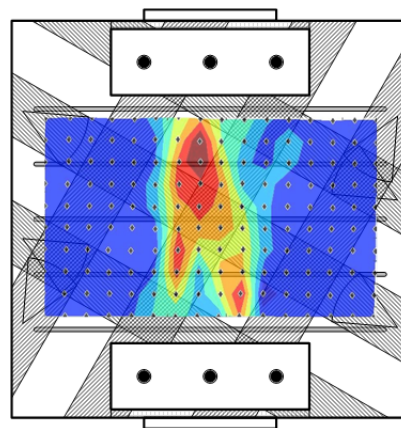
Strain distributions of U5-0-2-5 and B5-45-2-5 were similar. Figure 4.26 indicates that uniformly distributed strains can be obtained with bi-directional CFRP layouts and steel reinforcement. The peak load capacities were similar for all panels with bi-directional CFRP, however, larger strains could be seen in B5-60-2-5.



(a) U5-0-2-5 ($P=628$ kips)



(b) B5-45-2-5 ($P=628$ kips)



(c) B5-60-2-5 ($P=628$ kips)

Figure 4.27 Horizontal strain contours for panels reinforced with bi-directional CFRP strips and reinforcement

Figure 4.28 shows load comparisons for the bi-directionally strengthened panels. In the case of the bi-directional layout, the cracking load was increased more than 30 kips (15 %) compared to the control. Nearly equal maximum loads were reached in the bi-directional panels and indicates the panel strength is not dependent on the inclination of the bi-directional CFRP layout.

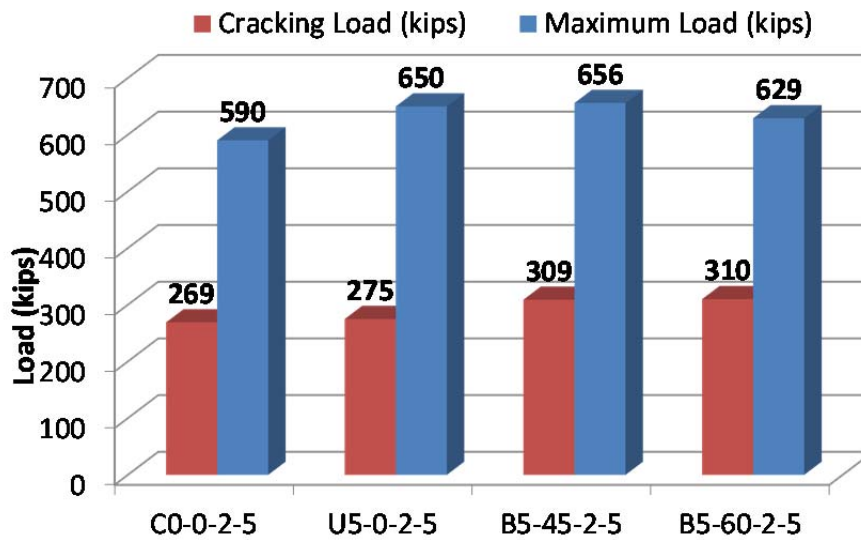


Figure 4.28 Load comparison of bi-directional CFRP layouts, panels with reinforcement

4.5 EFFECT OF CFRP LAYOUT

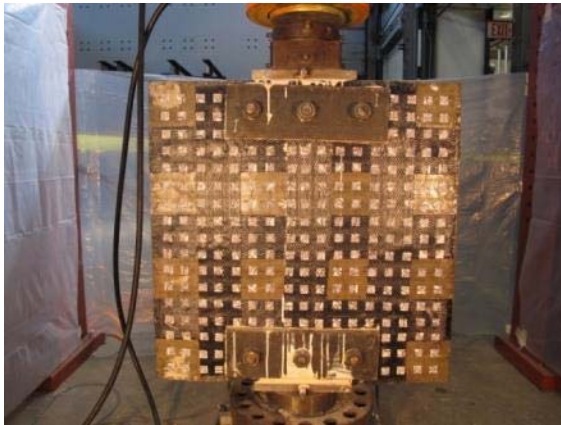
4.5.1 Panels reinforced with CFRP strips without steel reinforcement

4.5.1.1 Uni- and bi-directional CFRP strips with no inclination

Detailed test results are included in Appendix C. A number of representative plots were selected from that appendix and analyzed in this section.

As can be seen in Figure 4.29(a), the bi-directionally reinforced panel B5-0-0-5 was reinforced with 5 inch wide CFRP strips anchored at the edge of strips. The ratio of the CFRP anchor area to strip area was 1.2. Spacing of the strips was 10 inch from center to center. Cracking and maximum loads for B5-0-0-5 were 232 kips and 475 kips, respectively. Buckling of the vertical strip at the center of the panel can be seen in Figure 4.29(c). Center and bottom horizontal strips delaminated as the compressive strut formed and concrete crushing occurred. However, no anchors failed. Figure 4.29(e) was taken after the CFRP strips were removed.

As can be seen in Figure 4.29(b), the uni-directionally reinforced specimen U5-0-0-5 was reinforced with horizontal CFRP strips. The ratio of anchor to strip area was increased from 1.2 to 1.5 for U5-0-0-5. The cracking load of U5-0-0-5 was 201 kips and was smaller than that of B5-0-0-5 which cracked at 232 kips. Results therefore indicate that bi-directional CFRP applications allow a specimen to reach a higher cracking load than uni-directional applications. The maximum applied load was 486 kips and, as expected, was nearly the same as for U5-0-0-5. The vertical strips that were parallel to the loading direction had little influence on the response indicating that there is no need to test a panel with vertical strips.



(a) B5-0-0-5



(b) U5-0-0-5



(c) Failure mode of B5-0-0-5



(d) Failure mode of U5-0-0-5



(e) Crack pattern of B5-0-0-5



(f) Crack pattern of U5-0-0-5

Figure 4.29 Failure modes of bi- vs. uni-directional CFRP layouts at 0 and 90 degrees

A bar graph of maximum and racking loads is shown in Figure 4.30. The maximum loads were about the same for bi- and the uni-directionally reinforced panels and were about 30 % (116 kips) higher than those of the control panel. Cracking load was increased with bi-directional CFRP layout compared with the control.

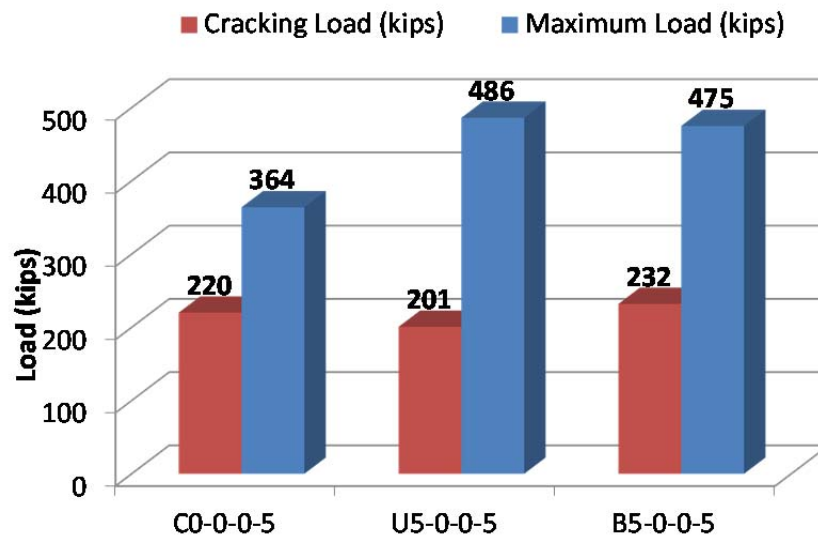
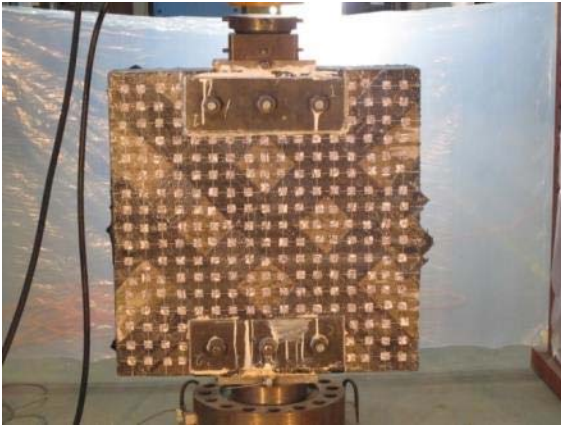


Figure 4.30 Load comparison of 0 and 90 degrees CFRP layout, no reinforcement

4.5.1.2 Uni- and bi-directional CFRP strips inclined at 45°, no reinforcement

The CFRP strip dimensions, ratio of anchor area to strip area (1.2), and the bi-directional layout scheme of B5-45-0-5 were identical to B5-0-0-5 but were inclined at 45 degrees. First of all, the most notable failure mode of this specimen was CFRP anchor failure. The cracking load was 210 kips and the maximum load was 431 kips. The maximum load carried by B5-0-0-5 was 475 kips, which is 44 kips higher than for B5-45-0-5. Figure 4.31(c) shows the CFRP anchor failure before the maximum load was reached. The anchor failure reduced the contribution of the strip to the panel strength, and resulted in a decrease of the panel capacity. The panel behavior before the anchor failure was discussed in Section 4.3. Figure 4.31(e) shows the crack pattern of the panel after removal of the CFRP. Early failure of the anchor may have influenced the direction of the primary inclined crack.

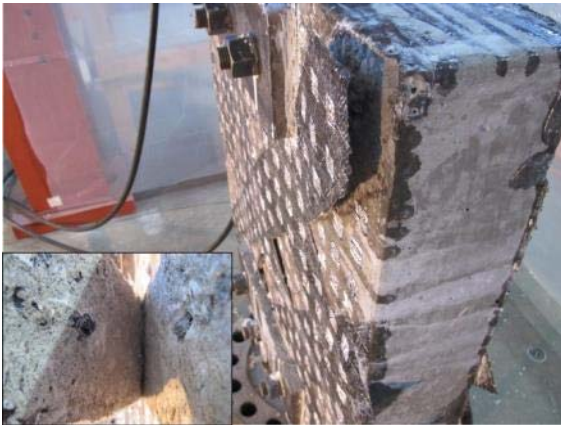
U5-45-0-5 (Figure 4.31(b)) was reinforced in only one-direction with CFRP strips inclined at 45 degrees. The cracking and the maximum loadings were 202 kips and 448 kips, respectively. The cracking load was almost identical to that of U5-0-0-5. Figure 4.31(d) shows a failure mode of this specimen. No CFRP strip rupture or anchor failure were seen in this test. Vertical cracks could be seen on the panel surface and out-of-plane concrete crushing between the strips was observed on the back side of the panel. Figure 4.31(f) shows concrete spalling after the maximum load was reached.



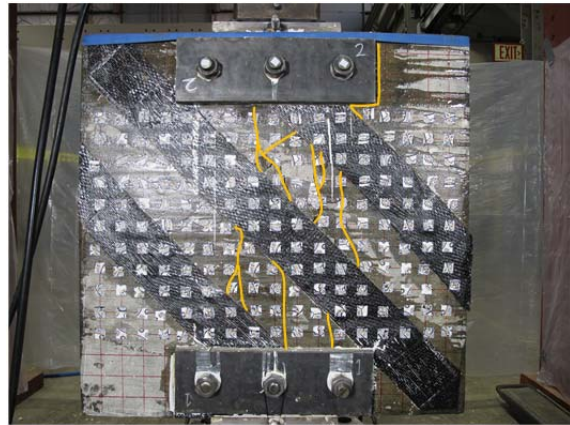
(a) B5-45-0-5



(b) U5-45-0-5



(c) Failure mode of B5-45-0-5



(d) Failure mode of U5-45-0-5



(e) Crack pattern of B5-45-0-5



(f) Crack pattern of U5-45-0-5

Figure 4.31 Failure modes of bi- vs. uni-directional CFRP layouts at 45 degrees

In Figure 4.32, the maximum and the cracking loads of specimens B5-45-0-5 and U5-45-0-5 are shown. Clearly, the performance of B5-45-0-5 was impaired by the premature anchor fracture. The performance of this specimen led to an increase in the anchor to strip material ratio from 1.2 to 1.5 in all subsequent tests. The performance of U5-45-0-5 was nearly the same as that of U5-0-0-5 with a small reduction in the peak load (448 kips vs 486 kips).

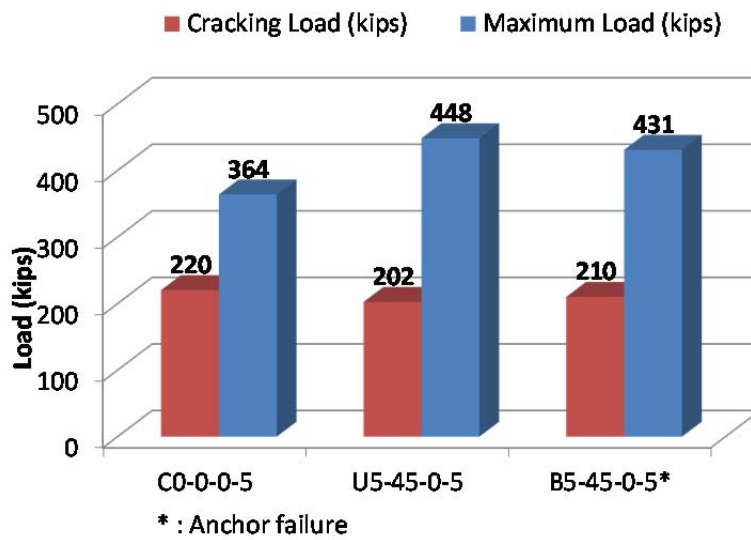


Figure 4.32 Load comparison of 45 degrees CFRP layout, no reinforcement

4.5.1.3 Uni- and bi-directional CFRP strips inclined at 30° and 60°, no reinforcement

The CFRP anchors that were used in B5-60-0-5 had an anchor to strip ratio of 1.2 and had anchor failure in B5-60-0-5 as in B5-45-0-5. The cracking and the maximum loads for B5-60-0-5 were 227 kips and 462 kips, respectively. The capacity of panel with the bi-directional CFRP layout (B5-60-0-5) was less than that of the uni-directional layout (U5-60-0-5). Strips that were oriented 60 degrees from the horizontal line exhibited buckling similar to that observed in B5-0-0-5. Crushing of the concrete strut between bearing plates is shown in Figure 4.33(e).

In U5-60-0-5, the uni-directional strips were inclined 60° (Figure 4.33(b)). Figure 4.33(f) shows the panel after the test. Concrete crushing between the strips occurred (Figure 4.33(d)), which led to delamination of the CFRP strips. No CFRP anchor failures occurred because the ratio of anchor to strip area was 1.5. Even though an anchor failed in B5-60-0-5, the loads on the two strengthened panels with 60° inclination were nearly identical (Figure 4.34).

The failure mode of specimen U5-30-0-5 is shown in Figure 4.15(b). No CFRP strip rupture or anchor failure was observed. The cracking load was 198 kips and the maximum applied load was 472 kips. The cracking load was almost identical to that of the U5-0-0-5 specimen. There were many vertical cracks on the panel surface after the test. In general, the uni-directional CFRP reinforced panels had similar failure modes regardless of the strip inclinations.



(a) B5-60-0-5



(b) U5-60-0-5



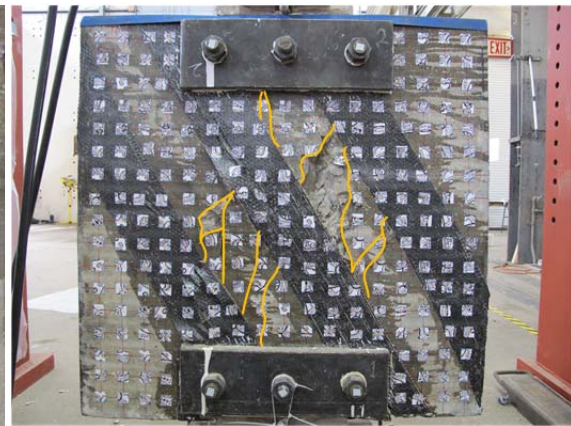
(c) Failure mode of B5-60-0-5



(d) Failure mode of U5-60-0-5



(e) Crack pattern of B5-60-0-5



(f) Crack pattern of U5-60-0-5

Figure 4.33 Failure modes of bi- vs.uni-directional CFRP layouts at 30 and 60 degrees

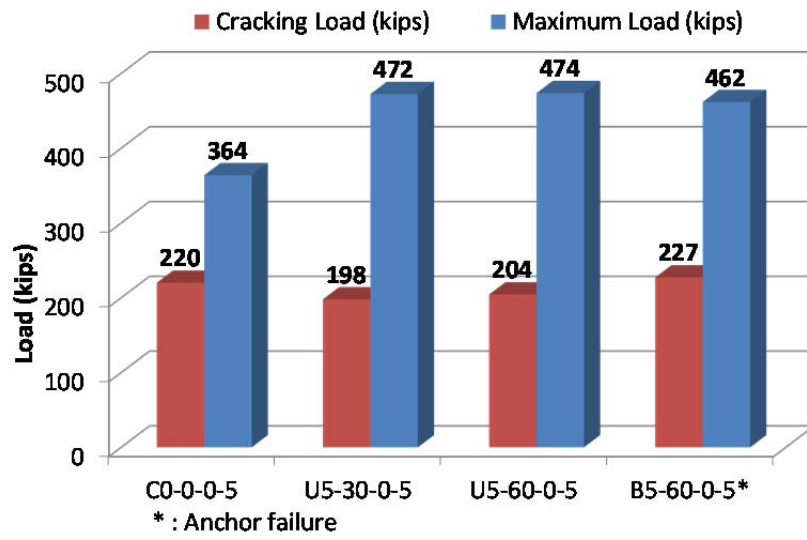


Figure 4.34 Load comparison of 30 and 60 degrees CFRP layout, no reinforcement

4.5.2 Panels reinforced with CFRP strips and bars

Uni-directional and bi-directional CFRP applications with two different strip angles (45° and 60°) are studied in this section. The bi-directional CFRP strip layout with vertical and horizontal strips was not constructed because the vertical CFRP strips were ineffective (See Figure 4.30).

4.5.2.1 Uni- and bi-directional CFRP strips inclined at 45°

Figure 4.35(a) shows a 3D model of B5-45-2-5. The panel was reinforced with two layers of the #3 rebar mats and 5 inch wide bi-directional CFRP strips placed at 45 degrees from horizontal. The cracking and maximum loads of B5-45-2-5 were 309 kips and 656 kips, respectively. Concrete crushing below the top steel plate was the main failure mode of that panel (Figure 4.35(c)).

Figure 4.35(b) shows the uni-directional CFRP strips and the embedded bars in U5-45-2-5. The failure mode of this specimen and the crack pattern are shown in Figure 4.35(d). The failure mode is similar to that of the bi-directional layout. Rupture of the CFRP strip on the back side of the panel can be seen. The cracking and the maximum loads of this specimen were 292 kips and 626 kips, respectively.

Load-strain behavior of the panel with a bi-directional layout was almost the same as that of the specimen with a uni-directional layout (Figure 4.36).



(a) 3D view of B5-45-2-5



(b) 3D view of U5-45-2-5



(c) Failure mode of B5-45-2-5



(d) Failure mode of U5-45-2-5

Figure 4.35 Failure modes of bi- vs. uni-directional CFRP layouts at 45 degrees

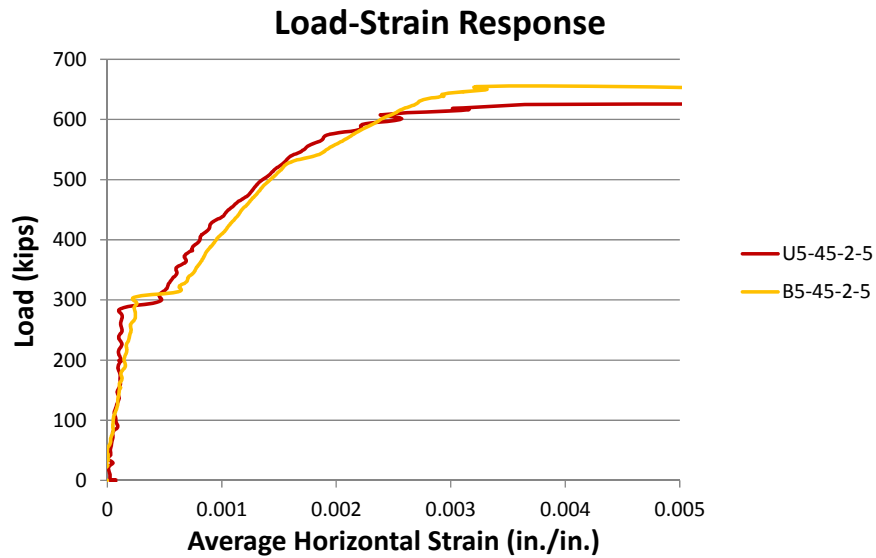
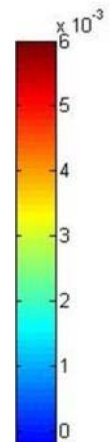
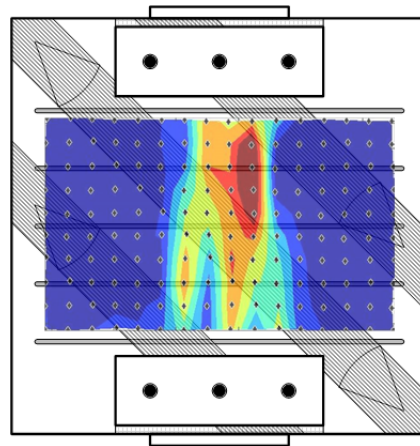


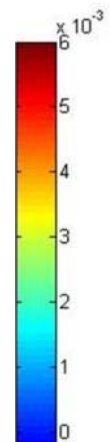
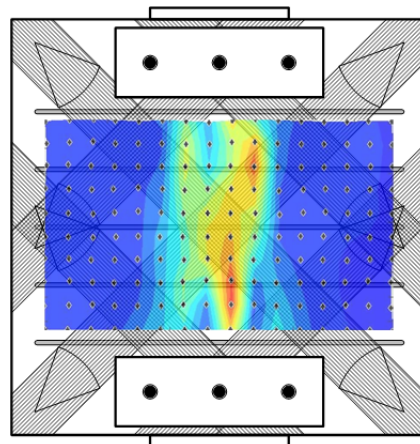
Figure 4.36 Load-strain responses of bi- and uni-directional CFRP layouts at 45 degrees from horizontal

In Figure 4.37(a) and (b), the horizontal strain contours at a load of 625 kips are shown for U5-45-2-5 and B5-45-2-5. At the same load level, the strain contours were quite different. The strain contours show that much higher strains and crack width developed between the strips with a uni-directional CFRP layout. Concrete crushing occurred in this area, as well. With a bi-directional CFRP layout, relatively uniform strain distributions were observed and the strains were lower.

The load comparison for the 45 degree layout with a control panel is shown in Figure 4.38. The bi-directional CFRP layout increased the maximum load of the panel by 66 kips (10 %) while the uni-directional CFRP layout resulted in a 36 kips (5 %) increase in maximum load. The cracking loads for both CFRP layouts were about 30 kips (10 %) higher than that of the control panel.



(a) U5-45-2-5 ($P=625$ kips)



(b) B5-45-2-5 ($P=625$ kips)

Figure 4.37 Horizontal strain contours for panels reinforced with a 45 degrees CFRP layouts

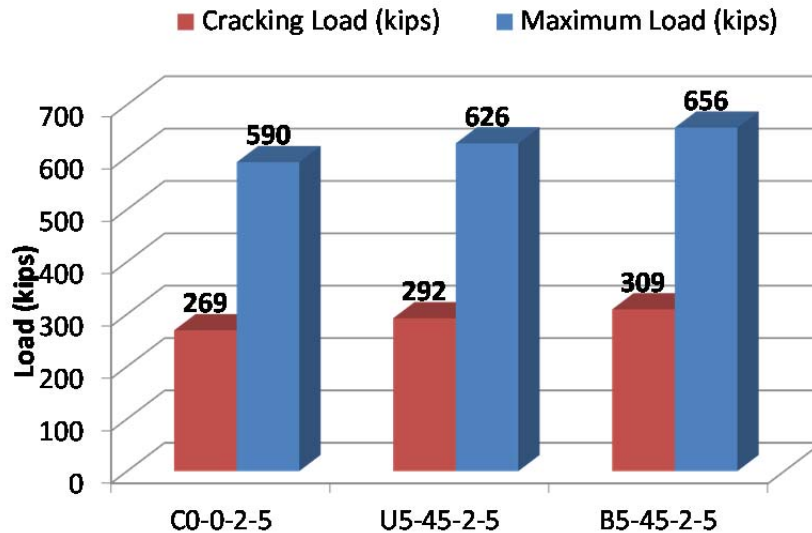


Figure 4.38 Load comparison for panels with a 45 degrees CFRP strip layouts, with reinforcement

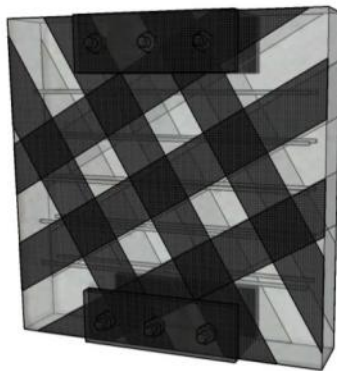
4.5.2.2 Uni- and bi-directional CFRP strips inclined at 30° and 60°

B5-60-2-5 (Figure 4.39(a)) was reinforced with two layers of steel bars and 5 inch wide CFRP strips inclined at 30 and 60 degrees from horizontal. The cracking load of this panel was about 310 kips and the maximum applied load was 630 kips. Figure 4.39(c) shows the failure mode of this specimen. CFRP strips that were placed over the center of the panel delaminated because of the concrete spalling as shown in bottom left corner of Figure 4.39(c). No CFRP anchor failure was observed in this test.

Figure 4.39(b) shows a 3D model of U5-30-2-5 specimen. The only difference between specimens U5-30-2-5 and B5-60-2-5 was the lack of CFRP strips inclined at 60 degrees in U5-30-2-5. For specimen U5-30-2-5, cracking and maximum loads were 265 kips and 588 kips, respectively. The general failure mode of specimen U5-30-2-5 was similar to that of specimen U5-60-0-5. Large concrete crushing occurred between the

CFRP strips. Spalling under the center CFRP strip can be seen in Figure 4.39(d). The failure mode of this panel was identical to that of U5-60-0-5 (Figure 4.33(d)).

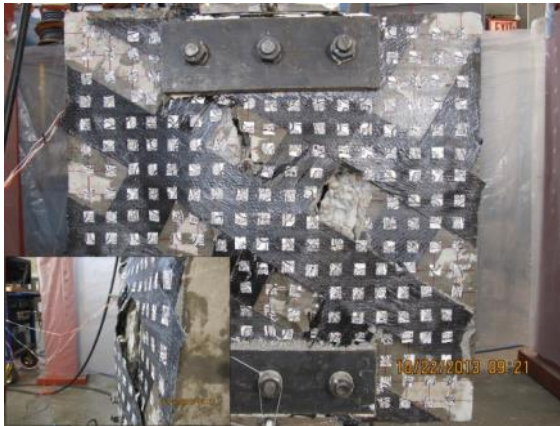
In Figure 4.40, load versus average horizontal strains are plotted for specimens U5-30-2-5 and B5-60-2-5. As can be seen in the figure, cracking and peak loads were higher with the bi-directional CFRP layout. Also, the average strain in the panel with the bi-directional layout was considerably smaller than in the panel with the uni-directional layout at the same load level.



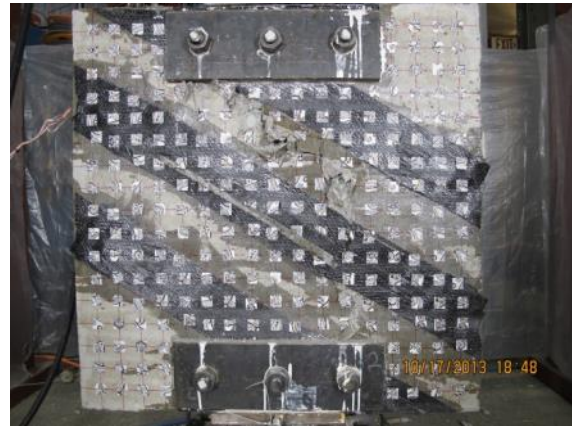
(a) 3D view of B5-60-2-5



(b) 3D view of U5-30-2-5



(c) Failure mode of B5-60-2-5



(d) Failure mode of U5-30-2-5

Figure 4.39 Failure modes of bi- vs. uni-directional CFRP layouts at 30 and 60 degrees

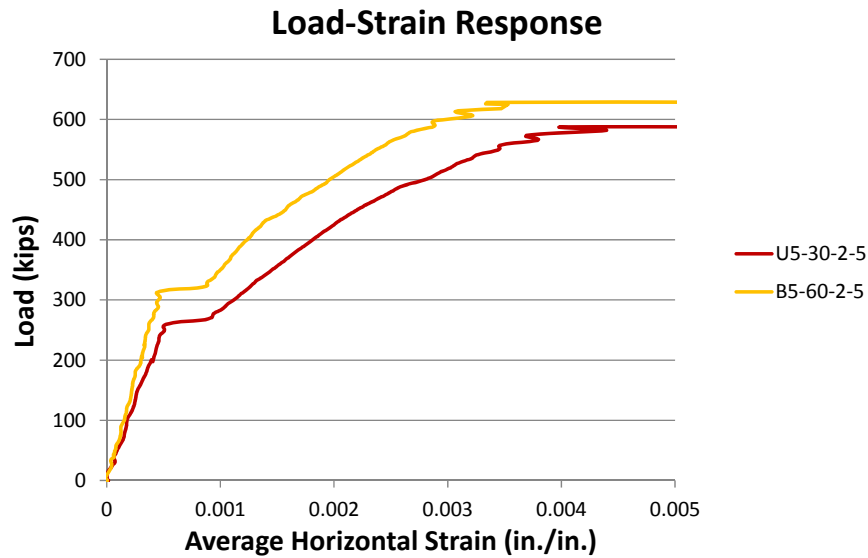
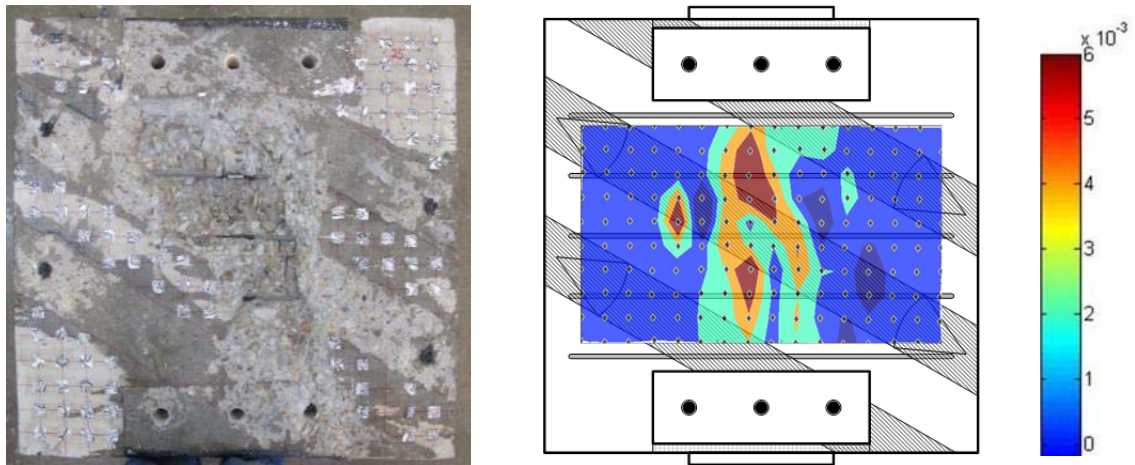


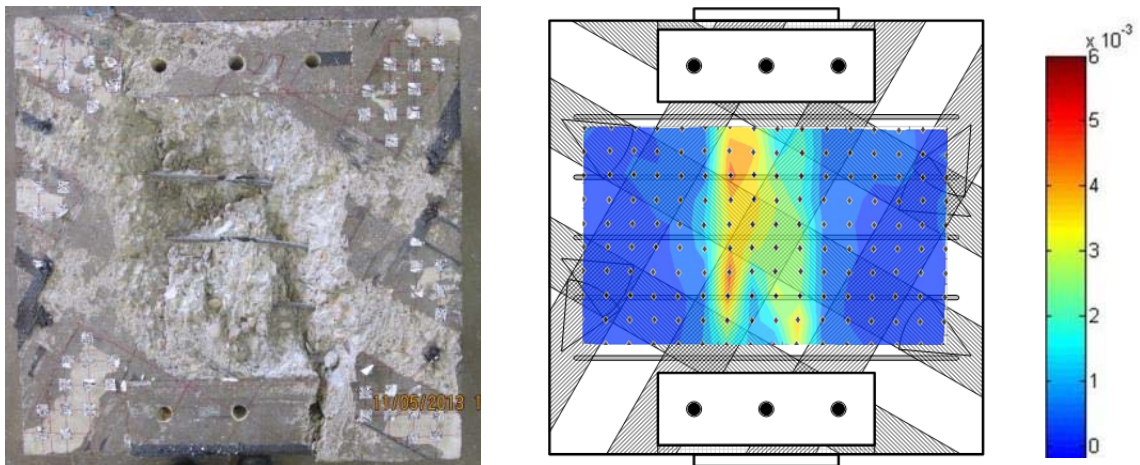
Figure 4.40 Load-strain responses of bi- and uni-directional CFRP layouts at 30 and 60 degrees from horizontal

The CFRP strips and the anchors were removed from the specimen after the test to expose the crack pattern. One critical crack formed in an oblique direction and this crack had separated the panel into two parts. Even though horizontal bar mats were used, the crack pattern was slanted due to the asymmetrical CFRP strip layout (Figure 4.41).

The horizontal strain contours are plotted at a load level of 587 kips for U5-30-2-5 and B5-60-2-5 in Figure 4.41. Horizontal strains exceeded 0.006 with the uni-directional CFRP layout. The area of large strains coincided with the location of crushing in U5-30-2-5. The locations of the dark red areas in the contour plot of U5-30-2-5 were between CFRP strips. A uniform strain distribution with lower strains was obtained for the bi-directional CFRP layout, with the maximum horizontal strain just exceeding 0.004. The maximum strain was slightly higher than 0.004. The strain contours provide clear evidence that a bi-directional CFRP layout can control cracks more effectively and results in more uniform strain distributions than a uni-directional CFRP layout.



(a) U5-30-2-5 ($P=587$ kips)



(b) B5-60-2-5 ($P=587$ kips)

Figure 4.41 Horizontal strain contours for panels reinforced with 30 and 60 degrees CFRP strip layouts

A comparison of loads can be seen in Figure 4.42. The maximum load of specimen B5-60-2-5 increased by 39 kips from that of the control panel. Despite the CFRP strip strengthening, the maximum load of specimen U5-60-2-5 decreased. Failure of this specimen initiated at the top steel plate area. The crack and the CFRP delamination propagated from the steel plate to the center of the panel and were likely caused by insufficient confinement from the steel plates.

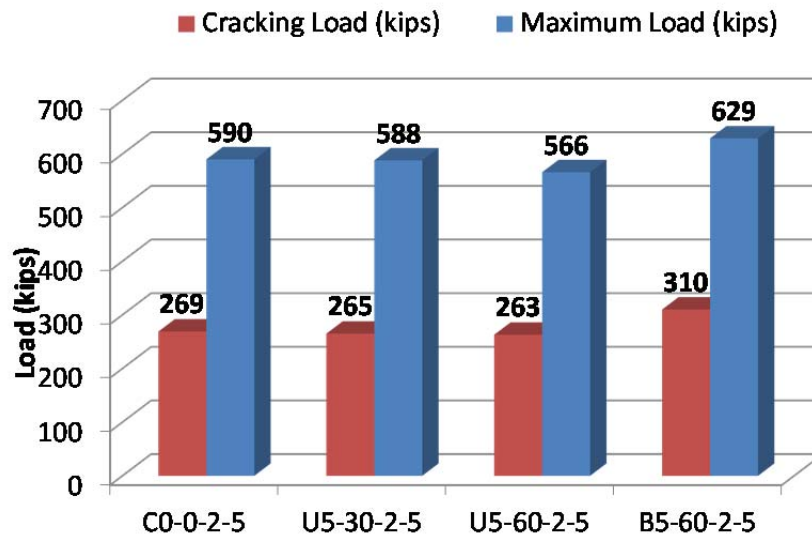


Figure 4.42 Load comparison of 30 and 60 degrees CFRP layout

4.6 EFFECT OF AMOUNT OF CFRP, STEEL REINFORCEMENT, AND INTERMEDIATE ANCHOR

4.6.1 Amount of CFRP material

Specimens B5-0-0-5 and B36-0-0-5 were compared to evaluate the effect of the CFRP material amount. Panel B5-0-0-5 was reinforced with 5 in. wide bi-directional CFRP strips and B36-0-0-5 specimen was fully strengthened in both directions. Figure 4.43 shows load-strain response of these panels. The cracking load of B36-0-0-5-0an was 79 kips (35 %) higher than the control panel. Since the orientation of CFRP strips were identical, stiffness after the cracking load of specimens B5-0-0-5 and B36-0-0-5 was similar but the fully wrapped panel reached a higher load.

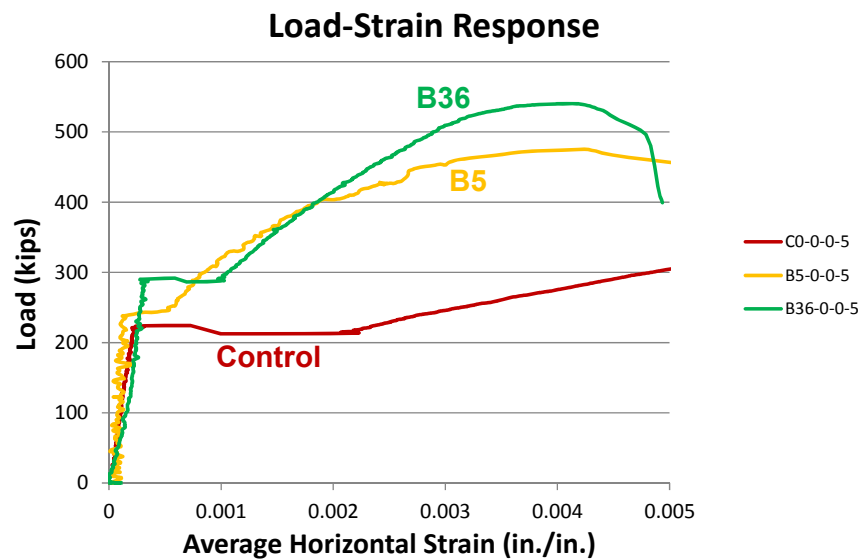
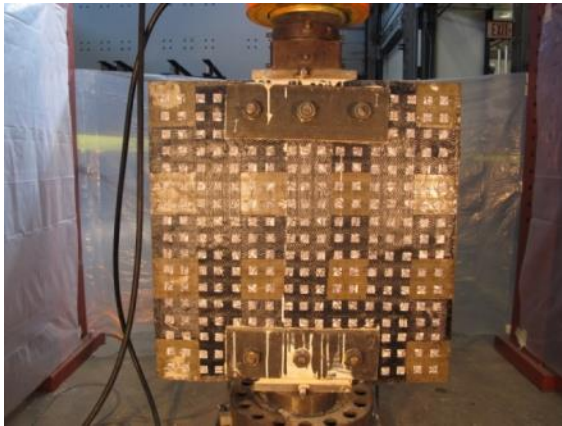
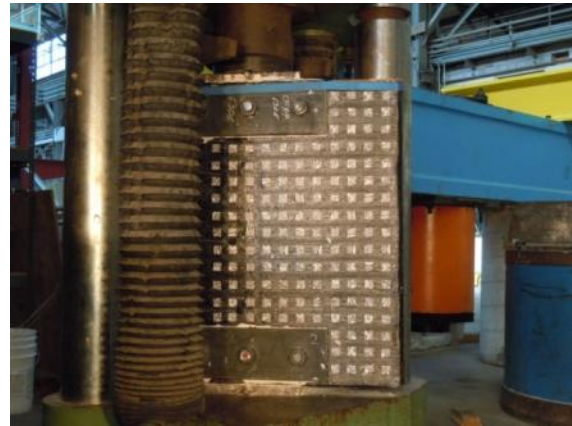


Figure 4.43 Load-Strain responses of strip vs. fully reinforced panel

Peak loads (blue bars) and CFRP material amounts (red line) in terms of surface area covered by CFRP are shown in Figure 4.45. The maximum load of the strip reinforced specimen was 475 kips (30 % increase over control) and that of the fully wrapped one was 540 kips (48 % increase). A 111 kip increase in maximum load was obtained with the use of CFRP strips. However, a maximum load increase of only 65 kips was achieved when the amount of CFRP material was doubled in the fully-wrapped application. The strength increase was not proportional to the increase in the amount of CFRP used.



(a) B5-0-0-5



(b) B36-0-0-5



(c) Failure mode of B5-0-0-5



(d) Failure mode of B36-0-0-5

Figure 4.44 Failure modes of strip vs. fully reinforced panel, no reinforcement

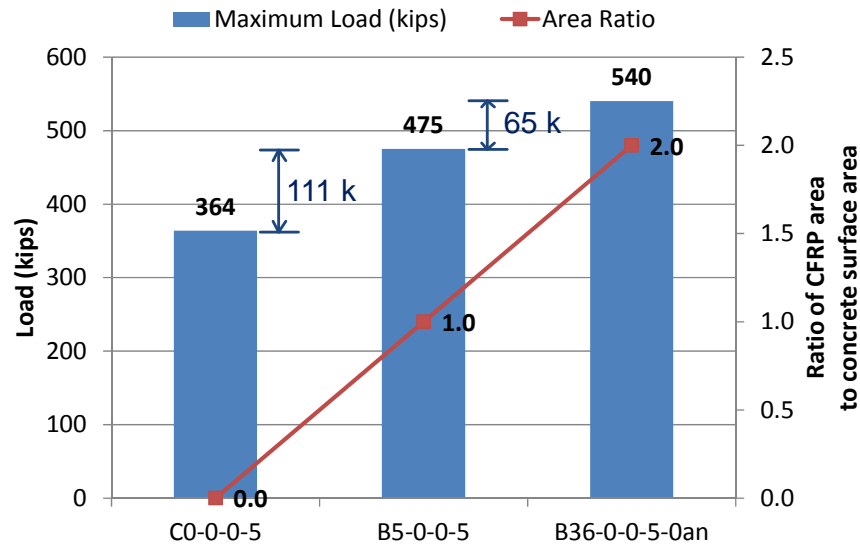


Figure 4.45 Effect of the CFRP amount

4.6.2 Intermediate CFRP anchors

Different numbers of the CFRP anchors were installed on the fully wrapped specimens to examine the effect of intermediate anchors. Figure 4.47(a), (b), and (c) show the layout of anchors. The panels had the same number of the anchors on the front and back sides. Details of the intermediate CFRP anchor are described in the Appendix B. All panels were fully wrapped horizontally. The horizontal CFRP strips were overlapped by 6 in. along the sides of the panels instead of having anchors at panel edge.

Figure 4.46 illustrates the load-strain responses of the fully wrapped panels with different numbers of intermediate CFRP anchor. The overall panel behavior was similar regardless of the number or presence of intermediate anchors. The only difference between tests was the behavior after the peak loads were reached. The load of the panel without intermediate CFRP anchors dropped after an average horizontal strain of 0.004

was reached. However, with the intermediate CFRP anchors, strains reached 0.008. The installation of the anchors allowed the horizontal fibers to nearly reach ultimate strain.

Strain contours of these specimen series are shown in Figure 4.47. The strain contours were taken at a load of 540 kips, which was the ultimate load on B36-0-0-5 specimen. Figure 4.47(a) shows that the location of the largest strain occurred at the node-strut interface and concrete crushed at that location. The failure modes show that the zone of concrete crushing was narrower in the panels with intermediate anchors. The horizontal CFRP delaminated from the concrete surface and reduced the restraint provided by the CFRP. Intermediate CFRP anchors however managed to distribute strains more uniformly over the critical crack and consequently reduce the peak strains. (Figure 4.47)

However, increasing the number of intermediate CFRP anchors did not improve the performance up to the peak load but resulted in a slower drop in capacity as the strains increased past the peak load.

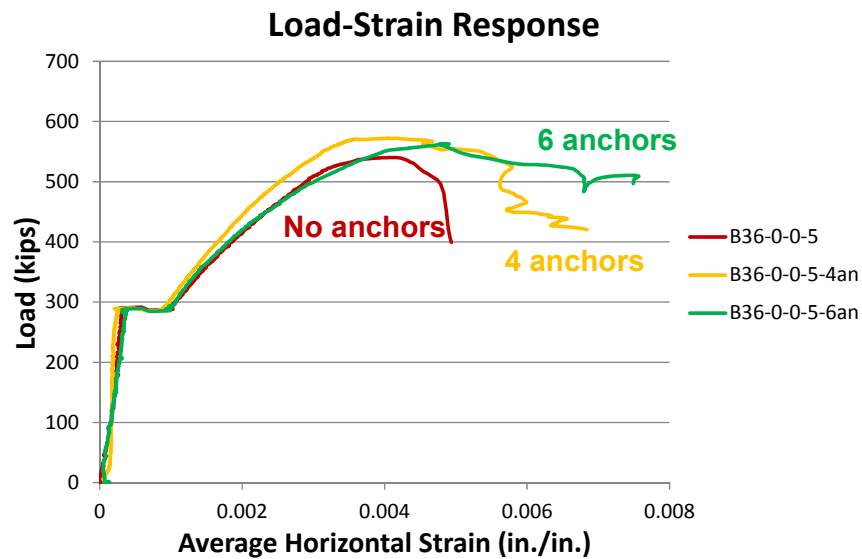
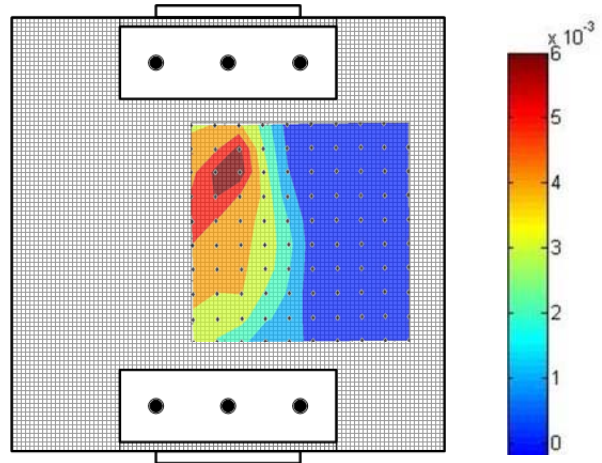
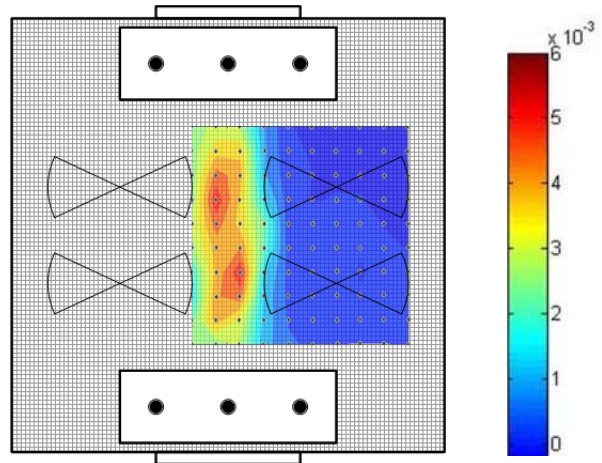


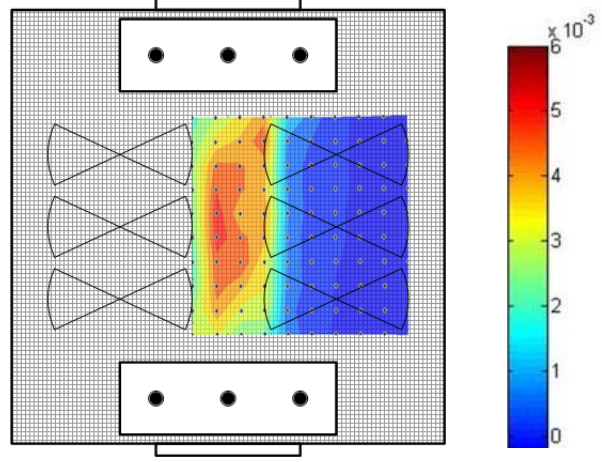
Figure 4.46 Load-strain responses of panels with intermediate CFRP anchors



(a) B36-0-0-5-0an ($P=540$ kips)



(b) B36-0-0-5-4an ($P=540$ kips)



(c) B36-0-0-5-6an ($P=540$ kips)

Figure 4.47 Horizontal strain contours for panels with intermediate CFRP anchors

The cracking loads of all three fully wrapped panels increased about 30 % compared with the control panel (Figure 4.48). The maximum load increased about 50 %. The failure modes show that the zone of concrete crushing was narrower in the panels with intermediate anchors but the capacity was nearly the same regardless of the intermediate anchors.

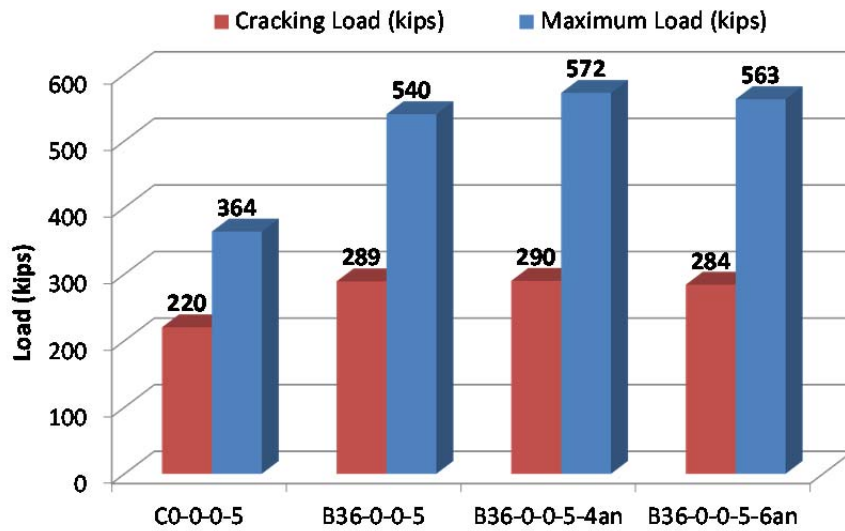
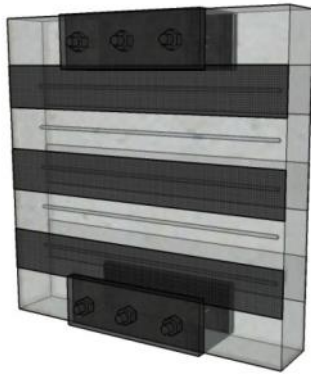


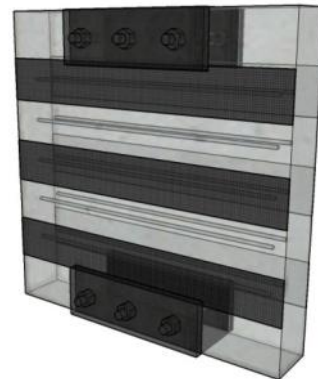
Figure 4.48 Effect of intermediate CFRP anchors

4.6.3 Amount of steel reinforcement

As shown in Figure 4.49(a), U5-0-1-5 was reinforced with horizontal 5 inch wide CFRP strips and one layer of #3 bars. U5-0-2-5 (Figure 4.49(b)) had two layers of bars. Figure 4.49(c) and (d) show failure modes of these specimens. Brittle compressive concrete crushing between the loading points occurred at the peak load.



(a) 3D view of U5-0-1-5



(b) 3D view of U5-0-2-5



(c) CFRP strip failure of U5-0-1-5



(d) CFRP strip failure of U5-0-2-5

Figure 4.49 Failure modes of panels reinforced with different amounts of reinforcement

Figure 4.50 shows the load-strain response of the three panels with different amounts of steel reinforcement. All the panels were reinforced with the same CFRP strip layout. The panels with steel reinforcement were considerably stiffer compared to U5-0-0-5. In the case of specimen U5-0-1-5, the rebar at the center of the panel yielded at a load of 490 kips. The rebar at the same location of specimen U5-0-2-5 specimen yielded at 590 kips.

The strain contours related to the different load states are shown in Figure 4.51. In Figure 4.51(a), (b), and (c), the contours at a load of 486 kips (the peak load of U5-0-0-5) can be compared. The panel that was only reinforced with CFRP strips had large strains (0.006) at this load level (Figure 4.51(a)). However, in the case of the bar reinforced panels, lower levels of tensile strain were recorded, and were limited to a narrow portion of the panel.

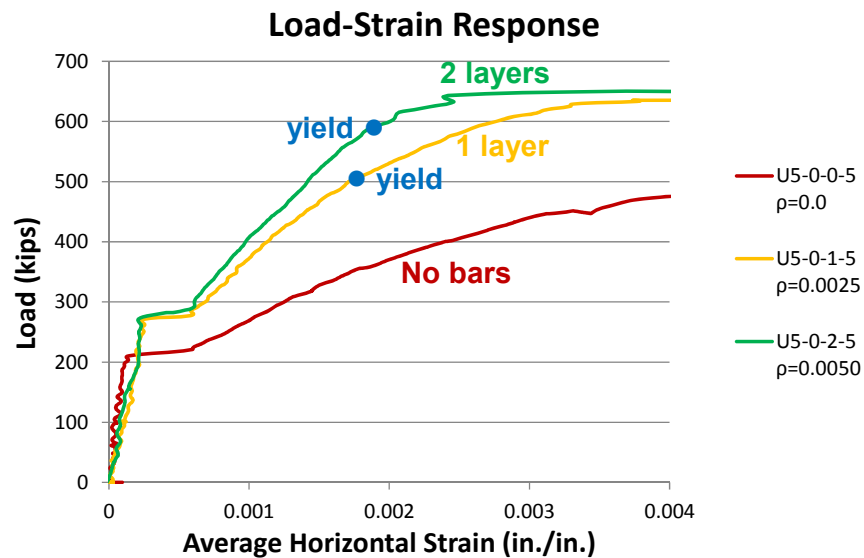
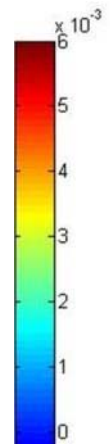
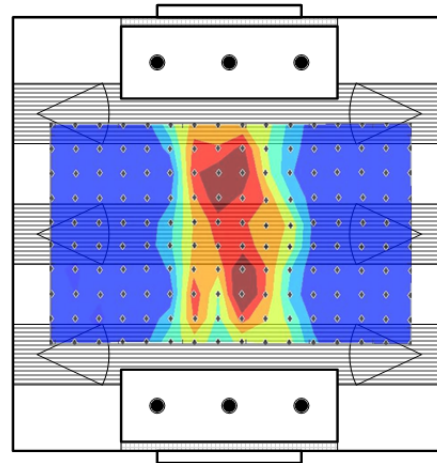
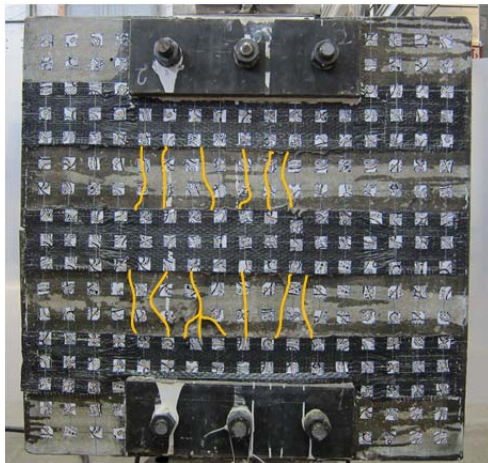
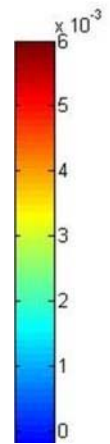
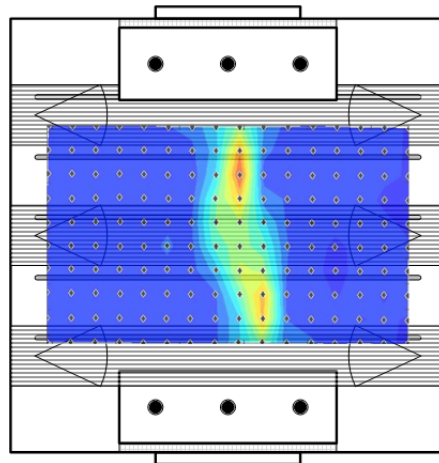


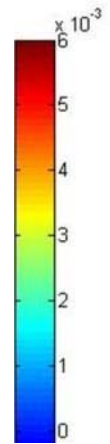
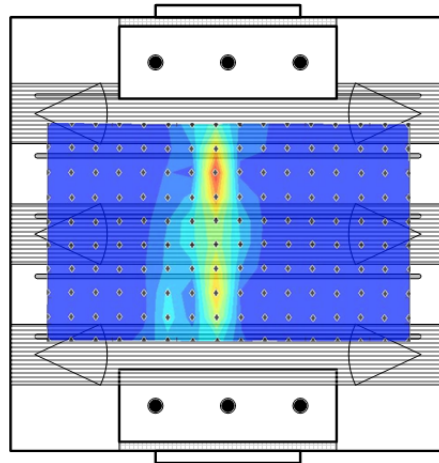
Figure 4.50 Load-strain responses of panels reinforced with different steel ratios



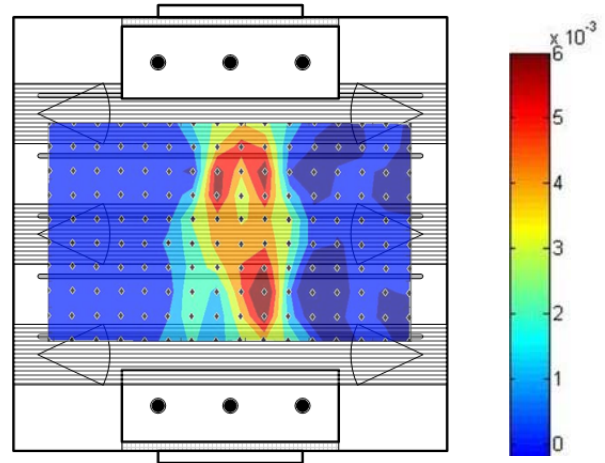
(a) U5-0-0-5 ($P=486$ kips)



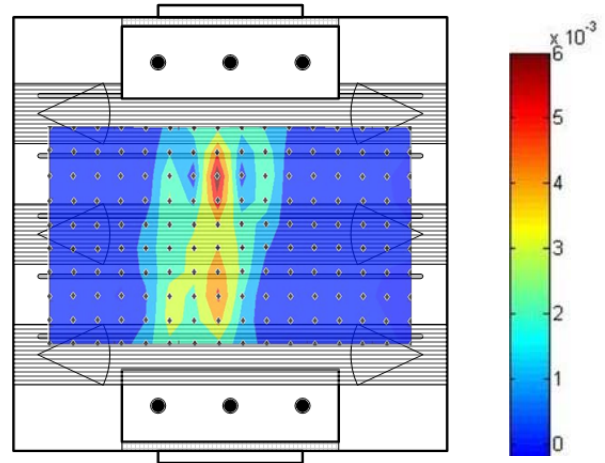
(b) U5-0-1-5 ($P=486$ kips)



(c) U5-0-2-5 ($P=486$ kips)



(d) U5-0-1-5 (P=635 kips)



(e) U5-0-2-5 (P=635 kips)

Figure 4.51 Horizontal strain contours for panels reinforced with various steel ratios

Since the panels with bars reached much higher loads, their strain contours are also plotted at a load of 635 kips in Figure 4.51. The strain contours in Figure 4.51(d) and (e) show different strain distribution between the steel-reinforced specimens. Right after bar yielding at 490 kips, large strains developed in the panel reinforced with one layer of bar (Figure 4.51(d)). On the other hand, a small strain increase was observed in the panel with two layers of bars. The CFRP strips allowed the panels to reach similar peak load level since the CFRP continued to restrain lateral expansion after the bars yielded.

A load comparison of the loads can be seen in Figure 4.52. The cracking and maximum loads of U5-0-1-5 were 274 kips and 635 kips, respectively. The cracking load was increased by 35 % with the steel reinforcement. The maximum load was increased by about 35 % with the steel reinforcement. Difference in loads between one and two layers of bars was insignificant.

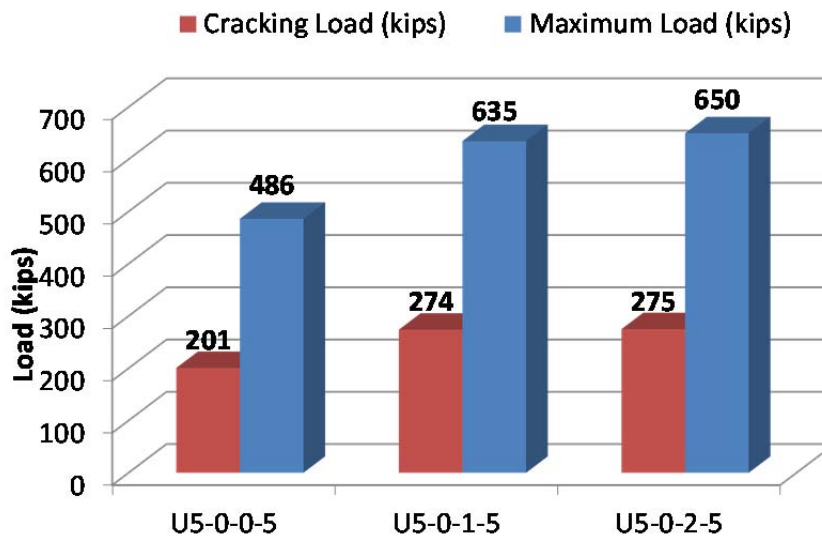


Figure 4.52 Effect of steel reinforcement ratio

4.7 LOAD CONTRIBUTION OF CFRP STRIPS AND STEEL REINFORCEMENT

In Figure 4.53, load-strain curves are plotted for panels with and without steel reinforcement. It should be noted that the bars increase the capacity of the panel and that the CFRP contribution is smaller when bars and CFRP are used together. This finding was reported by Kim (2011) and he developed interaction equations to take this effect into account for calculating contributions of steel and CFRP to shear capacity. Table 4.2 shows the cracking loads and the loads when an average horizontal strain of 0.004 was reached for the panels shown in Figure 4.54.

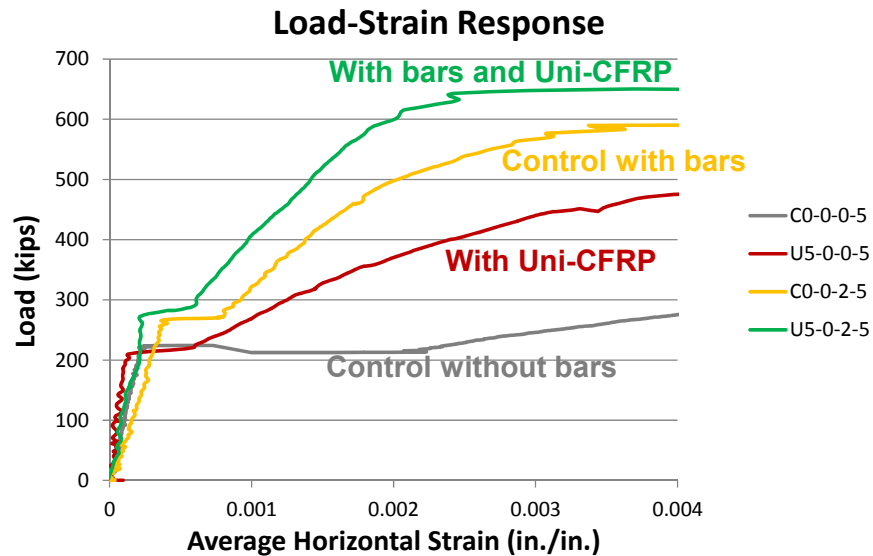


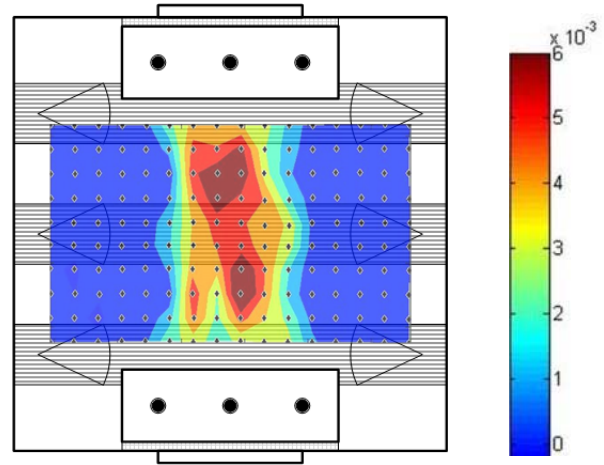
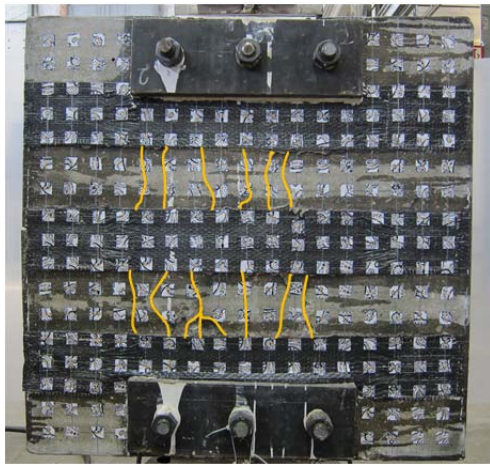
Figure 4.53 Load-strain responses of panels reinforced with various reinforcements

Table 4.2 Comparisons of load contributions of steel and CFRP to panel strength at 0.004 strain

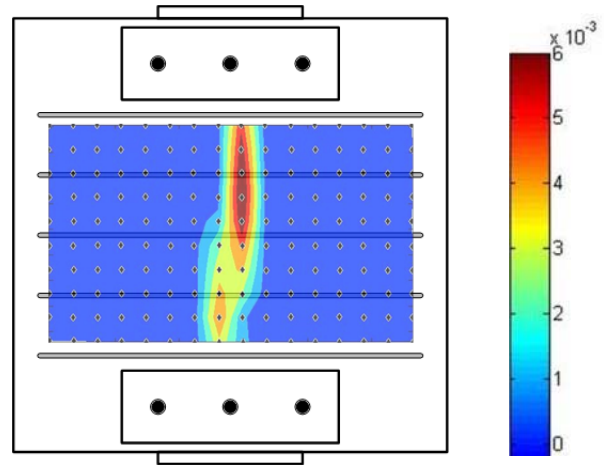
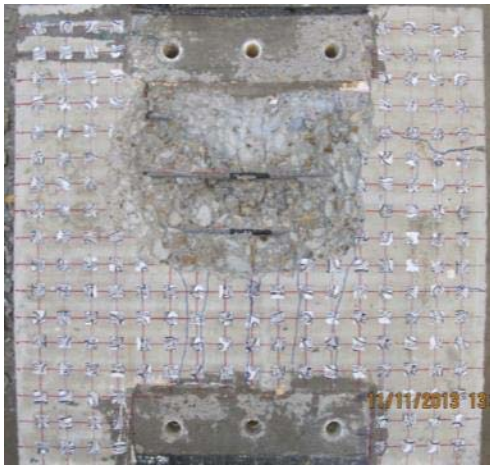
Test specimen	Cracking Load (kips)	Load recording at 0.4 % strain (kips)	Load increment relative to plain panel (kips) (% increase)
C0-0-0-5	220	276	0
U5-0-0-5	201	476	200 (73 %)
C0-0-2-5	269	590	314 (114 %)
U5-0-2-5	275	650	374 (136 %)

As can be seen in Figure 4.53 and Table 4.2, the cracking load increased by about 30 % when bars were added. Although significant horizontal deformations occurred after the cracking load was reached in the control panel C0-0-0-5, the panel essentially failed when cracking load was reached. However, different load increases were observed in the panels with different combinations of materials. The specimen with both CFRP strips and bars had the largest load increase (374 kips) and the lowest average horizontal strain at the same load levels. The force that could be caused by the CFRP strips and the bars were same (Appendix B). However, as shown in Figure 4.53, the load contribution of the steel reinforced panel to the panel strength was considerably greater (314 vs. 200 kips) than the CFRP contributed to the strengthened panel.

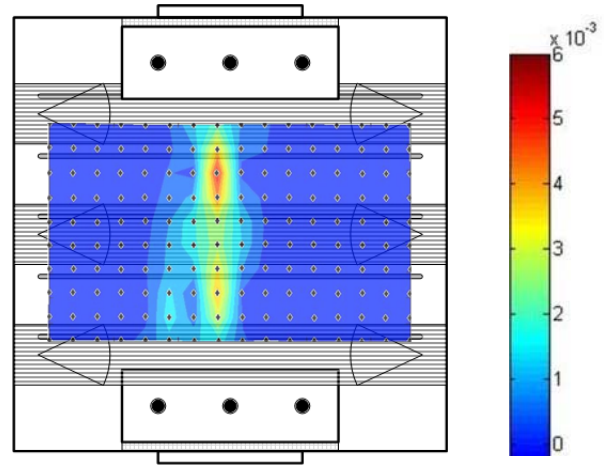
The strain contours of this series are shown in Figure 4.54 plotted at a load of 486 kips. Since C0-0-0-5 failed at cracking load, the strain contour was omitted from Figure 4.54. The contours for these panels indicate large area of high strains in U5-0-0-5 (Figure 4.54(a)). With CFRP only, the strains exceeded 0.006 at some locations and concrete crushing was observed at these locations. With bars only, large strains were observed on a narrow band where a vertical crack formed. With CFRP, delamination resulted in large strains spreading away from the crack. With bars, the crack is better controlled (opens less) since the bars transfer forces to the concrete through the deformations on the bars.



(a) U5-0-0-5 ($P=486$ kips)



(b) C0-0-2-5 ($P=486$ kips)



(c) U5-0-2-5 ($P=486$ kips)

Figure 4.54 Horizontal strain contours for panels reinforced with different materials

4.8 EFFECT OF CONCRETE STRENGTH

Figure 4.55 shows strengthened panels with different concrete strength. The peak load increase of the bi-directional CFRP reinforced panels can be seen in Table 4.3. Since B5-0-0-5 and B5-60-0-11 panels did not have premature anchor failure, these panels were chosen to evaluate CFRP strengthening effects with different concrete strength. In addition, bi-directional CFRP reinforced panels had nearly identical strength regardless of CFRP strip inclination (Figure 4.28). Therefore, B5-0-0-5 and B5-60-0-11 panels represent the bi-directional CFRP reinforced panels for 5 ksi and 11 ksi, respectively. Table 4.3 indicates a 111 kip of load increase with bi-directional CFRP layout in a 5 ksi concrete panel. In the case of 11 ksi concrete, the load increase was 116 kips. Nearly identical load increases were obtained with bi-directional CFRP layout regardless of concrete strength.

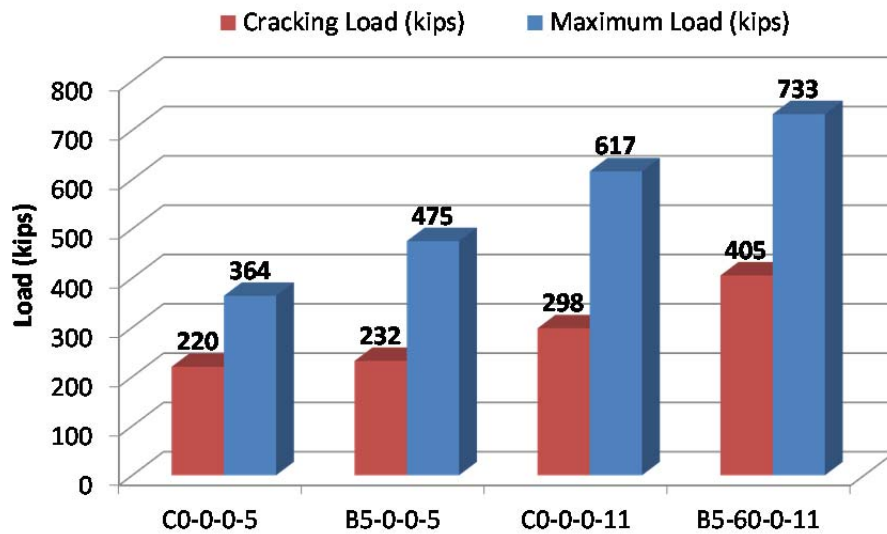


Figure 4.55 Load contribution of CFRP strip to panel strength

Table 4.3 Load increase in bi-directional CFRP strengthened panels

	C0-0-0-5	B5-0-0-5	C0-0-0-11	B5-60-0-11
Cracking load (kips)	220	232	298	405
Peak load (kips)	364	475	617	733
Increment of Peak load (kips, %)	111, 30 %		116, 20 %	

4.9 TRENDS OBSERVED IN PANELS AND I-BEAMS

The panels provide insight regarding the trends observed in the I-beam tests shown in Figure 2.6, even though shear-strain was plotted in Figure 2.6 and average horizontal strains are plotted for panel behaviors.

The increase in cracking load in the I-beams is similarly seen in the panels. The use of bi-directional CFRP layouts provided restraint across any potential crack orientations and it is likely that micro cracks did not develop into significant shear cracks until higher principal tensile stresses were reached.

The stiffness after cracking was improved using bi-directional layouts.

Bi-directional layouts resulted in increased strength. The bi-directional CFRP layouts increased the shear capacity of beams by adding a shear component to supplement the steel stirrup component and it is likely that there was more redistribution of stress in the concrete thereby improving the concrete contribution to the shear capacity. Although the panel strengths did not exhibit large increases in strength with bi-directional layouts compared with uni-directional layouts, it is likely that in a beam with a large area of the beam subjected to shear forces, the redistribution of tensile strains from regions of high strain to less strained regions is a significant factor for improving shear capacity.

CHAPTER 5 SUMMARY AND CONCLUSIONS

5.1 SUMMARY

The objective of this research was to evaluate the parameters that influence the effectiveness of CFRP materials in strengthening applications. Small scale panels were tested to study the compression struts similar to these in the shear span of I-beams. Panels could be tested faster and at less cost but do not have the same boundary conditions that develop in a beam. The experimental study using the concrete panels was carried out considering a number of parameters including the CFRP layout, the inclination of CFRP relative to the cracking direction, and the amount of steel reinforcement and CFRP material. Concrete panels were constructed and reinforced with various CFRP schemes and internal reinforcement. Monotonic loading was applied over a confined bearing area and the average horizontal strain was calculated using the vision system. The effectiveness of CFRP materials was evaluated based on the average horizontal strains across the middle of the panel.

5.2 CONCLUSIONS

The main findings from the experimental study are listed below.

Bi-directional vs. uni-directional CFRP layouts

1. **Nearly identical maximum panel strengths were observed in the bi-directional CFRP layout regardless of the CFRP angles.** The test results showed that the maximum load difference in the bi-directional CFRP layout at different inclinations was smaller than that of uni-directional CFRP layouts with different inclinations.
2. **The bi-directional CFRP layout controlled cracking better than uni-directional CFRP layouts.** The strain contours of the bi-directional CFRP layout showed lower strain readings compared to that of the uni-directionally strengthened panels at all load levels.
3. **Bi-directional CFRP layout reinforced panels had slightly higher cracking and maximum loads than that of uni-directional CFRP layout.** Average increments of cracking and maximum loads of the bi-directional CFRP layout were 12 % and 6 % compared to that of the uni-directional CFRP layouts, respectively.
4. **The influence of CFRP layouts on the panel strength was similar regardless of the concrete strength.**

5. **The effect of uni-directional CFRP layouts decreased as angle or inclination to the crack increased.** The results indicated that the influence of CFRP strengthening could only be maximized when the CFRP strip was perpendicular to the direction of cracking.

Effect of steel reinforcement

1. **Steel reinforcement was more effective in controlling the average horizontal strains in the cracked region than CFRP strips.** The panels reinforced with bars had lower average horizontal strains compared to the CFRP strip reinforced panels. The average strain recordings of the bar reinforced panel were 50 % of that of the CFRP strip reinforced panel. There was better bond between the bars and the concrete that deteriorated less rapidly than the debonding mechanism of the CFRP strips.
2. **Steel reinforcement contribution to the panel strength reduced the contribution of the CFRP strips.** Even though tensile capacity of the bars was the same as that of the uni-directional CFRP strips, the difference in bond properties limited the tensile force that could be developed in the CFRP.
3. **Panels with a higher steel ratio and CFRP strips exhibited lower average horizontal strain but did not increase maximum load capacity.** The CFRP strips allowed the panels to reach similar peak loads since the CFRP continued to restrain lateral expansion after the bars yielded.

Effect of CFRP anchors

- 1. Several panels failed due to anchor rupture. It is important that anchor strength was at least 50 % greater than that of the CFRP strip being anchored.**
- 2. Uniform strain distributions through cross section of the CFRP sheet could be obtained with intermediate CFRP anchors.**

5.3 FUTURE WORK

The intent of the panel test was to simulate compression struts in the shear region of I-beam. Since the boundary conditions of the panel were very different than in the beam web, the benefits of bi-directional CFRP strengthening must be determined through full-scale I-beam and U-beam test. The effects of bi-directional anchored CFRP layouts in the panel tests can only be verified under realistic boundary conditions before design guidelines for bi-directional CFRP shear strengthening can be established.

APPENDIX A

CONSTRUCTION OF PANEL SPECIMEN AND CFRP INSTALLATION

A.1 PANEL CONSTRUCTION WITH STEEL REINFORCEMENT

Installation procedure for strain gages is shown in Figure A.1. The strain gages attached to the bars were the product of Tokyo Sokki Kenkyujo Co. The gages have a 3 % strain limit and eliminate the need for a moisture-proof coating since transparent and flexible epoxy resin is applied on each gage. A water-proofing 1 mm thick tape-form coating was placed over the gages. Lastly, the strain gages were coated with duct tape.



(a) Strain gage



(b) SB tape



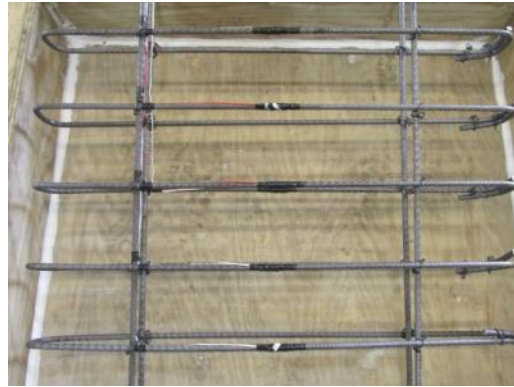
(c) Strain gage on the rebar



(d) Gage protection with SB tape



(e) Duct tape finishing



(f) Strain gages on the rebars



(g) Rebar mats in the wood forms



(h) After concrete casting

Figure A.1 Strain gage installation

A.2 CFRP INSTALLATION

A.2.1 Surface preparation

After removal of forms from the panels, the panel surfaces were smoothed using a grinder. The required hole size was calculated and holes were drilled into the panel specimen (Figure A.2(b)). Grinding stone bits were used to round the edge of all the anchorage holes to a radius of 0.5 inches. As can be seen in Figure A.2(c), the holes were ground along one side of the hole since one-way anchors were used.



(a) Removal of forms



(b) Concrete surface grinding



(c) Rounding the edge of the hole



(d) Panels positioned for CFRP application

Figure A.2 Surface preparation for CFRP installation

A.2.2 CFRP strip installation

The procedure for CFRP strip application is shown in Figure A.3(a) ~ (f). First, the required amount of component A and component B was measured and mixed for five minutes (Figure A.3(a) and (b)). Then the concrete surface and the CFRP strip were saturated by mixed epoxy using roller. After the saturation work, the CFRP strip was placed over the saturated location of the concrete surface. Then the CFRP patch was located over the strip end region with perpendicular direction to the CFRP strip. An opening for the anchor installation was created and saturated CFRP anchor was fully inserted into the hole. The anchor fan was spread out uniformly over the CFRP strip and excess epoxy was eliminated using plastic putty knife. Lastly, the second CFRP patch was placed over the anchor with the same direction.



(a) Mix component A and B



(b) Mixing



(c) Saturating the concrete surface



(d) Impregnating CFRP strip



(e) Attaching CFRP strip to concrete surface



(f) Panels after the CFRP application

Figure A.3 CFRP application

APPENDIX B

CALCULATIONS FOR THE SPECIMEN DESIGN

B.1 STEEL REINFORCEMENT DESIGN CALCULATION

As can be seen in Figure B.1, typical steel reinforced panels had 2 layers of rebar mat and each mat consisted with 5 layers of reinforcing bars. The tensile capacity of the steel reinforcement was determined to equal the tensile capacity of the CFRP strips. For the steel reinforcement, ASTM A615 Grade 60 steel was used in the calculation.

CFRP strip width: $w_f = 5$ in.

CFRP strip thickness: $t_f = 0.02$ in.

Tensile strength: $f_f = 150,131$ psi

Total number of strip: 6 ea

Total tensile force capacity: $T_{CFRP} = n \times w_f \times t_f \times f_f$
 $= 6 \times 5 \times 0.02 \times 150,131 = 90.08$ kips



Figure B.1 Layout of steel reinforcement

Steel reinforcement strength: $f_s = 80,000$ psi

Number of rebar layer: 5 layers

Required tensile force: $T_{s,required} = T_{CFRP}/n$
 $= 90.08/5 = 18.02$ kips/layer

Required rebar area: $A_{s,required} = T_{s,required}/f_s$
 $= 18.02/80 = 0.23$ in.²/layer

Use 2-No. 3 Rebar: $A_s = 2 \times 0.11 = 0.22$ in.²/layer

B.2 CFRP ANCHOR AREA CALCULATION

Figure B.2 shows a detail of the CFRP anchor. A strip of CFRP anchor that was cut to the calculated width and folded in half to allow easy insertion into the anchor hole. In Figure B.2, the inserted part of the anchor is illustrated in red color and the fan part is represented by blue color. Calculations for the dimension of the CFRP anchor are described in this section. The intermediate anchors used in Figure 3.9 were two-way anchors. Therefore, the anchor area of the intermediate anchors was double that of the typical and or one-way anchor.

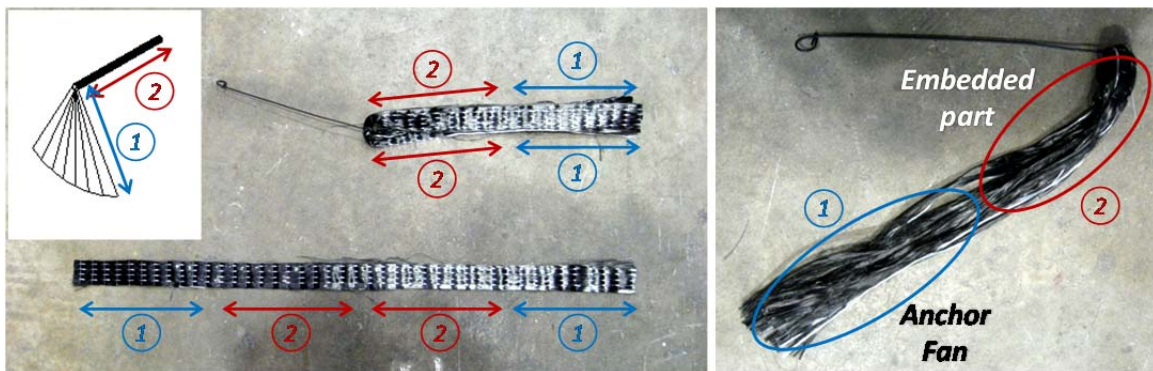


Figure B.2 CFRP anchor detail (Kim, 2011)

CFRP strip area: $A_{f,strip} = w_f \times t_f = 5 \times 0.02 = 0.1 \text{ in.}^2$

Required CFRP anchor area: $A_{f,anchor} = 1.5 \times A_{f,strip} = 1.5 \times 0.1 = 0.15 \text{ in.}^2$

Required Anchor width: $w_{f,anchor} = \frac{A_{f,anchor}}{2 \times t_f} = \frac{0.15}{2 \times 0.02} = 3.8 \text{ in.} \cong 4 \text{ in.}$

CFRP anchor length: $l_{f,anchor} = 2 \times (\text{inserted part} + \text{fan part})$
 $= 2 \times (4 + 6) = 20 \text{ in.}$

Therefore, final CFRP anchor cutting dimension: width \times thickness \times length
 $= 4 \text{ in} \times 0.02 \text{ in} \times 20 \text{ in.}$

B.3 ANCHOR HOLE AREA CALCULATION

Anchor hole area: $A_{hole} = 1.4 \times A_{f,anchor} = 1.4 \times 0.15 = 0.21 \text{ in.}^2$

Diameter of hole: $D_{hole} = \sqrt{\frac{4 \times A_{hole}}{\pi}} = \sqrt{\frac{4 \times 0.21}{\pi}} = 0.52 \text{ in.}^2$

Use $1/2$ in. drill bit for the anchor hole preparation.

B.4 REQUIRED DEVELOPMENT LENGTH OF REBAR MAT

Development length for deformed bar should be determined from ACI 318-11, Section 12.2.2. In the case of this specimen, all the rebars were smaller than No. 6 and satisfied the spacing and cover requirements.

Development length: $l_d = \left(\frac{f_y \psi_f \psi_e}{25 \lambda \sqrt{f'_c}} \right) d_b = \left(\frac{60,000 \times 1.0 \times 1.0}{25 \times 1.0 \times \sqrt{5,400}} \right) \times 0.375 = 12.25 \text{ in.}$

The rebars had 32 in. length and the development length from the center was 16 in. long. Therefore, 32 in. long rebar was adequate for the test specimen.

APPENDIX C

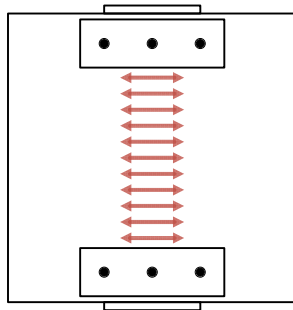
ADDITIONAL EXPERIMENTAL DATA

C.1 LOAD-STRAIN RESPONSE AND STRAIN CONTOUR OF THE PANEL SPECIMENS

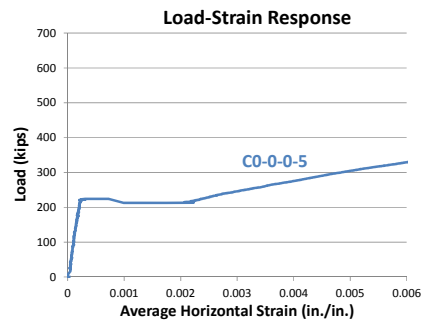
Additional load-strain responses of the panel specimens are illustrated in this section. All the strains are average strain in horizontal direction. The response of the control specimen is plotted in the same graph for comparison.

Final failure modes and strain contours at ultimate load are shown in the same figures. Loose concrete was removed to show crack patterns and pictures were taken after the test.

C.1.1 Panels reinforced without steel reinforcement



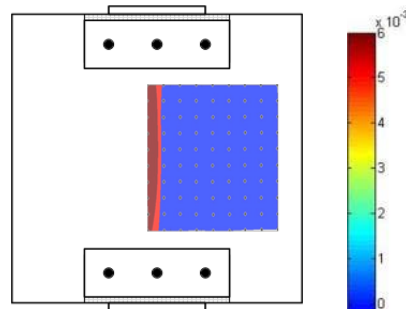
(a) Locations for strain measurement



(b) Load-average strain response

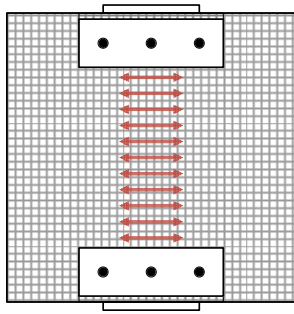


(c) Crack pattern



(d) Strain contour

Figure C.1 C0-0-0-5

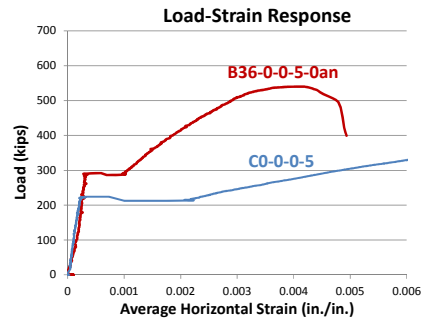


(a) Locations for strain measurement

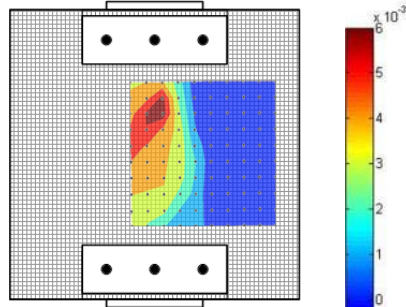


(c) Crack pattern

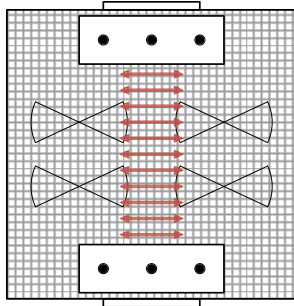
Figure C.2 B36-0-0-5-0an



(b) Load-average strain response



(d) Strain contour

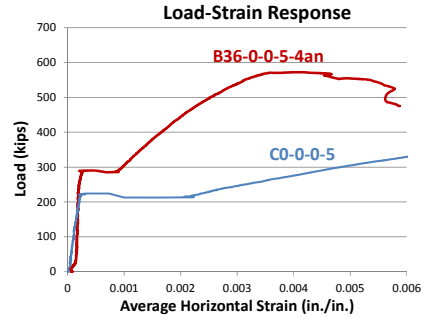


(a) Locations for strain measurement

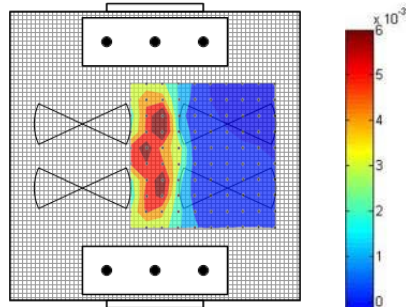


(c) Crack pattern

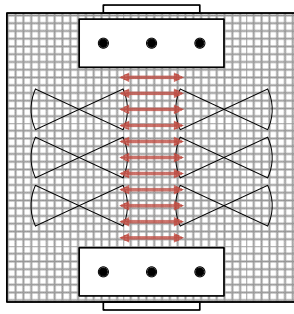
Figure C.3 B36-0-0-5-4an



(b) Load-average strain response



(d) Strain contour

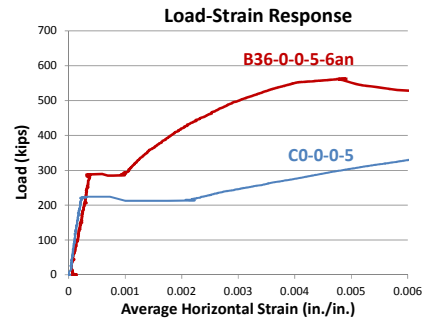


(a) Locations for strain measurement

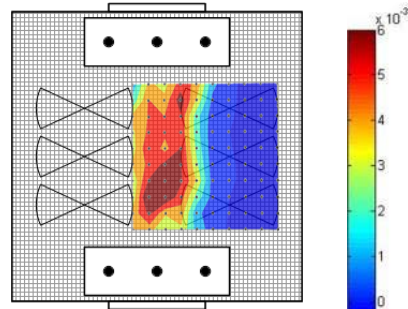


(c) Crack pattern

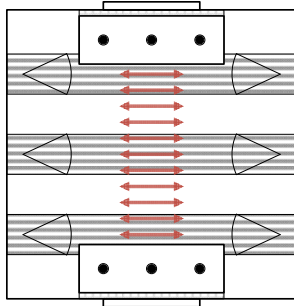
Figure C.4 B36-0-0-5-6an



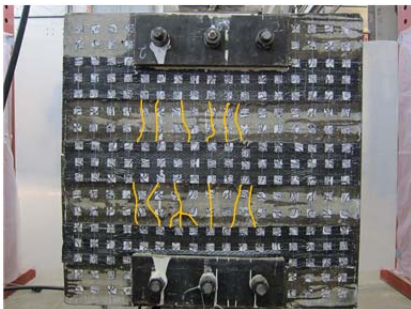
(b) Load-average strain response



(d) Strain contour

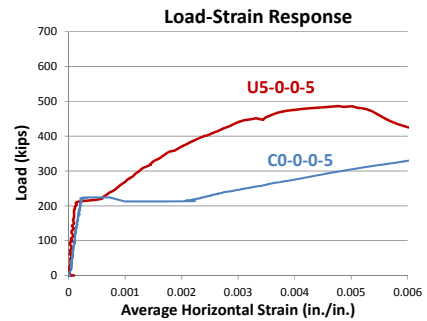


(a) Locations for strain measurement

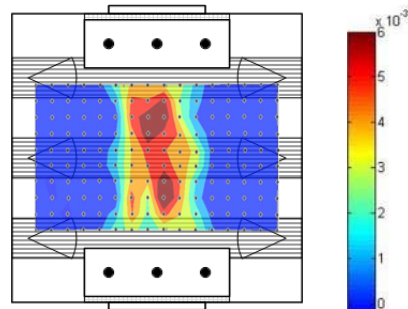


(c) Crack pattern

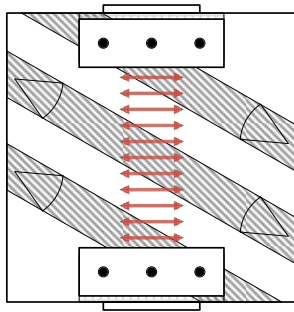
Figure C.5 U5-0-0-5



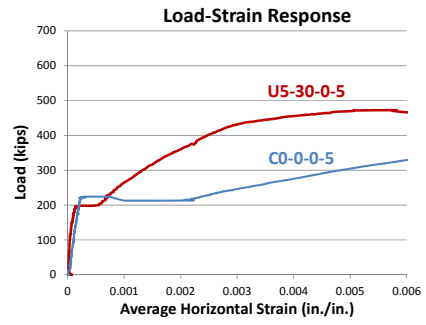
(b) Load-average strain response



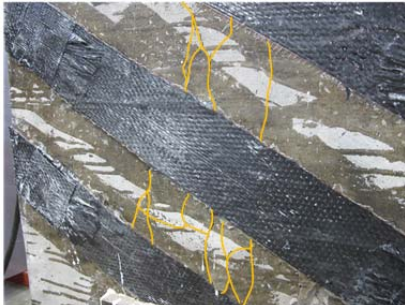
(d) Strain contour



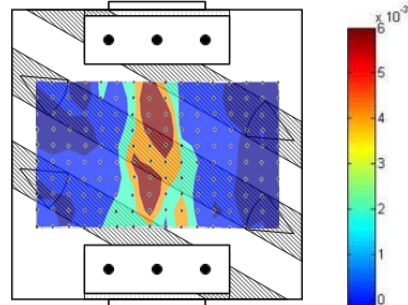
(a) Locations for strain measurement



(b) Load-average strain response

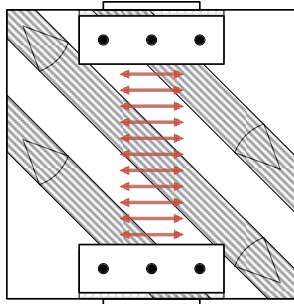


(c) Crack pattern

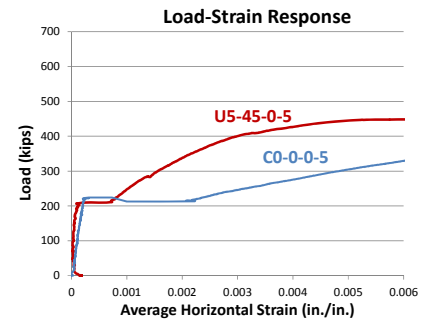


(d) Strain contour

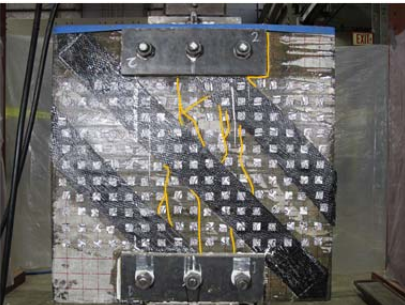
Figure C.6 U5-30-0-5



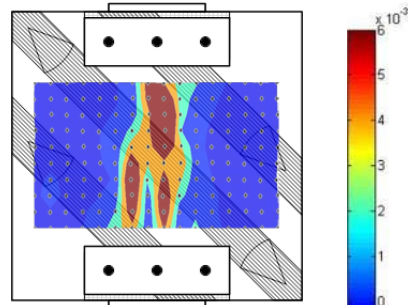
(a) Locations for strain measurement



(b) Load-average strain response

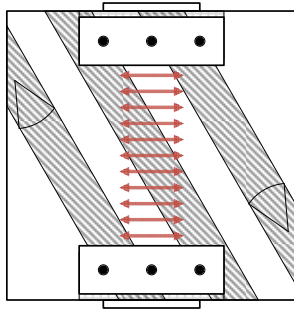


(c) Crack pattern

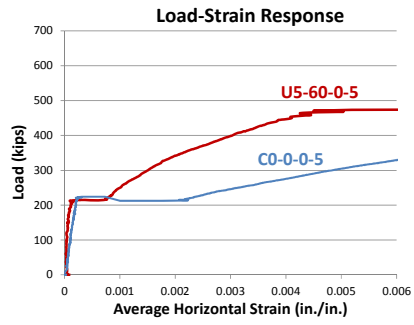


(d) Strain contour

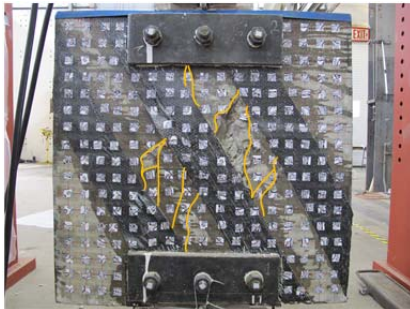
Figure C.7 U5-45-0-5



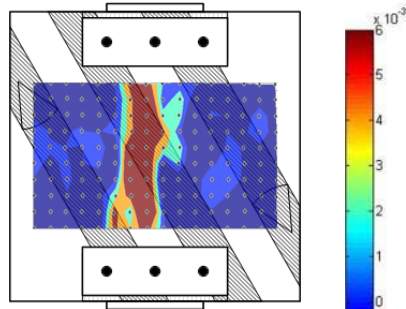
(a) Locations for strain measurement



(b) Load-average strain response

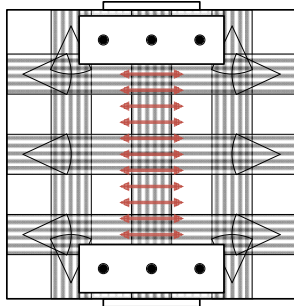


(c) Crack pattern

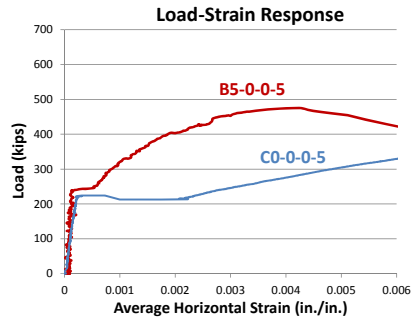


(d) Strain contour

Figure C.8 U5-60-0-5



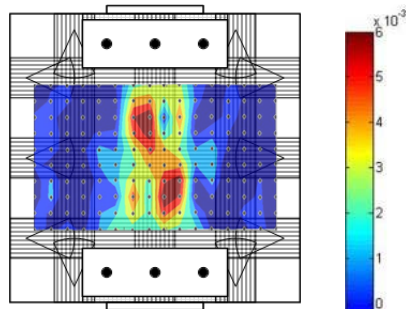
(a) Locations for strain measurement



(b) Load-average strain response

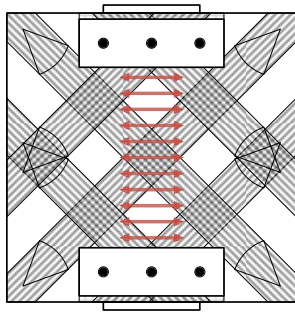


(c) Crack pattern

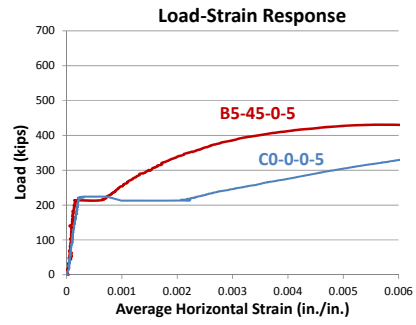


(d) Strain contour

Figure C.9 B5-0-0-5



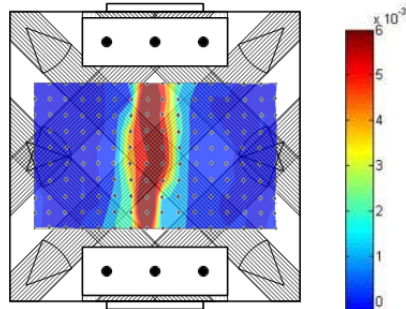
(a) Locations for strain measurement



(b) Load-average strain response

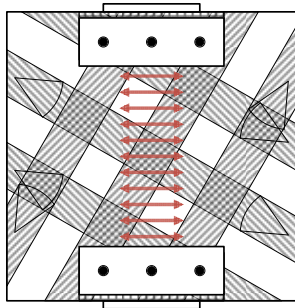


(c) Crack pattern

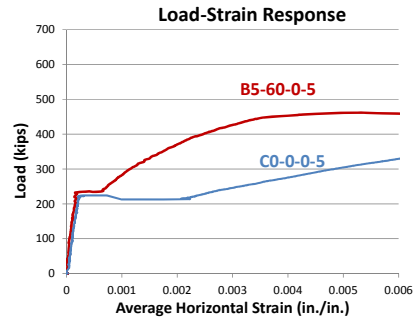


(d) Strain contour

Figure C.10 B5-45-0-5



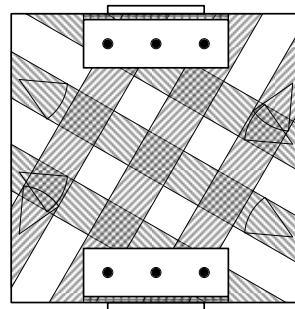
(a) Locations for strain measurement



(b) Load-average strain response



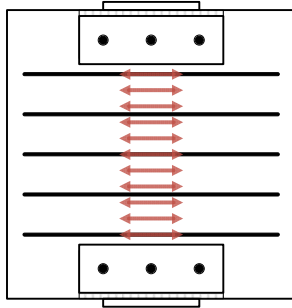
(c) Crack pattern



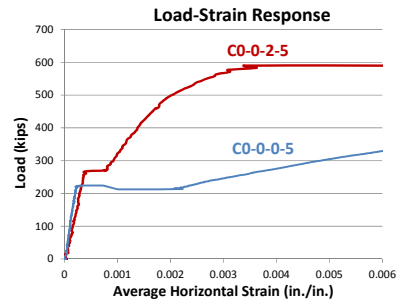
(d) Strain contour

Figure C.11 B5-60-0-5

C.1.2 Panels reinforced with steel reinforcement



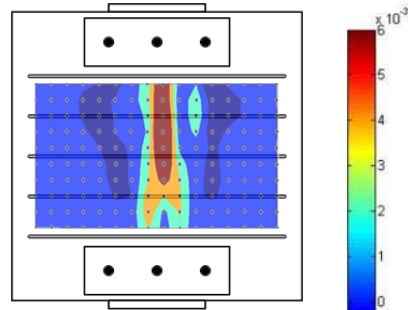
(a) Locations for strain measurement



(b) Load-average strain response

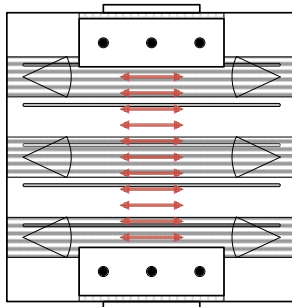


(c) Crack pattern

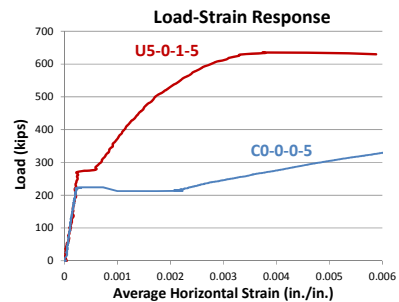


(d) Strain contour

Figure C.12 C0-0-2-5



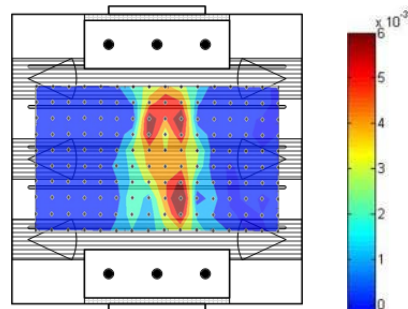
(a) Locations for strain measurement



(b) Load-average strain response

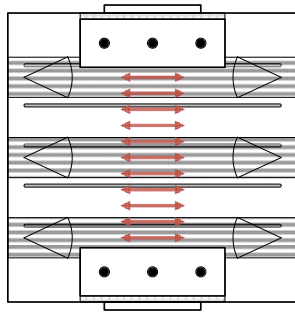


(c) Crack pattern

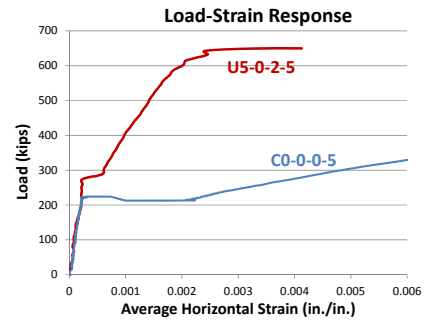


(d) Strain contour

Figure C.13 U5-0-1-5



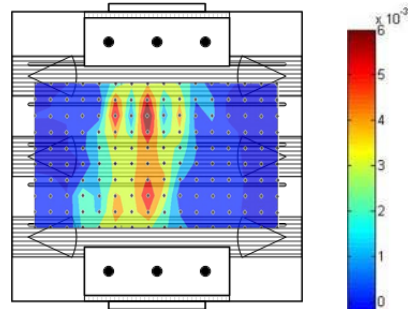
(a) Locations for strain measurement



(b) Load-average strain response

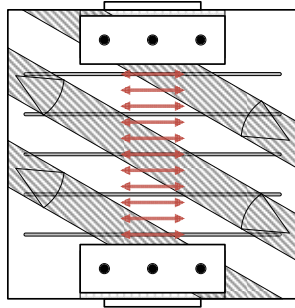


(c) Crack pattern

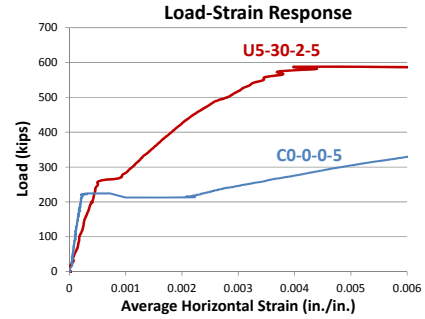


(d) Strain contour

Figure C.14 U5-0-2-5



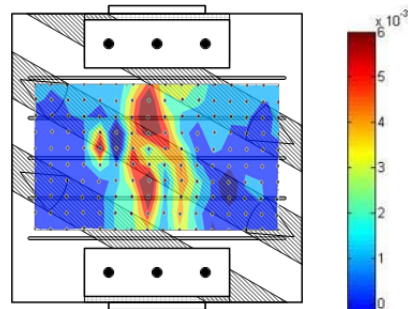
(a) Locations for strain measurement



(b) Load-average strain response

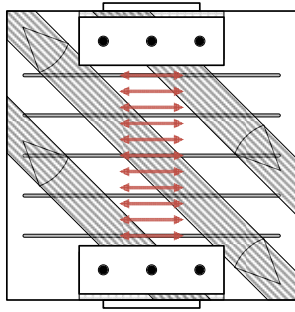


(c) Crack pattern

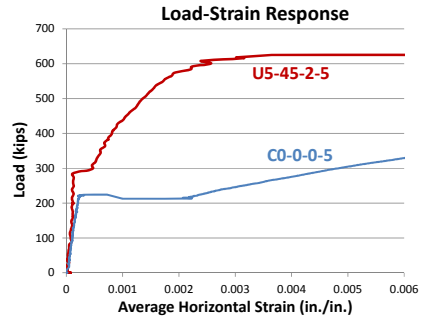


(d) Strain contour

Figure C.15 U5-30-2-5



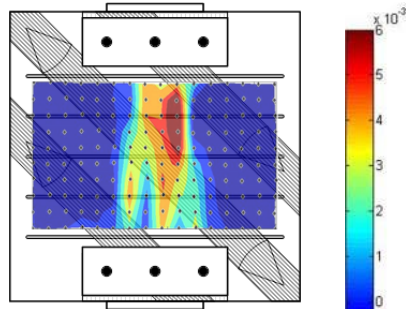
(a) Locations for strain measurement



(b) Load-average strain response

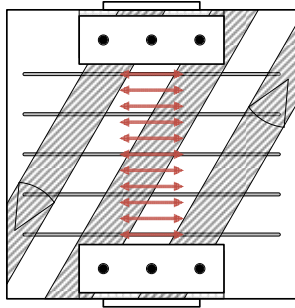


(c) Crack pattern

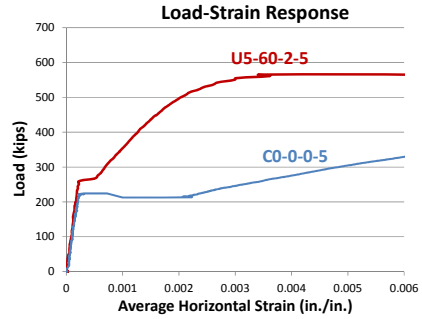


(d) Strain contour

Figure C.16 U5-45-2-5



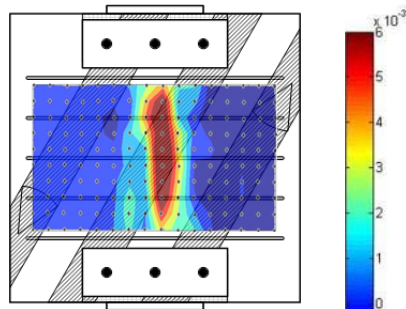
(a) Locations for strain measurement



(b) Load-average strain response

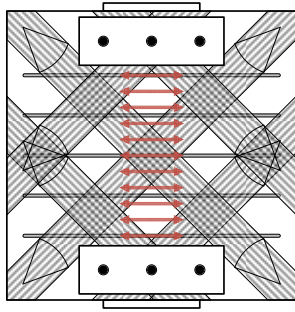


(c) Crack pattern

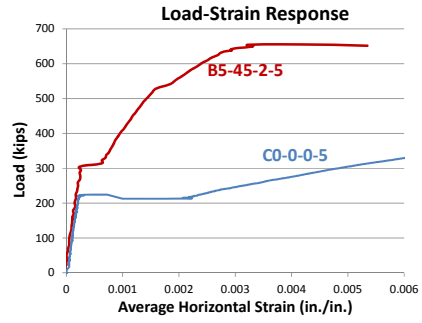


(d) Strain contour

Figure C.17 U5-60-2-5



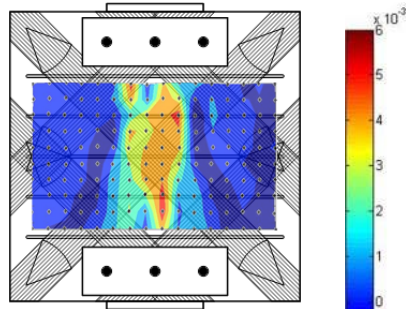
(a) Locations for strain measurement



(b) Load-average strain response

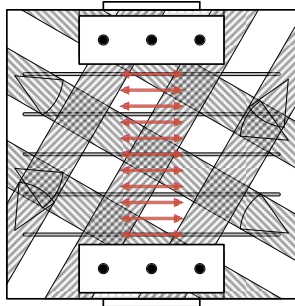


(c) Crack pattern

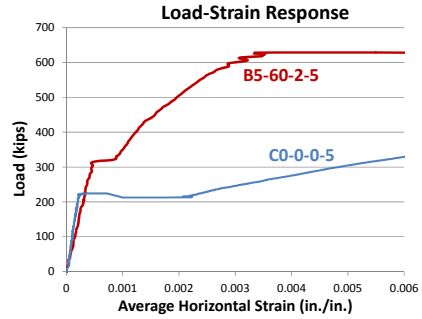


(d) Strain contour

Figure C.18 B5-45-2-5



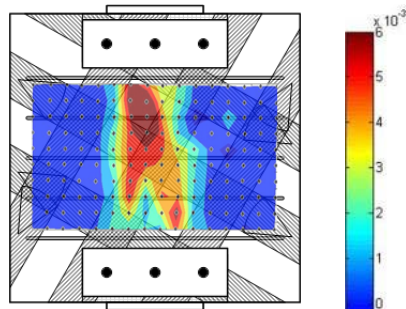
(a) Locations for strain measurement



(b) Load-average strain response



(c) Crack pattern



(d) Strain contour

Figure C.19 B5-60-2-5

APPENDIX D

STRAIN COMPARISON BETWEEN STRAIN GAGES AND VISION SYSTEM

Figure D.1 shows the locations for the strain measurement. Three different locations were selected to measure and compare the strain recordings. The red, yellow, and green square indicates the top, mid, and bottom side of the panel specimen, respectively. Two targets were chosen at each location for the vision system analysis and strain gages were attached on the embedded steel reinforcements.

Strain comparison plots can be seen in Figure D.2-D.9. The strain readings of the strain gages were plotted in solid curves and the strains of the vision system were represented by dashed curves. Strain gages were applied on the steel reinforcements in horizontal direction and the strain recordings from the vision system were in horizontal direction regardless of the CFRP strip orientations.

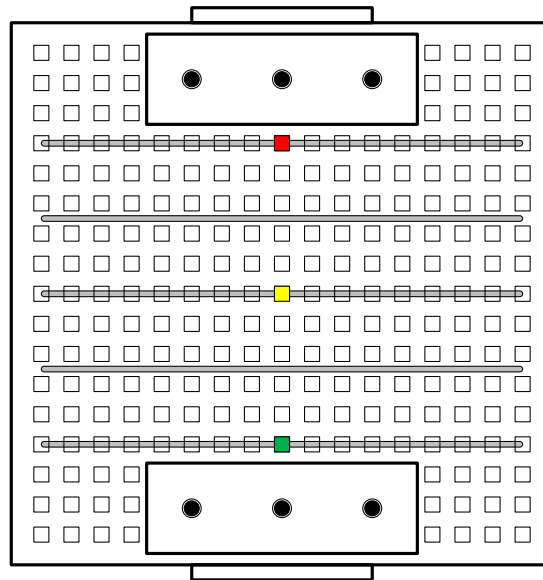
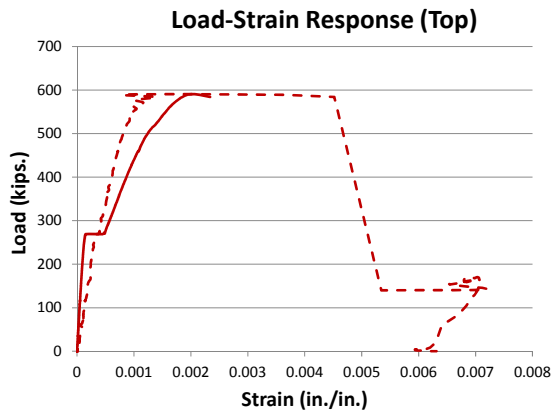
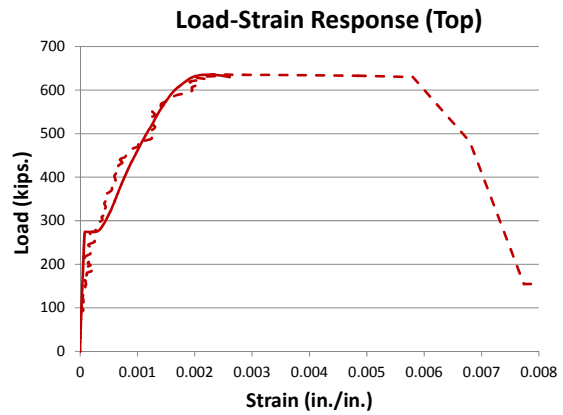


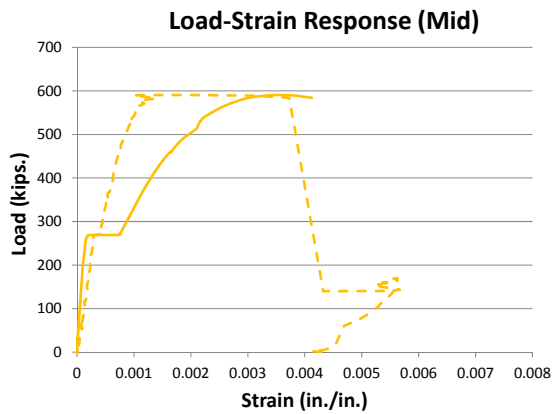
Figure D.1 Locations of the strain measurement



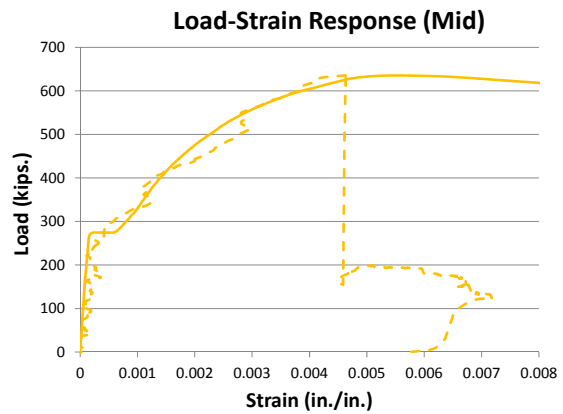
(a) Strains at the top side



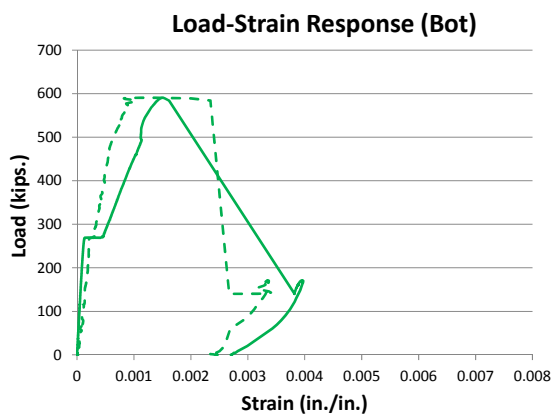
(a) Strains at the top side



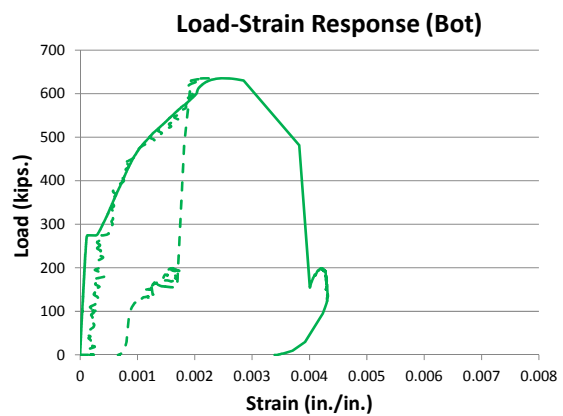
(b) Strains at the mid-height



(b) Strains at the mid-height



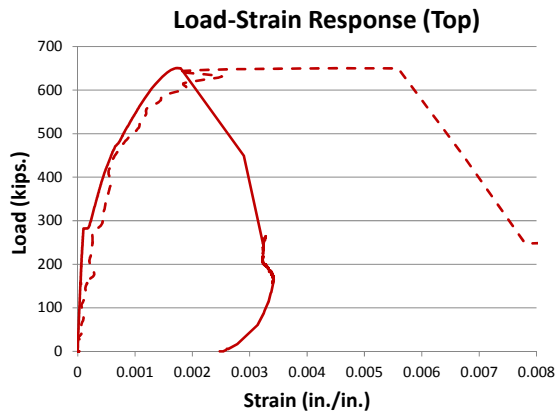
(c) Strains at the bottom side



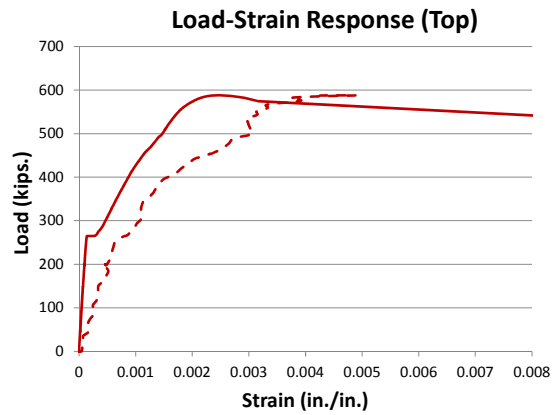
(c) Strains at the bottom side

Figure D.2 C0-0-2-5

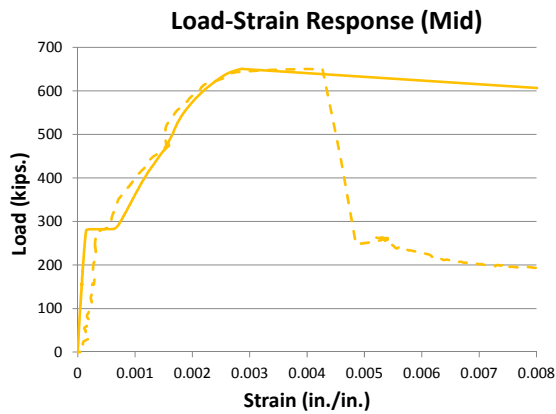
Figure D.3 U5-0-1-5



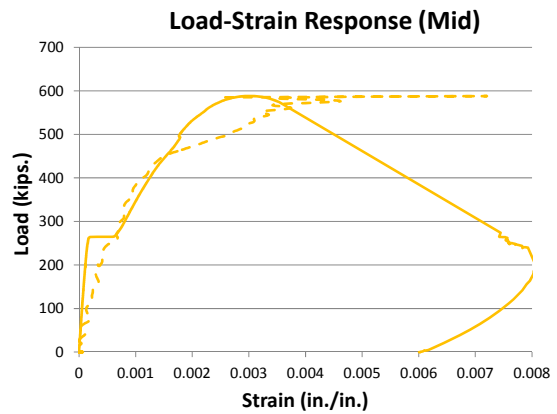
(a) Strains at the top side



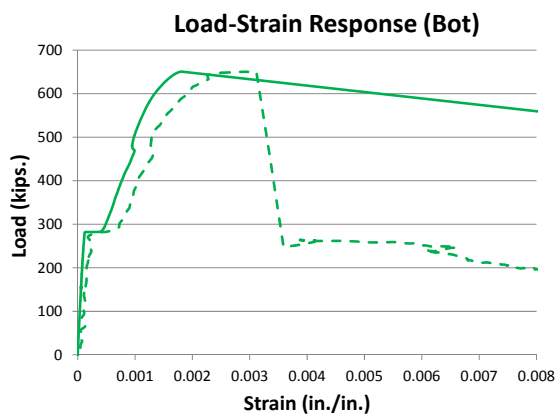
(a) Strains at the top side



(b) Strains at the mid-height

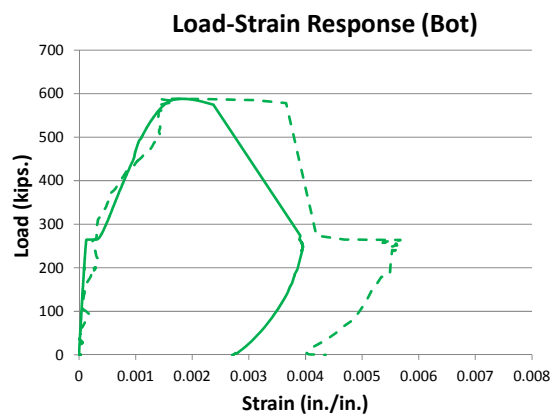


(b) Strains at the mid-height



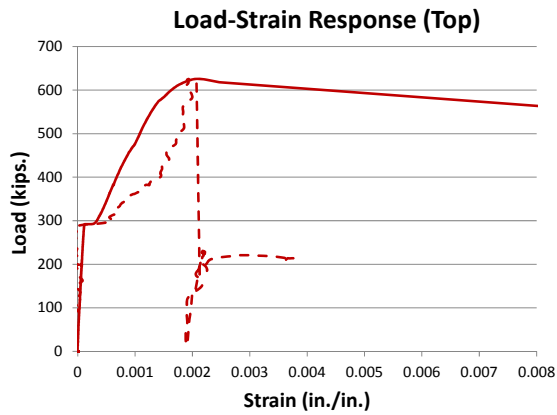
(c) Strains at the bottom side

Figure D.4 U5-0-2-5

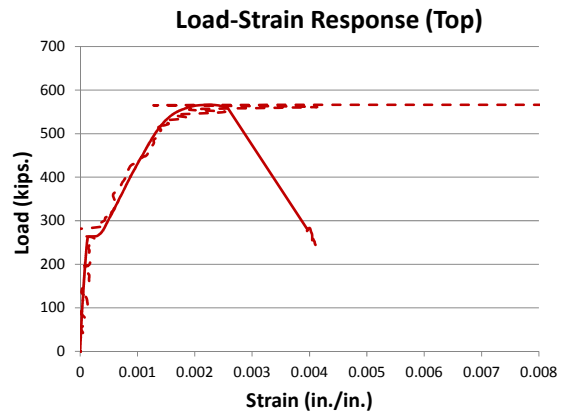


(c) Strains at the bottom side

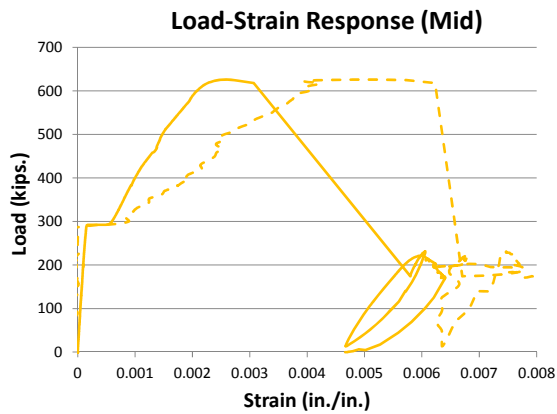
Figure D.5 U5-30-2-5



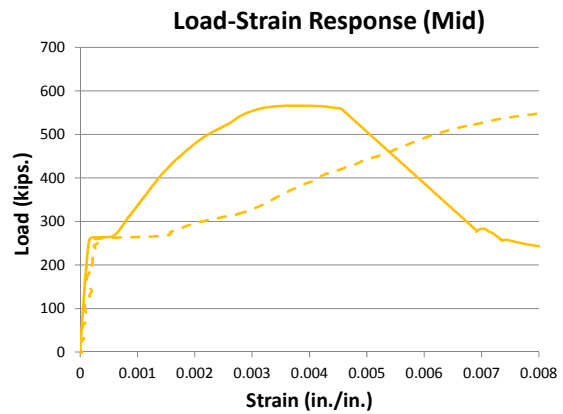
(a) Strains at the top side



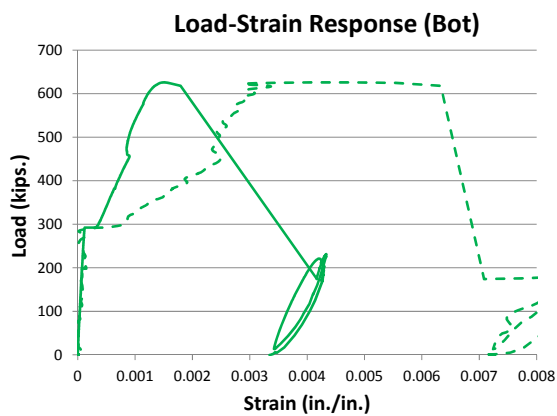
(a) Strains at the top side



(b) Strains at the mid-height

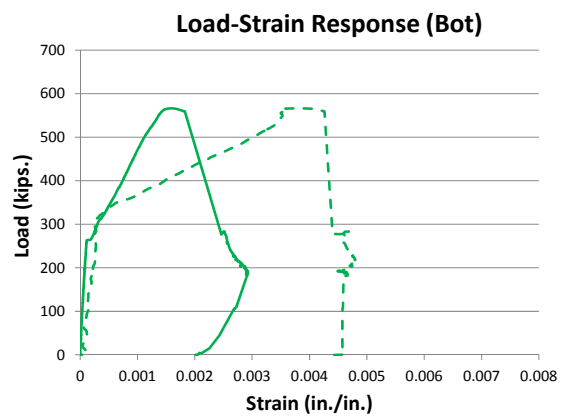


(b) Strains at the mid-height



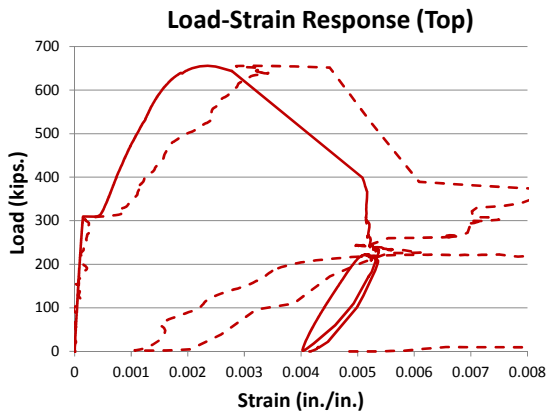
(c) Strains at the bottom side

Figure D.6 U5-45-2-5

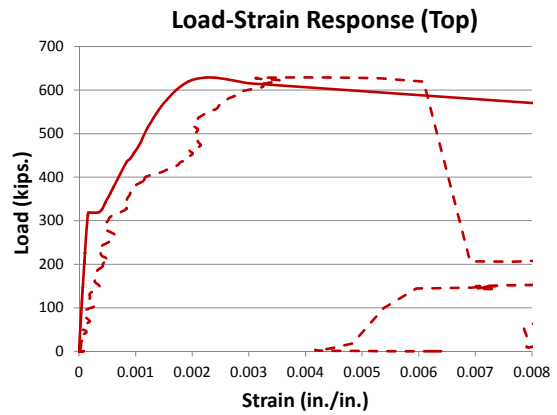


(c) Strains at the bottom side

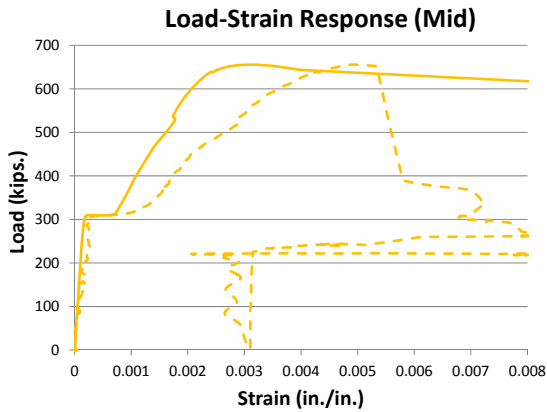
Figure D.7 U5-60-2-5



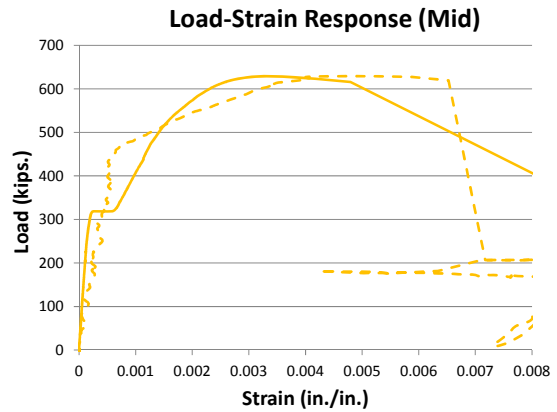
(a) Strains at the top side



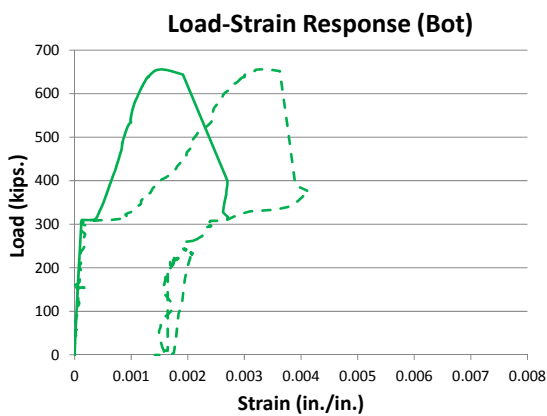
(a) Strains at the top side



(b) Strains at the mid-height

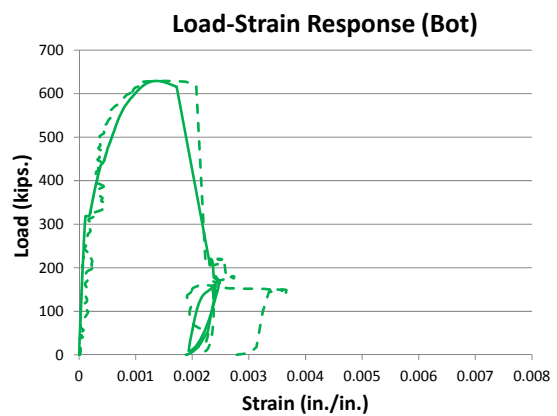


(b) Strains at the mid-height



(c) Strains at the bottom side

Figure D.8 B5-45-2-5



(c) Strains at the bottom side

Figure D.9 B5-60-2-5

REFERENCES

- ACI Committee 318, "Building Code Requirements for Structural Concrete (ACI 318-11)," American Concrete Institute, Farmington Hills, Michigan, USA, 2011.
- ACI Committee 440, "Guide for the Design and Construction of Externally Bonded FRP Systems for Strengthening Concrete Structures (ACI 440.2R-08)," American Concrete Institute, Farmington Hills, Michigan, USA, 2008.
- Brown, M.D., "Design for Shear in Reinforced Concrete Using Strut-and-Tie and Sectional Models," Ph.D. Dissertation, Department of Civil, Architectural, and Environmental Engineering, The University of Texas at Austin, Austin, Texas, 2005.
- Chajes, M., Januska, T., Mertz, D., Thomson, T., and Finch, W., "Shear Strengthening of Reinforced Concrete Beams Using Externally Applied Composite Fabrics," *ACI Structural Journal*, V. 92, No. 3, May-June. 1995, pp. 295-303.
- Kachlakev, D., and McCurry, D., "Testing of Full-Size Reinforced Concrete Beams Strengthened with FRP Composites: Experimental Results and Design Methods Verification," *Report No. FHWA-OR-00-19*, U.S. Department of Transportation Federal Highway Administration, 2000, 109 pp.
- Kim, Insung., "Use of CFRP to Provide Continuity in Existing Reinforced Concrete Members Subjected to Extreme Loads," Ph.D. Dissertation, Department of Civil, Architectural, and Environmental Engineering, The University of Texas at Austin, Austin, Texas, 2008.
- Kim, I., Jirsa, J. O., and Bayrak, O., "Use of CFRP to Strengthen Poorly Detailed Reinforced Concrete Beams," *Third International Conference on FRP Composites in Civil Engineering*, CICE 2006, Miami, 2006.
- Kim, Y., "Shear behavior of Reinforced Concrete T-beams Strengthened with Carbon Fiber Reinforced Polymer (CFRP) Sheets and CFRP Anchors," Ph.D. Dissertation, Department of Civil, Architectural, and Environmental Engineering, The University of Texas at Austin, Austin, Texas, 2011.

- Kim, Y., et al, "Shear Strengthening of Reinforced and Prestressed Concrete Beams Using Carbon Fiber Reinforced Polymer (CFRP) Sheets and Anchors," *CTR Technical Report 0-6306-1*, Center for Transportation Research at The University of Texas at Austin, 2012, pp. 226-229.
- Kobayashi, K., Fujii, S. et al., "Advanced Wrapping System with CF Anchor-Stress Transfer Mechanism of CF Anchor," *Proceedings of the 5th International Symposium on Fiber-Reinforced Polymer (FRP) Reinforcement for Concrete Structures.*, FRPRCS-5. Cambridge, U.K., 2000, pp. 379-388.
- Malvar, L., Warren, G., and Inaba, C., "Rehabilitation of Navy Pier Beams with Composite Sheets," *Second FRP International Symposium on Non-Metallic (FRP) Reinforcement for Concrete Structures*, Ghent, Belgium, Aug. 1995, pp. 533-540.
- Monti, G. and Liotta, M. A., "FRP-Strengthening in Shear: Tests and Design Equations," SP 230 *7th International Symposium on Fiber-Reinforced Polymer (FRP) Reinforcement for Concrete Structures*, American Concrete Institute, 2005, pp. 543-562.
- Norris, T., Saadatmanesh, H., and Ehsani, M., "Shear and Flexural Strengthening of R/C Beams with Carbon Fiber Sheets," *Journal of Structural Engineering*, V. 123, No. 7, 1997, pp. 903-911.
- Orton, S.L., Jirsa, J.O., and Bayrak, O., "Design Considerations of Carbon Fiber Anchors," *Journal of Composites for Construction*, ASCE, Nov.-Dec. 2008, pp. 608-616.
- Sim, J., et al, "Shear Strengthening Effects with Varying Types of FRP Materials and Strengthening Methods," SP 230 *7th International Symposium on Fiber-Reinforced Polymer (FRP) Reinforcement for Concrete Structures*, American Concrete Institute, 2005, pp. 1665-1680.
- Wollman, G., "Anchorage Zones in Post-Tensioned Concrete Structures," Ph.D. Dissertation, The University of Texas at Austin, Austin, Texas, 1992.

VITA

Changhyuk Kim was born in Seoul, South Korea in 1982, the son of Namhae Kim and Junghee Lee. He graduated Seoul high school and entered Inha University in 2001. He served military service from 2003 to 2005. He received the degree of Bachelor of Science in Engineering in 2007. In March of 2007, he entered the graduate school at Inha University, and he received Master of Engineering degree in February of 2009. In 2010, he started Ph.D. program under the supervision of James O. Jirsa and Wassim Ghannoum at the University of Texas at Austin.

Permanent address:107-1901, Dongcheon Hyundai Hometown Apt.,
Dongcheon-dong, Suji-gu, Yongin-si,
Gyeonggi-do, 448-511, South Korea
changhyuk82@gmail.com

This dissertation was typed by the author.